INHIBITION OF AUTOPHAGY INCREASES HNSCC SENSITIVITY TO CANCER THERAPIES

By

Yong-Syu Lee

A dissertation submitted in partial fulfilment of the

requirements for the degree of

Doctor of Philosophy

(Comparative Biomedical Sciences)

at the

University of Wisconsin-Madison

2021

Date of final oral examination: November 24th, 2021

The dissertation is approved by the following members of the Final Oral Committee:

Randall J. Kimple, Associate Professor, Human Oncology
Deric L. Wheeler, Professor, Human Oncology
Dustin A. Deming, Associate Professor, Medicine
Lisa M. Arendt, Assistant Professor, Comparative Biosciences
Lauren A. Trepanier, Professor, Medical Sciences

Acknowledgements

This thesis represents the sum of four years of work that absolutely could not have been accomplished on my own. I want to take this first opportunity to thank each and every individual who took the time to help me throughout this process, in whatever capacity you helped. This would not have been possible without you. I want to thank my lovely and amazing advisor, Dr. Randall Kimple, for his supportive guidance throughout these years. For teaching me not only how to ask the right scientific questions, but also to help patients through improving our understanding of cancer therapy. I could never forget your great and heartwarming help during the toughest time in my PhD years. Your mentorship and advice have proven invaluable, and I cannot truly thank you enough for your support.

The other members of my thesis committee, Dr. Deric Wheeler, Dr. Dustin Deming, Dr. Lisa Ardent, and Dr. Lauren Trepanier have also been instrumental during my time in graduate school. I have benefited greatly from the collective advice and wisdom of these scientists, for which I will always be grateful. By the way, I always enjoy giving little surprise to all of you in each meeting. I am always delighted to recall that all of you were impressed by the “bar” I prepared for my second meeting and posted selfies to Twitter. I swear that I almost ignored the policy and brought some beers.

Research is a team effort, and to that end the members of the Kimple lab have been invaluable in helping to progress this work to where it is today. I want to specifically thank those students that worked with me during their undergraduate years as well as their post-baccalaureate time in helping me with my projects. These include Justin Skiba and Samantha Bradley, both of whom have been critical in collecting the data in this work.

In addition, thank you to Lindsey Abel and Cristina Paz for having fun with me at lots of fun nights and events, which brings a lot of smiles to my graduate life. Another special shoutout to my lovely friend Dr. Mari Iida. I will never forget the first time we met and the long talk we had. You definitely change my whole graduate life in a good way and now bring me to this position. As described above, my thanks to you will never end.

I also wish to share my gratitude for the other members, research teams and laboratories that have assisted in my training and data collection. Justin Jeffery, Ashley Weichmann, and the Small Animal Imaging and Radiotherapy Facility assisted in scanning mice and performing biodistribution experiments. Lance Rodenkirch, working in Optical Imaging Core, assisted in analyzing confocal IF images. Lastly, Kathryn Fox, thank you for indulging my endless barrage of questions, for taking the time to teach me how to properly design a staining panel, and for ensuring that only the highest quality work would come from someone trained by your hands.

As part of the Comparative Biomedical Sciences Program, this PhD is part of a milestone that I finally step on over the past four years. Thank you to the coordinator, Susan Thideman, you always give me the greatest welcome no matter how much I bother you. I also wish to thank those who made the decision to accept my application. I am truly fortunate to have been given the opportunity to train as a scientist in this program at UW-Madison.

Lastly, I wish to thank my family, who have supported me throughout my graduate training, and long, long before either. Last and biggest thank to my fallen father, who was always proud of me and even now still watch me in the heaven. I am so honored to watch you baptized at the last day I stayed in my lovely hometown. Always love and miss you.

Abstract

INHIBITION OF AUTOPHAGY INCREASES HNSCC SENSITIVITY TO CANCER THERAPIES

By
Yong-Syu Lee

Under the supervision of Professor Randall J. Kimple, M.D., Ph.D.

At the University of Wisconsin-Madison

Head and neck squamous cell carcinomas (HNSCC) are responsible for over 600,000 new cases, and 380,000 deaths in the world annually. A combination of surgery, radiation (RT), and chemotherapy is used in the multidisciplinary management of patients with locally advanced HNSCC. Despite this aggressive treatment, five-year survival rates with optimal therapy for HNSCC hover around 50%. Response rates to cetuximab (CTX), a monoclonal antibody targeting the epidermal growth factor receptor (EGFR) are <20% when delivered alone and <35% when combined with cytotoxic chemotherapy. Within the radiation field, 30-40% of these patients experience local recurrence. In general, over 50% of patients recur after their initial therapy and 4-26% are diagnosed with metastatic (i.e., incurable) disease, highlighting the unmet need for a better understanding of therapeutic resistance and novel approaches to the treatment of these patients.

Autophagy is a cellular process that protects both normal and cancer cells from cellular stress. Autophagy can be activated by harsh conditions such as nutrient deprivation, chemotherapy, or radiation therapy and functions to maintain cellular energy by recycling damaged organelles to generate energy and raw materials to support cell survival. It is our hypothesis that these treatments may be unintentionally activating the

autophagic pro-survival process in tumors that would help explain the limited responses seen from patients. The goal of this thesis was to determine the role of autophagy in HNSCC therapeutic resistance and identify improved approaches for the treatment of HNSCC.

Both CTX and RT caused a significant increase in autophagy as assessed using the reporter assay and immunoblotting. Higher basal levels of autophagy were found in therapeutic resistant cell lines (UM-SCC1-C5, CTX-resistant cell; MOC2, radiation-resistant cell). Using a clonogenic survival assay, the combination of SAR405 (autophagy inhibitor) and CTX/RT resulted in significant loss of cell survival suggesting a treatment sensitizing effect and indicating the cellular protective role of autophagy in HNSCC tumorigenesis. To bridge the autophagy and clinical relevance, our group generated patient-derived xenograft models to study the LC3B expressions, an autophagy marker, in CTX/RT-resistant patient tissues. It turned out that higher LC3B levels were observed in resistant tissues. Tissue microarray (TMA) was also used to assess the LC3B expression in 107 HNSCC patients with varied stages of tumor, and this data suggests that there are higher LC3B in the recurrent and advanced staged tumors.

Knockdown of EGFR and lysosomal-associated transmembrane protein 4B (LAPTM4B), two proteins important in growth-factor deprivation induced autophagy, in CTX-treated but not RT-treated cells showed significant decrease in autophagy. RT did increase the accumulation of ROS (~50%), leading to the increased autophagy in HNSCC by two times. RT-induced mitochondrial autophagy (mitophagy) as confirmed by knockdown of Pink1, a critical mediator of mitophagy. *In vivo*, SAR405 treatment improved tumor control when combined with CTX/RT when compared to single treatment.

Taken together, our findings suggest that inhibition of autophagy can improve the efficacy of anticancer treatments and suggest that future drugs which target specific subtypes of autophagy may be needed to personalize treatment combinations for HNSCC patients.

Table of Contents

Chapter 1

Introduction and background

1.1 Overview

This thesis represents the collective work of four years focused on studying the effect of autophagy inhibition particularly on the resistance to cetuximab or radiation in head and neck squamous cell carcinomas (HNSCC). Autophagy is an evolutionarily conserved cell survival mechanism that degrades damaged proteins and organelles to generate cellular energy during times of stress. Recycling of these cellular components occurs in a series of sequential steps with multiple regulatory points [1]. Mechanistic dysfunction can lead to a variety of human diseases and cancers due to the complexity of autophagy and its ability to regulate vital cellular functions. Current HNSCC therapeutical methods may unintentionally induce cellular protective autophagy leading to therapeutic resistance. The role that autophagy plays in both the development and treatment of cancer is highly complex, especially given the fact that most cancer therapies modulate autophagy [2].

In this introduction chapter, it covers a brief conceptual summary of the types of autophagy, the signaling pathway of autophagy, as well as the correlation of autophagy and apoptosis.It next discusses the regulation of autophagy in tumor development and introduces the concept of targeted autophagy as a potential therapeutical strategy for HNSCC. This chapter closes with a discussion of the potential role of autophagy as a predictive or prognostic cancer biomarker, as well as the need for a deeper understanding into what is still unknown about autophagy. It lastly summarizes the hypothesis and experimental approach used in the remaining chapters.

1.2 Introduction of autophagy

1.2.1 Types of autophagy

Autophagy can be classified into three types (Figure 1.1): microautophagy, macroautophagy, and chaperon-mediated autophagy (CMA) [1]. It is important to note that both macro- and microautophagy can be further classified as either selective or nonselective. Nonselective autophagy is primarily utilized for cell survival purposes and involves the random engulfment of damaged cytoplasmic components destined for non-specific degradation in a lysosome. Selective autophagy targets specific organelles and can be classified according to its target; for example, mitochondrial autophagy is termed mitophagy, peroxisomal autophagy termed pexophagy, ribosomal autophagy termed ribophagy, etc [3].

While macroautophagy involves the formation of a phagophore and subsequent fusion of the autophagosome with a lysosome for cargo digestion, microautophagy involves the direct engulfment of cytoplasmic substrates within lysosomes via tubular invaginations. In this sense it is non-selective; however, there are three forms of selective microautophagy that each target specific organelles for lysosomal degradation, these being micropexophagy (peroxisomes), piecemeal microautophagy of the nucleus (PMN), and micromitophagy (mitochondria) [4]. It has been found that microautophagy is involved in many neurodegenerative diseases such as Alzheimer's [5] and Huntington's disease [6], but its specific link to cancer development is unknown [4].

Unlike both micro- and macroautophagy, chaperon-mediated autophagy (CMA) is a highly specific form of autophagy that recognizes the amino acid motif KFERQ through binding to the cytosolic chaperone protein (HSC70). The lysosomal protein LAMP2A then delivers this specific substrate to the lysosome for internalization and subsequent

degradation [2, 7].

The term “autophagy” commonly refers to macroautophagy, as it is the most studied of the three. We will use the term autophagy to refer to macroautophagy throughout this review. Double membraned vesicles known as autophagosomes first sequester the damaged cytoplasmic organelles and proteins. The autophagosome then fuses with hydrolase-containing lysosomes to form an autolysosome; this structure is then able to enzymatically degrade the original cargo into its constituent macromolecules and free amino acids for metabolic reuse [8, 9].

1.2.2 Signaling pathways of autophagy

The signaling pathway of autophagy is highly complex and involves over 30 autophagy related genes (Atgs, Figures 1.2 and 1.3); these genes are involved in various stages such as initiation, nucleation of the autophagosome, elongation of the autophagosome, lysosome fusion, and finally degradation [7]. The presence of Atg homologs in multiple higher eukaryotes suggests that the autophagy pathway is highly evolutionarily conserved [8].

Initiation of autophagy begins with the formation of the autophagosome at the phagophore assembly site (PAS), where Atg proteins are recruited and the phagophore expands [8]. Formation of the PAS is regulated by both the mTOR/Atg13/ULK1 complex and the Beclin/Vps34 complex [7]. The ULK1 complex goes on to activate the class III PI3K complex, itself consisting of the vacuolar protein sorting-associated protein 34 (Vps34), Atg14, vp63, and BECN1-regulated autophagy protein 1 (AMBRA1), all scaffolded by the tumor suppressor Beclin-1 to allow for their interaction with each other [9]. Vps34 is required for the formation of new autophagosomes; inhibition of Vps34 via

3-methyladenine inhibits autophagosome formation [10]. Likewise, inhibition of ULK1 via the pre-clinical compound SBI-0206955 [11] prevents autophagosome formation. The mechanistic target of rapamycin (mTOR) is able to directly phosphorylate ULK1 as a method of autophagy inhibition, making it a popular target for anticancer therapies [12]. Inhibition of Beclin-1 via binding of the B-cell lymphoma 2 (Bcl-2) antiapoptotic proteins is an additional route to autophagy inhibition [13]. Finally, inositol 1,4,5-triphosphate receptor (IP_3R) complexes with Beclin-1 to inhibit autophagy; this effect can be reversed using the IP_3R antagonist, xestospongin B, that disrupts this complex [14].

Autophagosome membrane expansion requires two ubiquitin-like reactions, the Atg5-Atg12 complex and MAP1-LC3/LC3/Atg8 complex [7]. Atg12 is conjugated to a lysine residue of Atg5 in a series of activation reactions by Atg7 and Atg10, forming the Atg5-Atg12 complex [15]. Atg5-Atg12 is further linked to Atg16, creating the Atg5-Atg12-Atg16 complex required for autophagosome membrane elongation and eventually dissociates from the membrane [16]. The second conjugation involves microtubule-associated protein 1A/1B-light chain 3 (LC3 or Atg8) and phosphatidylethanolamine (PE), whereby LC3 is cleaved to form LC3-I via Atg4 [17]. LC3-I undergoes conjugation with PE to form LC3-II in a reaction with Atg7 and Atg3. Unlike LC3-I or other complexes, LC3-II continues to be associated with the autophagosome membrane until its final degradation in the autolysosome [18]. Crosstalk exists between these two complexes. For example, the Atg5-Atg12-Atg16 complex may help in the conjugation of LC3-I to PE [19]. Dysfunction in any of the conjugation systems will result in unsuccessful autophagosome membrane formation [20].

Autophagosomes first fuse with endosomes to begin maturation. To engulf cellular

substrates, p62 (Sequestosome 1 or SQSTM1) binds to ubiquitin to allow for the delivery of cargo to the autophagosomes [21]. There are several proteins required to mediate the fusion process as well as provide GTPase activity, such as the endosomal sorting complexes required for transport (ESCRT) machinery, soluble NSF attachment protein receptors (SNAREs), Ras-related protein 7 (Rab7), and the class C Vps proteins; loss of function of each of these can lead to dysregulated maturation [22-25]. Autophagosomes ultimately fuse with lysosomes to form autolysosomes in the final step of the autophagy mechanism, in which damaged proteins and organelles are degraded. Autophagic flux can be calculated as a measure of autophagy by examining LC3-II and p62 levels, as both are degraded in the autolysosome [18].

1.2.3 Autophagy and apoptosis

Cytoplasmic organelles and whole cells are constantly regulated by both autophagy, the process of self-eating, and apoptosis, the process of self-killing [26]. The relationship between these mechanisms is highly complex and may be triggered by common upstream signals, resulting in their concurrent activation. These common regulators include the tumor suppressor protein TP53, BH3-only proteins, death-associated protein kinase (DAPK), and JUN N-terminal kinase (JNK) [27].

TP53 is a well-studied tumor suppressor protein, having effects on metabolism, antioxidant defense, genomic stability, proliferation, senescence, cell death, and most notably is able to induce autophagy following DNA damage [28]. While TP53 has not been found to directly interact with any of the core Atg proteins, it can activate pro-autophagic genes such as AMPK, TSC2, PTEN, DRAM, or Sesn1/2 to induce autophagy [29]. The BH3-only proteins BAD, BID, NOXA, and PUMA interact with Bcl-2 to release Beclin-1,

an autophagy initiator [27]. Conversely, the BH3-only protein BIM inhibits autophagy through interaction with Beclin-1, as well as mediating apoptosis [30]. Beclin-1, after being unbound from BCL-2, complexes with VPS34 to help facilitate autophagy protein localization to autophagosome membranes [13].

Further investigations into the relationship between autophagy and apoptosis has been conducted in colon cancer cells. It has been shown that a shift from autophagy to apoptosis can occur through a caspase-8 dependent manner wherein caspase-8 co-localizes with the proteins LC3-II and LAMP2, autophagic markers on autophagosomes. Caspase-8, normally involved in signaling apoptosis, can be degraded by the autophagic machinery, hindering its activity [31]. Conversely, activation of apoptosis can also suppress autophagy through Bax-mediated cleavage of Beclin-1. Cleavage of Beclin-1 interrupts its interaction with VPS34, a required step in the initiation of autophagy [32].

1.3 Autophagy in the development and progression of cancer

1.3.1 The association of autophagy with cancers

The precise role of autophagy in cancer remains highly complex. Autophagy has been shown to play a role in both evasion of cell death and maintenance of homeostasis through cellular recycling programs, and in the promotion of cell death through large-scale degradation of cellular components [33]. While autophagy can be induced to limit cancer proliferation and progression, tumor cells can also take advantage of this machinery to promote metastasis and survival in times of nutrient deprivation. For example, tumor suppressor proteins including TP53, PTEN, DAPK, TSC1, and TSC2 are commonly mutated in cancer and can provide the cell with signals to activate autophagy [33]. The precise role of autophagy as a pro- or anti-survival process may be both stage and

environment specific [34].

During the early stages of tumorigenesis, autophagy can act as a tumor suppressor. For example, Bif-1 can interact with Beclin-1 through UV radiation-resistance-associated gene (UVRAG) to act as a tumor suppressor and positive regulator of autophagy [35]. The gene encoding Beclin-1 is decreased or deleted in 70% of breast cancer, 52% of prostate cancer, and 75% of ovarian cancer [36-38]; this loss of Beclin-1 promotes apoptosis and mitigates the cytoprotective role autophagy typically plays [39]. This finding suggests that Beclin-1 functions as a tumor suppressor, as it usually is involved in the formation of the phagophore in the autophagy mechanism [40]. Conversely, overexpression of Beclin-1 has been found to promote apoptosis and suppress tumorigenesis in MKN-45 gastric cancer cells [41]. Additionally, frameshift mutations in Atg2B, Atg5, Atg9B, and Atg12 are common in gastric and colorectal carcinomas, suggesting that impaired activation of autophagy might contribute to cancer development [42]. The observation that mutations in autophagy core proteins results in carcinogenesis suggests that autophagy is an important mechanism involved in tumor inhibition. Not surprisingly, the most commonly mutated gene in cancer, TP53, plays a complex role in autophagy where it can act as either as an autophagy promotor or autophagy inhibitor. Wild type TP53 can activate autophagy genes in response to conditions of cellular stress, such as oncogenesis, whereas mutated cytoplasmic TP53 has been shown to repress autophagy [43].

Although autophagy can help to suppress initial tumor development, it can also help tumor cells overcome the extreme stressors they face, such as hypoxia and nutrient deprivation [40]. To fulfill the increased metabolic and energetic needs, tumors cells take

advantage of autophagic machinery to recycle intracellular components, supplying the necessary substrates to promote cell survival [44]. A study found that Ras-mutated cancer cells maintained higher levels of basal autophagy and possessed an “autophagy addiction” required to sustain cell survival and tumor growth during times of limited nutrients [45]. There also is evidence that low Atg5 expression in melanoma promotes tumorigenesis, as Atg5 normally inhibits proliferation and induces cell senescence [46]. Together, these findings imply that autophagy is used to increase stress tolerance and provide tumor cells with the appropriate nutrients to support their survival.

1.4 Autophagy in the treatment of head and neck cancer

1.4.1 The challenges of modulating autophagy in cancer therapy

Autophagy’s dual role of cytotoxicity and cytoprotection poses an immense challenge to anticancer treatment approaches. Drug-induced autophagy has been employed as an attempt to kill cancer cells, particularly in those that have adopted anti-apoptotic strategies. However, an opposite approach has been taken wherein autophagy is inhibited as an attempt to overcome the therapeutic resistance conferred by autophagy [47]. It should be noted that there are currently no FDA approved compounds that were developed specifically to inhibit autophagy. Rather, autophagy modulation was discovered as an off-target effect. Our group and others are actively investigating whether chemotherapy and radiotherapy can be enhanced with the addition of autophagy modulators to improve tumor control and prevent the development of therapeutic resistance, as autophagy has numerous effects on cancer treatments. There remains a significant need for an improved understanding of how autophagy can be modulated to improve the care of cancer patients.

1.4.2 Effect of chemotherapy on autophagy

Current cancer therapies such as radiation and chemotherapy induce cytotoxic stress capable of triggering pro-survival autophagy in cancer cells, demonstrating the complicated role of autophagy in anticancer therapy [48, 49]. Many cancers, including nearly all (i.e. 90%) HNSCCs, are associated with EGFR overexpression, with more aggressive phenotypes corresponding to increased EGFR levels [50, 51]. EGFR is an upstream regulator of the PI3K/Akt/mTOR signaling pathway, which is itself activated in 47% of HNSCCs with EGFR activation, making it an attractive target for cancer therapies [52]. This pathway controls cell proliferation, survival, and modulates gene expression, as well as governing autophagy regulation [53]. Many commonly used chemotherapy agents can induce autophagy, emphasizing a need to better understand this mechanism [54].

Gefitinib, also known as Iressa or ZD1839, is an EGFR tyrosine kinase inhibitor that acts by binding to the ATP site on EGFR, blocking activation of downstream AKT/ERK/STAT3 signaling [55, 56]. Clinical efficacy is unfortunately minimal, with a 10-15% patient response to treatment [56]. The anticancer effects of gefitinib were found to be enhanced when used in combination with MK-2206, an allosteric inhibitor of Akt, a kinase family with inhibitory effects on apoptosis [57]. However, gefitinib is also able to activate autophagy and promote cell survival through an EGFR-independent pathway, which suggests that the use of autophagy inhibitors in combination with gefitinib could work together to improve treatment efficacy [58].

Erlotinib, also known as Tarceva or OSI-774, is another EGFR tyrosine kinase inhibitor that targets the ATP binding site within EGFR and prevents downstream signal activation [59]. Treatment with erlotinib leads to a 29% response rate in patients with HNSCC [60]. The NADPH oxidase 4 (NOX4) enzyme is increased by erlotinib treatment,

leading to erlotinib-induced cytotoxicity and production of H_2O_2 to drive cell death. This points to a potential therapeutic approach in which erlotinib could be used in combination with conventional therapies that additionally increase oxidative stress to amplify its effects [61]. At low concentrations, erlotinib triggers autophagy to provide cells with necessary energy and nutrients as an attempt at survival. Conversely, high doses of erlotinib have been found to cause autophagic cell death; this effect is further increased with the addition of autophagy inhibitors to treatment [62].

Saracatinib, also known as AZD0530, is a small molecule inhibitor of Src family kinases (Src, Yes, Fyn, Lyn, Lck, Hck, Fgr, Blk, Yrk) which are involved in cellular processes including proliferation, adhesion, invasion, migration, and tumorigenesis [63]. Higher levels of Src have been correlated with more advanced cancers [64, 65]. The ability of saracatinib to block Src through the Vimentin/Snail signaling pathway suppresses cancer cell metastasis in HNSCC, both *in vitro* and *in vivo* [66]. Unfortunately, a phase II clinical trial of single agent saracatinib failed to demonstrate efficacy [67]. The disappointing clinical results suggest that underlying mechanisms of resistance such as autophagy may play a key role in determining which cancers respond to these targeted therapies; for example, in non-small cell lung cancer (NSCLC) Src inhibition induces cytoprotective autophagy through PI3K signaling. Simultaneous inhibition of autophagy with saracatinib increased cytotoxicity [68]. Similarly, Src was seen to induce high levels of autophagy through the PI3K signaling pathway in prostate cancer cells. Combining saracatinib and chloroquine (CQ), an autophagy inhibitor, resulted in higher levels of apoptosis as well as a 64% inhibition of tumor growth in mouse models [69]. This combination of saracatinib plus autophagy inhibition may reveal better tumor control in

clinical settings.

Cetuximab, also known as Erbitux or IMC-225, is a IgG1 monoclonal antibody that binds to the EGFR ligand binding domain resulting in both inactivation and receptor internalization [70]. Blocking EGFR ligand binding has many anticancer effects including inhibition of tumor growth, impairment of DNA damage repair, and increased cell death [71]. Due to the extremely high rate of EGFR overexpression in HNSCC, cetuximab has been a popular treatment option, particularly for those patients unable to tolerate cytotoxic chemotherapy. However, responses to cetuximab monotherapy hover around 20% [72]. Cetuximab promotes EGFR translocation to the nucleus, which has been linked to resistance to cetuximab [73]. Fortunately, the Src protein family inhibitor dasatinib has showed promising results in inhibiting cetuximab-mediated EGFR nuclear translocation [74]. Another promising multi-drug treatment for HNSCC is the combination of cetuximab and cisplatin, in which response to treatment increased from 20% to 35% [72, 75]. Cetuximab induces autophagy both by inhibition of the PI3K/Akt/mTOR pathway and activation of the Vps34/Beclin-1 pathway as indicated by an increase in LC3-II accumulation, characteristic of increased autophagic flux. Interestingly, the addition of rapamycin, an mTOR inhibitor and autophagy inducer, to cetuximab treatment increased apoptosis in cetuximab-resistant cells [76].

Panitumumab, also known as Vectibix or ABX-EGF, is a monoclonal IgG2 antibody which inhibits EGFR [77]. As compared to IgG1 antibodies like cetuximab, IgG2 antibodies are not anticipated to induce antibody-dependent cellular toxicity (ADCC) [78, 79]. Panitumumab improved progression-free survival and caused low cytotoxicity in a phase III HNSCC clinical trial, although it did not improve overall patient survival in

combination with cytotoxic chemotherapy [80]. In combination with radiotherapy, panitumumab augmented in vitro efficacy by enhancing radiation-induced DNA damage as well as blocking EGFR nuclear translocation, both of which can increase apoptosis [79]. Little is known regarding the connection between panitumumab and autophagy; nonetheless it has been found that Beclin-1, a marker of autophagy, is increased in cells treated with panitumumab [81].

1.4.3 Effect of radiation therapy on autophagy

Although radiation therapy (RT) is a common treatment for many cancer patients, it has been shown to increase autophagy significantly in cancer cells [48]. Autophagy appears to enhance cancer cell killing following radiation [82]. Consistent with this, rapamycin increases the efficacy of radiotherapy by increasing radiation-induced cell death [83, 84]. Combination treatment with radiation and rapamycin increases autophagy and leads to increased cell death in an oral squamous cell carcinoma (OSCC) cell line, showing that induction of autophagy may help increase the anticancer effects of radiotherapy [85]. Pretreating radiation-resistant cells with 3-methyladenine (3-MA) or chloroquine (CQ) can increase efficacy of irradiation treatment compared to irradiation alone [86]. While this helps establish autophagy's role as a tumor suppressor, it has also been reported that autophagy can exhibit cytoprotective effects in radiation-treated cells, acting as a tumor promotor Gracio [87]. The precise relationship between autophagy and radiotherapy continues to be elucidated and may be partially dependent on where in the autophagy pathway inhibition occurs and the dose of radiation utilized [88].

1.4.4 Induction of autophagy in head and neck cancer

Given the dual role that autophagy plays in cells as both a tumor suppressor and tumor promotor, several drugs have been developed to regulate either the induction or inhibition of autophagy (Figure 3). The main pathway targeted by autophagy inducers is the mTOR/Akt signaling pathway as it normally is a negative regulator of autophagy [27].

Rapamycin, also known as Rapamune or sirolimus, targets and inhibits mTOR through the formation of a FKBP12-rapamycin-mTOR complex, and through this induces autophagy [89]. Rapamycin can also induce apoptosis in HNSCC and additionally has a synergistic effect in combination with other cytotoxic agents such as cisplatin, carboplatin, doxorubicin, paclitaxel, topotecan, and mitoxantrone [90]. While rapamycin can induce autophagy, inhibition of autophagy decreased the cytotoxicity of rapamycin, demonstrating that autophagy is an important aspect of rapamycin treatment efficacy [91].

Everolimus, also known as Afinitor or RAD001, is a derivative of rapamycin that also inhibits mTOR and activates autophagy. Induction of autophagy by everolimus enhances sensitivity to other therapies such as doxorubicin and radiation, as well as promoting autophagy-mediated programmed cell death. Everolimus-mediated autophagy leads to Met inactivation and Src activation, suggesting that Src inhibitors may synergize with everolimus [92].

Temsirolimus, also known as Torisel or CCI-779, is yet another derivative of rapamycin that partially inhibits mTOR by complexing with the FK506 binding protein [93]. Temsirolimus improves the efficacy of traditional therapies when combined with irradiation, anti-EGFR, and anti-angiogenic therapies in HNSCC [94]. It should be of no surprise that temsirolimus is able to induce autophagy due to its effects on the PI3K/Akt/mTOR pathway. Temsirolimus was also found to promote G1 cell cycle arrest

through the downregulation of p21, and although not cytotoxic, did modestly increase cell death when used at high concentrations [95].

1.4.5 Inhibition of autophagy in head and neck cancer

Autophagy activation is known to be involved in the progression of many types of cancers; regulating autophagy induction would be beneficial for improving treatment. Two potential inhibitors of autophagy, chloroquine (CQ) and its derivate hydroxychloroquine (HCQ), have been investigated for their ability to block autophagy in cancer. Other autophagy inhibitors are currently in development but have not yet received FDA approval (Figure 3).

The anti-inflammatory drug chloroquine (CQ) blocks autophagy by inhibiting lysosomal fusion with autophagosomes; hypothesized to occur due to CQ-induced Golgi and endosomal disorganization [96]. Increased cell death was achieved using combination treatment of CQ with cisplatin, erlotinib, and saracatinib *in vitro* [62, 69, 97]. CQ greatly improved glioblastoma treatment response both when treated alone [98] and in combination with conventional therapies [99]. Another study reported that CQ has additional autophagy-independent methods of reducing cancer cell invasion and metastasis [100].

Hydroxychloroquine (HCQ), also known as Plaquenil, functions similarly to CQ and synergizes with CYT997, a microtubule-disrupting agent, to trigger oxidative stress-associated apoptosis in HNSCC [101]. HCQ is a successful autophagy inhibitor on its own, but combination with current therapies demonstrate the largest effect. A clinical trial on canines with lymphoma showed a 93.3% response rate when treated with HCQ and doxorubicin [102]. Combination treatment of HCQ with gemcitabine, a chemotherapy

drug, yielded a 61% response rate in patients with pancreatic adenocarcinoma with additional improvements in overall survival [103].

1.5 Potential application of autophagy in clinic

Autophagy not only controls cellular homeostasis but also plays a critical role in cancer development leading from healthy cells to metastatic or drug-resistant tumors (Figure 1.4). This multistep regulation highlights the opportunities for pharmacologic intervention in the multistep process of autophagy, as well as its potential for serving as a predictive or prognostic cancer biomarker. Initially, autophagy protects healthy cells from malignant transformation. However, defects in the autophagic process might facilitate the acquisition of malignant features by healthy cells. Once malignancy is established, autophagy assumes the role of cell protector against cellular stresses from microenvironments including alkylating agents and irradiation. This may help establish therapeutic resistance in cancer cells. In this phase, the restoration of autophagic responses may be essential to support cancer cell survival and proliferation in the presence of adverse microenvironmental conditions. The exact strength of these autophagic responses required to fight against cellular stresses remains unknown, as evidence in support of this model is lacking. Lastly, autophagy inhibitors have exhibited an ability to be useful additives to current alkylating agents or irradiation in several studies, but convincing evidence from clinical trials has not yet been presented. These emphasize the unmet experimental and medical needs to further understand the use of autophagy in HNSCC therapies and ultimately improve treatment outcomes for patients suffering from this disease, which motivates us to start this thesis project.

1.6 Thesis hypothesis and structure

The core hypothesis of this body of work is that autophagy helps head and neck cancer cells survive from current cancer treatments and ultimately establishes therapeutic resistance. To adequately address this question, the role of autophagy in HNSCC must be determined. In **Chapter 2**, we provide clear evidence regarding the autophagy status in treatment resistant cells, malignant tissues, and recurrent HNSCC patients. These data describe a critical role for autophagy in therapeutic resistance. Using a tissue microarray (TMA) from HNSCC patients we show increased LC3B expression in more advanced stage primary cancers and in recurrent cancers when compared to primary ones. **Chapter 3** determines the cellular protective role of autophagy in HNSCC treated with CTX or RT and describes that combination therapy can improve the response to both CTX and RT in the *in vitro* and *in vivo* models of HNSCC. **Chapter 4** determines the different subtypes of autophagy activated by CTX and RT respectively, leading to a better understanding of the mechanisms by which these treatments stimulate autophagy. **Chapter 5** summarizes these findings and their potential implications, and discusses additional questions raised by this work.

1.7 Acknowledgment

This introduction chapter has just been accepted to published in the latest issue of the journal Molecular Carcinogenesis as a review paper. Thank you to Samantha Bradley and Dr. Randall Kimple for finishing this great work with me in a short period.

Figure 1.1

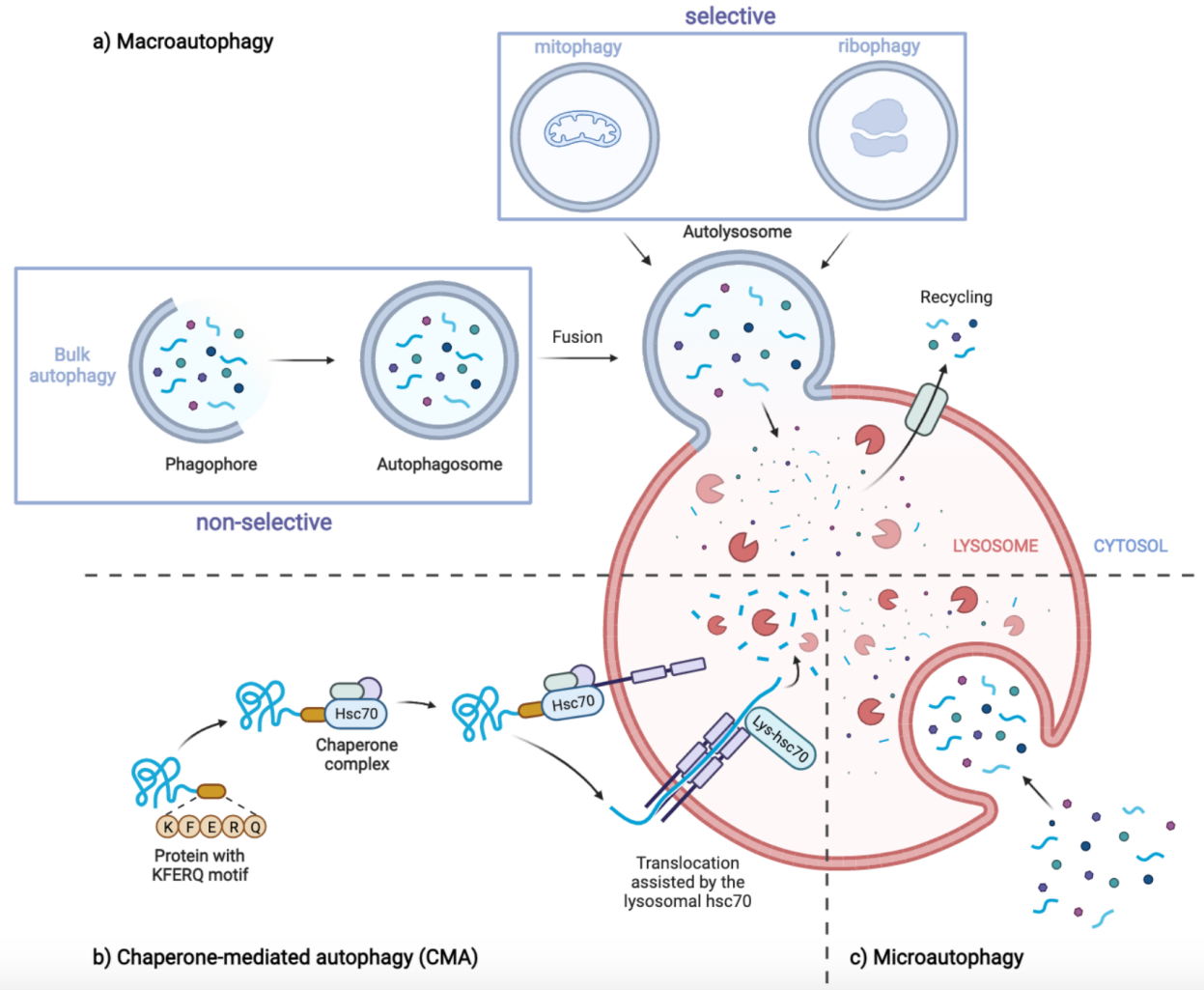
a) Macroautophagy
selective
mitophagy
ribophagy
Autolysosome
Bulk autophagy
Phagophore
Autophagosome
Fusion
non-selective
Recycling
LYSOSOME
CYTOSOL
Hsc70
Chaperone complex
Hsc70
Lys-hsc70
K F E R Q
Protein with KFERQ motif
Translocation assisted by the lysosomal hsc70
b) Chaperone-mediated autophagy (CMA)
c) Microautophagy

Figure 1.1 Types of autophagy

There are three major types of autophagy. **a)** Macroautophagy involves the fusion of the autophagosome and lysosome to degrade damaged cytosolic cargos. Autophagy can occur either via non-selective (bulk) degradation or through selective elimination of cytosolic components including different dysfunctional organelles such as mitochondria and ribosomes. **b)** Chaperone-mediated autophagy (CMA) occurs independent of the autophagosome and lysosomal invagination. Chaperone proteins, such as Hsc70, recognize cytosolic cargo destined by degradation by their consensus sequence known as the KFERQ-like motif. **c)** Microautophagy is the process where lysosomes directly engulf cytosolic components via invagination of the lysosomal membrane.

Figure 1.2

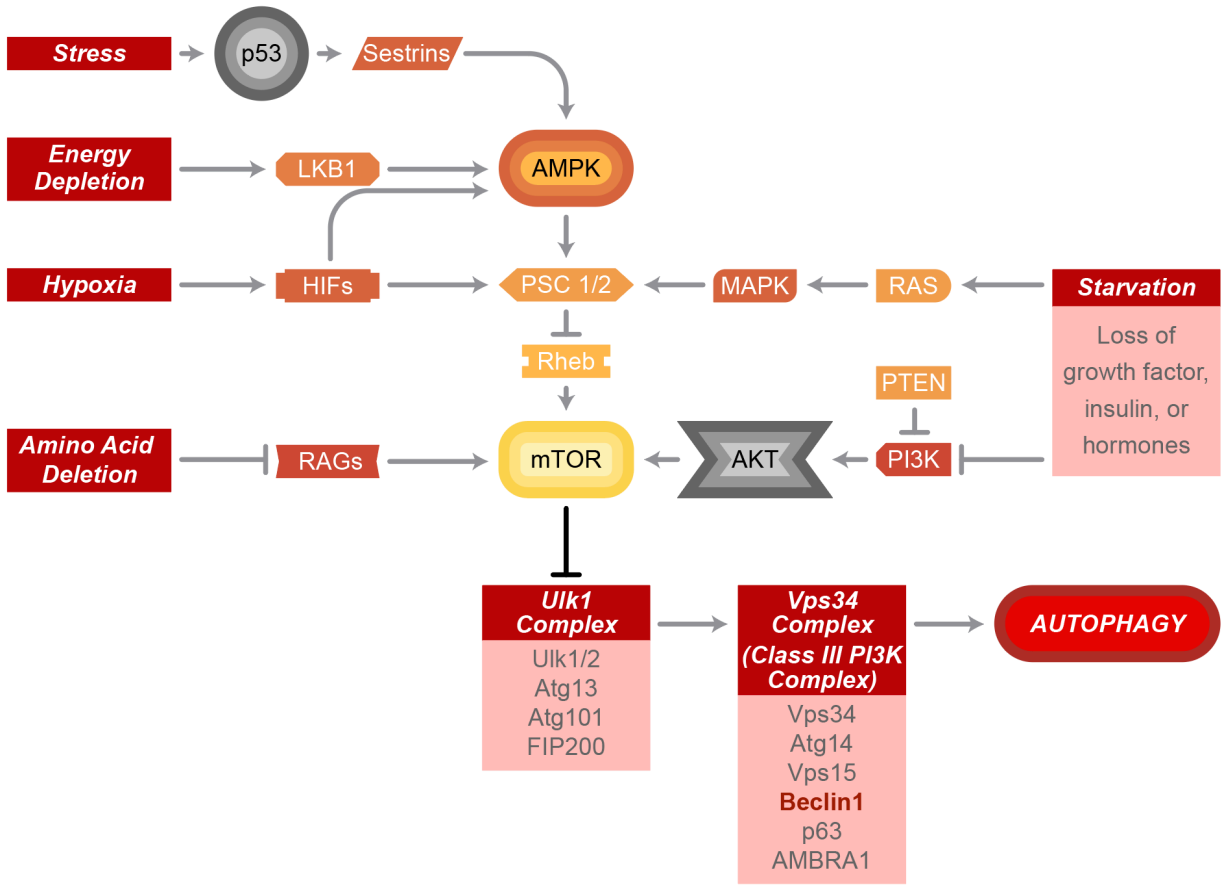
Stress
p53
Sestrins
Energy Depletion
LKB1
AMPK
Hypoxia
HIFs
PSC 1/2
MAPK
RAS
Starvation
Loss of growth factor, insulin, or hormones
Rheb
PTEN
Amino Acid Deletion
RAGs
mTOR
AKT
PI3K
Ulk1 Complex
Ulk1/2
Atg13
Atg101
FIP200
Vps34 Complex (Class III PI3K Complex)
Vps34
Atg14
Vps15
Beclin1
p63
AMBRA1
AUTOPHAGY

Figure 1.2 Cellular stress-induced autophagy

Autophagy induction can be mediated by the AMPK-mTOR pathway in response to various cellular stresses, such as starvation, hypoxia, amino acid depletion, energy depletion and stress. Once mTOR has been inhibited, the downstream Ulk1 and Vps34 complex will be activated and then further initiate autophagy maturation.

Figure 1.3

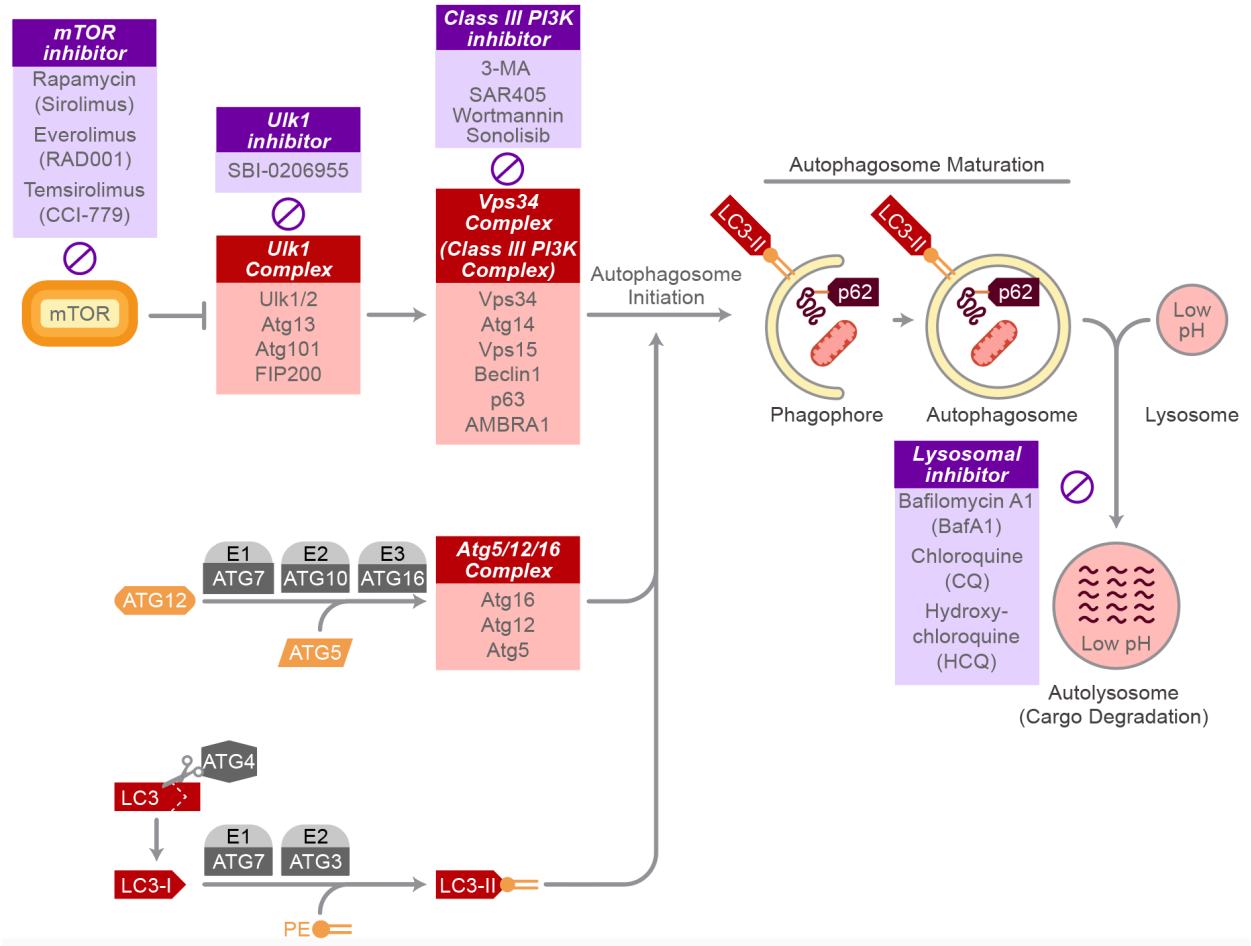
mTOR inhibitor
Rapamycin (Sirolimus)
Everolimus (RAD001)
Temsirolimus (CCI-779)
mTOR
Ulk1 inhibitor
SBI-0206955
Ulk1 Complex
Ulk1/2
Atg13
Atg101
FIP200
Class III PI3K inhibitor
3-MA
SAR405
Wortmannin
Sonolisib
Vps34 Complex (Class III PI3K Complex)
Vps34
Atg14
Vps15
Beclin1
p63
AMBRA1
Autophagosome Initiation
Autophagosome Maturation
LC3-II
p62
Phagophore
Autophagosome
Low pH
Lysosome
Lysosomal inhibitor
Bafilomycin A1 (BafA1)
Chloroquine (CQ)
Hydroxy-chloroquine (HCQ)
Low pH
Autolysosome (Cargo Degradation)
E1 ATG7
E2 ATG10
E3 ATG16
ATG12
ATG5
Atg5/12/16 Complex
Atg16
Atg12
Atg5
ATG4
LC3
LC3-I
E1 ATG7
E2 ATG3
PE
LC3-II

Figure 1.3 Signaling pathway of autophagy and autophagy inhibitors
Activated Vps34 complex cooperates with the Atg5/12/16 complex and LC3II to maturate autophagosomes. Damaged proteins or organelles labeled with p62 are engulfed in autophagosomes and ultimately fuse with lysosomes for degradation or recycling. Several inhibitors have been developed (purple boxes) to suppress autophagy at different steps.

Figure 1.4

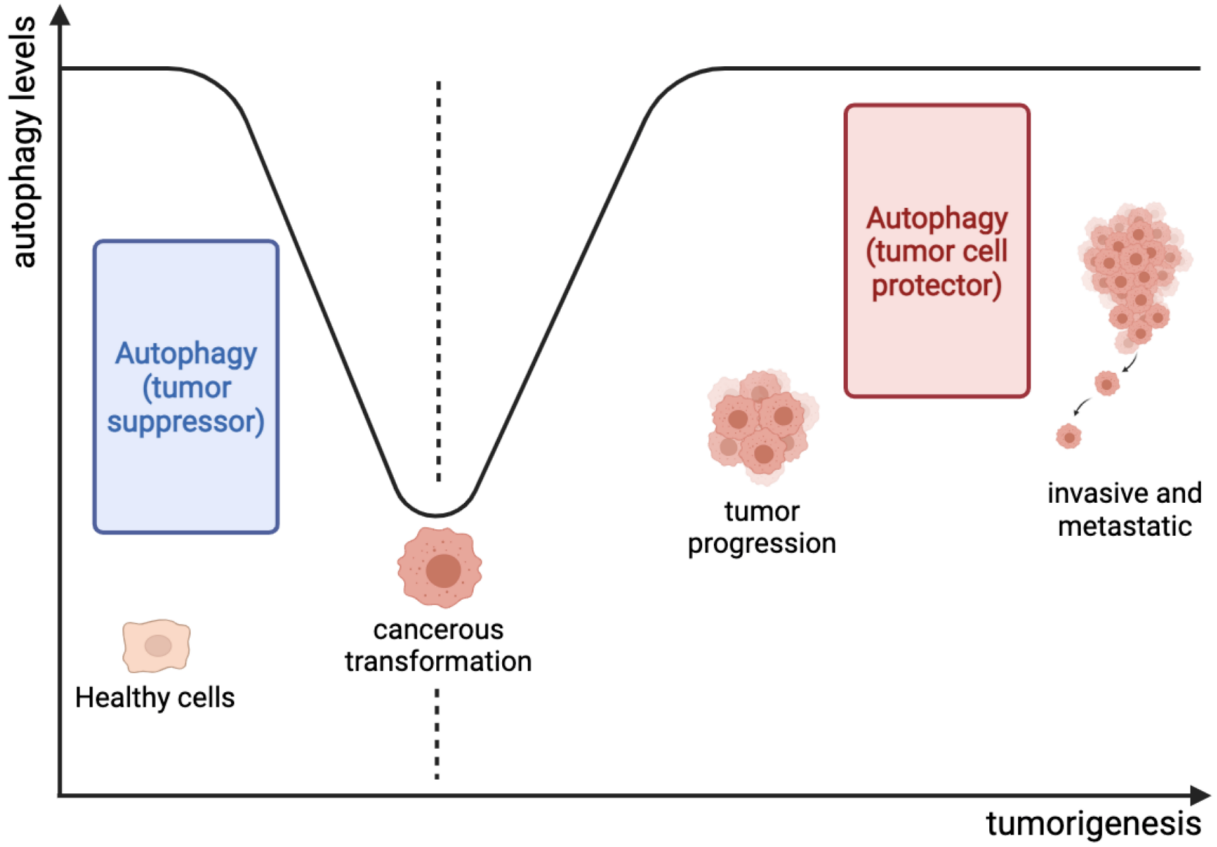
autophagy levels
Autophagy (tumor suppressor)
Autophagy (tumor cell protector)
Healthy cells
cancerous transformation
tumor progression
invasive and metastatic
tumorigenesis

Figure 1.4 The role of autophagy in tumorigenesis

Autophagy acts to protect healthy cells from malignant transformation. Once the malignancy has been established, the loss of autophagy has been proposed as a biomarker for the initiation of early-stage cancers. As tumors progress, autophagy becomes a cellular protector to help cancer grow and survive in a resource-limited microenvironment.

Chapter 2

Autophagy status in HNSCC with diverse malignancies

Preface

This chapter pertains to a series of experiments focused on determining the autophagy status in HNSCC with different malignant stages. To characterize autophagy in HNSCC, it is required to assess autophagy activation and autophagy flux using different biotechniques. In addition to the traditional methods for autophagy flux measurement, we developed an imaging cytometry based high throughput method to assess autophagy flux *in vitro*; this enabled us to quickly examine the cellular autophagy levels in response to different treatments. We have submitted our manuscript describing the high throughput autophagy screening for publication as a novel method and it is under review at the time of this writing. Therapy resistant cell lines (UM-SCC1-C5, cetuximab resistant cells; MOC2, radiation resistant cells) were also used to determine the autophagy status in tumor progression. Patient-derived xenograft (PDX) tissues and tissue microarray (TMA) database enabled us to analyze autophagy status in a pre-clinical and clinical setting.

2.1 Abstract

Autophagy is considered not only a mechanism of cell protection due to its ability to mitigate cell stresses and recycle metabolic precursors, but also as a driver of cell death in autophagy deficient cells or through excessive destruction of cellular components [104]. This paradoxical feature is highly associated with tumor formation in different stages [105]. We hypothesize that autophagy assists HNSCC to build the resistance in response to varied therapeutical methods; this highlights the need for the assessment of autophagy status in HNSCC in different conditions (i.e., resistant cells vs. sensitive cells). However, assessing autophagy changes in the microenvironment of progressing tumors may be a challenge due to the complex of the autophagy regulatory pathway. In this chapter, we measured autophagy activation and autophagy flux using several techniques, providing the objective evidence to observe the bona fide autophagy status. In addition, we also displayed a high throughput method to measure autophagy flux while screening the effectiveness of several autophagy inhibitors. This fast and reliable system is based on the imaging cytometry and acridine orange staining for autophagosomes.

We established our own patient-derived xenograft (PDX) library to unveil the LC3B expressions, an autophagy marker, in different PDX tissues derived from patients with certain therapeutic resistance. Lastly, our group collaborated with the TRIP lab at UW-Madison to analyze the tissue microarray (TMA) database for 107 HNSCC patients, and the pre-clinical evidence showed the positive correlation between autophagy and clinic patients, implying the predictive and prognostic features of autophagy for HNSCC.

2.2 Introduction

Autophagy is one of major conserved cellular mechanisms in response to cellular

stresses including tumorigenesis and cancer chemotherapy. Constructive autophagy may protect cancer cells from therapy-induced cellular stress, leading to therapeutic resistance and refractory cancer [106]. Therapeutic resistance accounts for a major cause of chemotherapy failure. Recent evidence has indicated that autophagy pathways are involved in the development of certain anticancer drug resistance [107]. Although several studies have explored approaches of managing the drug resistance using autophagy modulators [108], the underlying mechanisms between autophagy and therapeutic resistance have not been fully disclosed, indicating the unmet need for the further study.

To investigate the autophagy status within treatment resistant cells, we thankfully obtained the cetuximab resistant HNSCC cell, UM-SCC1-C5, from Dr. Deric Wheeler. UM-SCC1-C5 is a subclone cell line derived from its parental cell UM-SCC1 (University of Michigan Squamous Cell Carcinoma). [109]. For the radiation sensitive (MOC1) and resistant cell line (MOC2), they were established using syngeneic C57BL/6 (B6) mouse OSCC cell lines and were kindly provided by Dr. Ravi Uppaluri (Dana-Farber Cancer Institute). Patient-derived xenograft tissues with different malignant stages of tumor were established in our group and supported by Wisconsin Head and Neck Cancer SPORE. HNSCC tissue microarray database was a resource to enable us to not only investigate the autophagy status across a large cohort of patients but also to examine the potential role of autophagy as a prognostic marker.

Autophagy assessment can be categorized into two different approaches: 1) direct observation of autophagy-related structures and their fate; and 2) quantification of autolysosome-dependent degradation of proteins [110, 111]. TEM is a conventional method to observe the double-membraned structures of autophagosomes. On the other

hand, antibody-based techniques – immunofluorescence (IF), immunoblot and flow cytometry – rely on autolysosome formation to detect LC3-II degradation, and therefore inhibitors of autolysosome formation such as Bafilomycin A1 (Baf) are used to accumulate LC3-II for a set amount of time to study autophagic flux [112, 113]. Another method to assess autophagy is measuring changes in autolysosome levels. Autolysosome levels can be altered by autophagy induction and the efficiency of autolysosome formation resulted from the fusion of autophagosomes and lysosomes, indicating the importance of late-stage autophagy. Completion of late-stage autophagy can be used to represent the completion of autophagy but not the initiation of autophagy [112, 114]. We developed an imaging cytometry-based methodology, which combines the technique of acridine orange staining. Acridine orange is a fluorophore that accumulates in a protonated form inside acidic vesicular organelles such as autolysosomes. At high concentrations, acridine orange dimerizes, causing a metachromatic shift from green to red, which can be measured for studying late-stage autophagy [115].

In this chapter, we assessed autophagy status in varied types of sources ranged from resistant cell lines, PDX tissues to patients. These data led to a conclusion that more active autophagy occurred in resistant, malignant, and recurrent HNSCC tumor tissues.

2.3 Materials and methods

2.3.1 Cell lines and cetuximab treatment

Human head and neck cancer cell lines (HPV-positive: UM-SCC47, and HPV-negative: A253, UM-SCC1) were obtained from the UW Head and Neck SPORE cell line repository. Cetuximab resistant cell lines, UM-SCC1-C5, -C8, and -C11 derived from UM-SCC1, were kindly obtained from Dr. Deric Wheeler. Syngeneic C57BL/6 (B6) mouse

OSCC cell lines, MOC1 and MOC2, were kindly provided by Dr. Ravi Uppaluri (Dana-Farber Cancer Institute). All cells were cultured at low passage in standard conditions (at 37 °C in 5% CO2). All human HNSCC cells were cultured in Dulbecco's modified Eagle's Medium (DMEM) (Corning Inc.) supplemented with 10% fetal bovine serum, 1% penicillin/streptomycin, L-glutamine, 4.5g/L glucose, and sodium pyruvate. Mouse cell lines (MOC1 and MOC2) were maintained in modified DMEM medium/F12 at a 2:1 mixture with 5% fetal bovine serum, 1% penicillin/streptomycin, 1% amphotericin, 5ng/mL epidermal growth factor (EGF), 400 ng/mL hydrocortisone, and 5mg/mL insulin. Cetuximab, provided by Erbitux, was stored at 4^{o}C.

2.3.2 Immunoblot analysis

Cells were harvested and washed with PBS before freezing at -80°C. Cells were lysed with RIPA buffer supplemented 1% (v/v) with phosphatase/protease inhibitor cocktail (Cell Signaling Technologies, #5872) and sonicated. Equal amounts of protein were analyzed by SDS-PAGE, transferred to polyvinylidene diflouride membranes, and probed with specific primary antibodies overnight at 4°C. Targets were detected with NIR-conjugated anti-mouse and anti-rabbit secondary antibodies (LiCOR) and imaged on a LiCOR Odyssey FC. Specific antibodies and sources are listed in Table 1. For autophagy flux analysis, after certain drug treatments, cells were treated with or without 100nM bafilomycin A1 four hours prior to cell lysis. Protein samples were probed with LC3B primary antibody and were quantified for each sample to obtain LC3 number A (sample without Baf) and LC3 number B (sample with Baf). Subtract A from B and you have the number for autophagy flux.

2.3.3 Irradiation

Cells were irradiated with an Xstrahl X-ray System, Model RS225 (Xstrahl, UK) at a dose rate of 3.27 Gy/minute at 30 cm FSD, tube voltage of 195 kV, current of 10 mA and filtration with 3 mm Al. Animals were irradiated with an X-RAD320 (Precision X-Ray, North Branford, CT) with 1 Gy/minute delivered at 320 kV/12.5 mA at 50 cm FSD with a beam hardening filter with half-value layer of 4 mm Cu. The delivered dose rate was confirmed by ionization chamber. Mice were shielded with custom-built lead jigs to limit radiation exposure to the rear quarter of the body.

2.3.4 LC3B puncta immunofluorescence (IF) staining

Cells were plated in 8-well chamber slides at densities ranging from 10,000 to 30,000 cells/well depending on cell type size and growth rate. Twenty-four hours post-plating cells were treated with DMSO control, 100nM CTX, or irradiated with 8 Gy and incubated at 37 °C in 5% CO2 for 36 hours. 100nM bafilomycin A1 (Baf) was added to cells 4 hours prior to fixing cells with 100% methanol in PBS at indicated time points. Cells were permeabilized with 0.1% Triton-X 100 in TBST for 15 minutes, blocked with goat serum for 1 hour at 25°C, and incubated with anti-LC3B primary antibody overnight at 4°C (Table 1). Cells were then probed with Alexa Fluor 555 conjugated secondary antibody (CST #4413) for 1 hour at 25°C in the dark, and cover-slipped with Fluoromount containing DAPI. The next day, they were imaged at 60x magnification using a Nikon A1RS inverted point scanning confocal microscope system.

2.3.5 Imaging cytometry-based autophagy flux assay

Cells were cultured in black-wall, clear-bottom 96-well plates. Cells were treated

with and without 100nM Baf, 100nM for 24 hours. For the image-cytometer based acridine orange (AO) assay, 24 hours post-treatment, 96-well plates were washed three times (100µL/well) with 1xPBS. 50µL of 1µg/ml AO was added to each well and the plates were incubated at room temperature for 30 minutes. Cells were then washed two times (100µL/well) with 1X PBS. 50µL of 1X PBS was added per well, and then the plates were read on the SpectraMax i3 Multi-Mode Microplate Reader Platform with MiniMax 300 Imaging Cytometer (Molecular Devices, Sunnyvale, CA) using the SoftMax Pro software (v6.4). The monochromator and MiniMax settings were used on the software. The monochromator setting was used to measure excitation/emission wavelengths of 500/526 (green) to assess intensity of unprotonated, diffuse AO staining DNA (non-autophagic staining), and 460/650 (red) to assess intensity of dimerized, protonated AO concentrated in acidic vesicular organelles (autophagic staining) [115]. The MiniMax setting was used to count the number of cells per well as we have previously described [116]. The red intensity signal per well was divided by the green intensity or the cell count to assess the level of autophagy and to assess the efficacy of the two normalization methods: controlling to green intensity as recommended by Thome et al. vs. controlling to cell count as previously done by Fowler et al. [115, 116].

2.3.6 Autophagy LC3 HiBiT reporter assay

The autophagy LC3 HiBiT reporter vector (Promega) contains a HiBiT tag and a sequence encoding the MAP1LC3B gene. LC3 reporter proteins are trapped in autophagosomes and degraded upon autophagy flux. HEK293-LC3 and U2O2-LC3 were obtained from Promega. HNSCC A253 cells were transduced with the lentiviral packaged autophagy LC3 HiBiT reporter vector and selected with G418 for 2 weeks to obtain the

A253-LC3 stable cell line. Thereafter, reporter cells were plated in white 96-well plates and treated with 100nM CTX or 8Gy irradiation as indicated time point. Then, 100 µL of Nano-Glo HiBiT lytic reagent (Promega) was added to each well and the samples were mixed using an orbital shaker for 10 min. Luminiscence was measured on a SpectraMax i3 Multi-Mode Microplate Reader Platform.

2.3.7 In vivo immunohistochemistry (IHC)

5 µm sections from formalin fixed paraffin embedded samples were deparaffinized with xylene and hydrated through graded solutions of ethanol. Antigen retrieval was conducted in sodium citrate retrieval buffer (pH 6.0) followed by washing in running water. Slides were washed in PBS and then incubated with 0.3% hydrogen peroxide solution. Blocking was carried out using 10% goat serum in PBS and then incubated with the primary antibody diluted in 1% goat serum in PBS containing 0.1% Triton X-100 overnight at 4°C. Slides were washed with PBS next day; secondary antibody was used (SignalStain® Boost IHC Detection Reagent HRP Rabbit, CST #8114). Staining was detected using diaminobenzidine (Vector Laboratories, Inc. #SK-4100). The slides were counterstained with 1:10 hematoxylin (Thermo Scientific #TA-125-MH) solution for 2 minutes, then dehydrated in ethanol and xylene solutions and sections were covered with coverslip with Cytoseal (Thermo Scientific #8312–4). Three sections were taken from three independent tumors for each control and experimental condition.

2.3.8 Tissue microarray (TMA)and LC3B immunofluorescence staining

Immunofluorescence (IF) staining for LC3B expression was assessed in 107 patients from the UW Head and Neck SPORE oropharynx tissue microarray treated

between 1989 and 2017. 5 μm formalin-fixed, paraffin-embedded tissue sections arranged in a tumor microarray were probed using LC3B and pan-cytokeratin (PCK) primary antibody. Sections were dehydrated, and coverslipped with Cytoseal XYL (Thermo Fisher Scientific). PCK staining was used to identify tumors and then exclude stromal tissues. Percentages for LC3B and PCK double positive area was assessed using inform software with specific algorithm setting.

2.3.9 Statistical analysis

A two-tailed Student's t test was used to evaluate the differences between two groups. One-way ANOVA, followed by Dunnett's or Holm-Sidak's multiple comparisons test, was used for multiple group comparisons. Data were analyzed with Prism 8 (GraphPad Software). $P < 0.05$ was considered statistically significant. All experiments were repeated at least three times and presented as means ± SEM.

2.4 Results

2.4.1 CTX and RT increase autophagy in HNSCC

To determine whether autophagy is modulated by common treatments for HNSCC, we first examined the autophagy levels in CTX- and RT- treated cells using an LC3B-based reporter assay (LC3B HiBit, Promega). The treatment time point (36 hours) was previously determined in a time-course dependent study (Figure 2.1A). Using a model cell line stabling expressing the LC3 reporter, treatment with either CTX (100nM) or RT (8Gy) increased LC3 flux in U2OS cells 36 hours after treatment (Figure 2.1B). We established a similar HNSCC reporter cell line (A253-LC3B) to test whether CTX and RT increased autophagy in head and neck cancer cells. Again, LC3B flux was increased by

both CTX and RT compared to control treated cells (Figure 2.1C).

2.4.2 CTX- and RT-induced autophagy are seem in both HPV- and + cells

HNSCCs arise in the mucosal lining of the upper aerodigestive tract ranged from the nasal cavity to the esophagus. Infection with high-risk human papillomaviruses (HPVs) has recently been implicated in the pathogenesis of HNSCCs. Statistically, HPV infection is the major cause of 12% of pharyngeal cancer, 3% of oral cancer, and 30–60% of oropharyngeal carcinoma cases [117]. Several studies have shown that patients with HPV-positive (HPV+) oropharyngeal cancer have a significantly improved overall and disease-free survival when compared with HPV-negative (HPV-) oropharyngeal cancer patients [118-122].

To determine the correlation of HPV with treatment-induced autophagy, we measured LC3B flux in untransfected A253 cells (HPV-) and UM-SCC47 (HPV+) using immunoblotting. Cells were treated with either CTX or RT with and without the addition of bafilomycin A1, Baf, to allow the determination of LC3B flux. LC3B flux was increased in A253 cells 36 hours after treatment with CTX or RT (Figure 2.2A). Similar findings were also observed in the HPV+ HNSCC cell line UM-SCC47 (Figure 2.2B). Assessment of LC3B puncta using immunofluorescence staining following either CTX or RT treatment again demonstrated an ability of both treatments to induce autophagy (Figure 2.2C). These findings demonstrate that both CTX and RT induce autophagy in HNSCC cell lines and indicate that autophagy induction by CTX or RT treatment was able to be detected in both HPV- and HPV+ cells.

2.4.3 Higher autophagy existed in treatment resistant HNSCC cells and malignant

tissues

We next shifted to study the effects of autophagy in HNSCC cells and patient-derived xenograft (PDX) tissues that exhibit resistance to standard therapies. We utilized a panel of cells with acquired resistance to CTX originally established by the Wheeler lab [109]. These cells were treated with increasing concentrations of CTX to establish resistant clones. Immunoblotting data showed greater LC3B flux in CTX resistant cell lines (UM-SCC1-C5, -C8, and -C11) when compared to their parental cell line UM-SCC1 (Figure 2.3A). We also demonstrated that these resistant cell lines were able to further activate autophagy by treating them with the mTOR inhibitor PP242 which acts as an autophagy activator (Figure 2.3B). Immunofluorescence staining also demonstrated increased LC3B puncta in CTX resistant cells UM-SCC1-C5 than in parental UM-SCC1 cells (Figure 2.3C). MOC1 and MOC2 are isogenic oral cancer cell lines derived from a murine host [123-125]. Because they do not express human EGFR they are both CTX resistant (data not shown). In accordance with the data obtained from CTX resistant cells, higher LC3B flux was observed in radiation resistant MOC2 cells when compared to the radiation sensitive MOC1 cells (Figure 2.3D). H&E staining for LC3B in patient-derived xenograft (PDX) samples with different drug sensitivities was consistent with our immunoblotting results. Patient tissues with CTX or RT resistance were observed to have higher LC3B levels when compared to the sensitive patient tissue (Figure 2.3E). These findings suggest that autophagy protects HNSCC cells from CTX and RT leading to therapeutic resistance.

There is no straightforward way to assess LC3B flux in fixed patient tissues as LC3B IHC captures only a single moment in time. Despite this limitation, we stained a TMA of 153 HNC patients for LC3B to determine whether we could correlate LC3B

expression with stage at diagnosis (Figure 2.3F). Using a cytokeratin mask to assess only tumor tissue, we quantified the percentage of cancer cells with LC3B expression. Patients diagnosed with stage III or IV tumors had more expression of LC3B than those with stage I or II tumors (18.79% vs 8.16%). Interestingly, when assessing LC3B expression in recurrent tumors we saw no difference based on original stage at diagnosis: recurrent stage I/II (14.30%) vs. recurrent stage III/IV (12.49%). As compared to the LC3B expression rate in the primary tissues with stage I/II (8.16%), all recurrent tumors (R) posed higher LC3B levels. The TMAs suggest an important role for autophagy in tumor progression and recurrent disease.

2.5 Discussion

Depending on the stage (early stage, locally advanced stage, and metastatic stage) and resectability of the tumor, the therapeutic approach to HNSCC patients is usually surgical resection, radiotherapy or chemotherapy or a combination of these three methods. In addition, EGFR targeting monoclonal antibodies (cetuximab, CTX) is commonly combined with standard RT as bioradiotherapy (BRT) to improve the patient response due to the high levels of EGFR observed in HNSCC [126]. Statistically, the 5-year overall survival rate for HNSCC patients with optimal therapy is approximately 50% [127], but patients are associated with 30-40% of locoregional recurrences and 20-30% of distant metastasis (R/MHNSCC, recurrence/metastatic HNSCC) [128]. Therapeutic resistance occurs frequently after long-term anticancer treatment, resulting in refractory cancer and tumor recurrence. This highlights the unmet need for a better understanding of therapeutic resistance and novel approaches to the treatment of these patients.

In this chapter, we describe that autophagy is activated in HNSCC cells treated

with CTX or RT. We saw therapy induced autophagy in both HPV-negative and HPV-positive HNSCC cells but determining the precise role for HPV oncoproteins in this process is beyond the scope of this manuscript. In both acquired and intrinsic resistance models, autophagy was higher than in related sensitive lines. This is consistent with the finding of increased autophagy in patient samples with recurrent as compared to primary tumors and in more advanced stage, compared to early-stage cancers. We readily acknowledge the limitation that LC3B immunohistochemistry in fixed tissues only provides a snapshot and does not permit one to comment on autophagic flux in these tissues. This indicates the need of a clinically straightforward biomarker for autophagy measurement from patients.

However, autophagy can be a double-edged sword for tumors. It may participate in the development of therapeutic resistance and protect cancer cells from anticancer treatment, but overactive autophagy can also kill cancer cells due to the autophagy-induced cell death. Therefore, research on the regulation of autophagy to combat therapeutic resistance is expanding and is becoming increasingly important. In the next chapter, we will focus on the role of autophagy in HNSCC and how autophagy modulation benefits the anticancer effect.

Figure 2.1

A

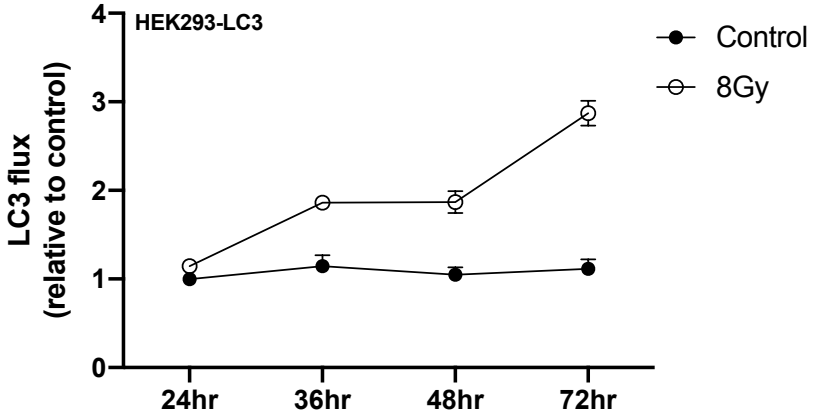

B

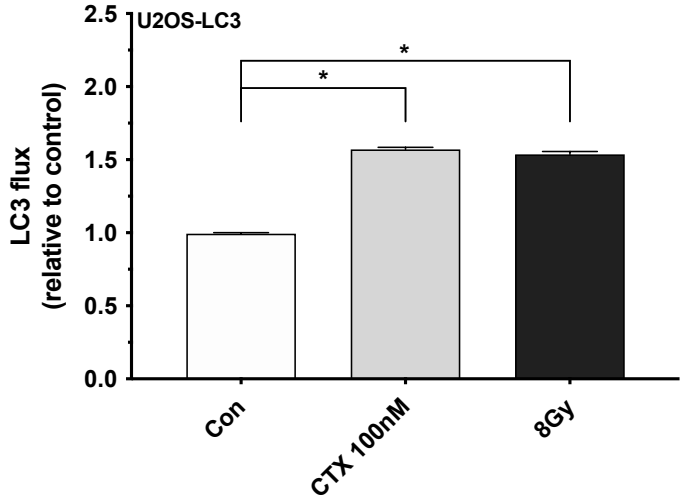

C

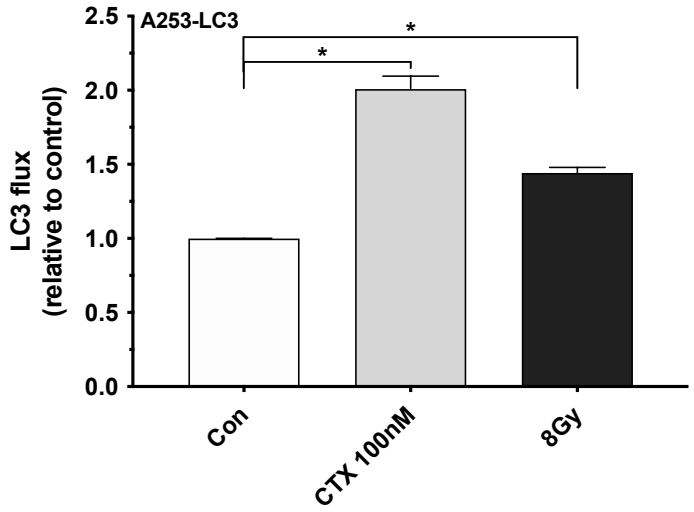

Figure 2.1 Cetuximab (CTX) and radiation (RT) increase autophagy in HNSCC
(A) HEK293-LC3 cells were irradiated with 8Gy for several time points to determine the treatment time for the assessment of autophagy using Progema LC3B HiBit Kit. (B) U2OS-LC3 was treated with 100nM CTX, 8Gy irradiation, or DMSO control for 36 hours to compare the autophagy induction with the control group. (C) Using the HNSCC A253-LC3 stable cell line to confirm the autophagy induction by 100nM CTX and 8Gy irradiation with the same treatment hours (36 hours).

Figure 2.2

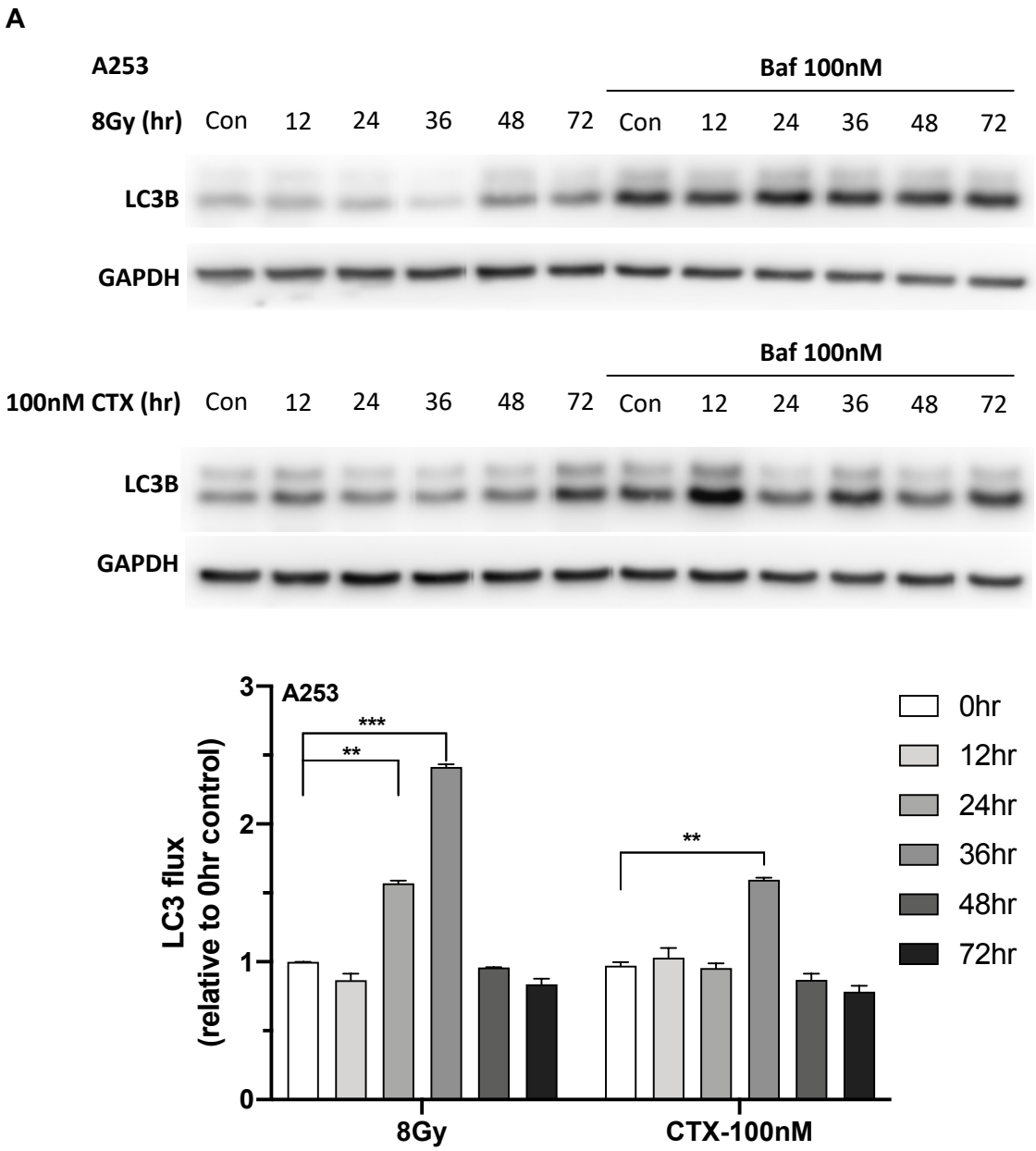
A
A253
Baf 100nM
8Gy (hr) Con 12 24 36 48 72 Con 12 24 36 48 72
LC3B
GAPDH
Baf 100nM
100nM CTX (hr) Con 12 24 36 48 72 Con 12 24 36 48 72
LC3B
GAPDH
A253
LC3 flux
(relative to 0hr control)
0
1
2
3
***
**
**
8Gy
CTX-100nM
0hr
12hr
24hr
36hr
48hr
72hr

Figure 2.2

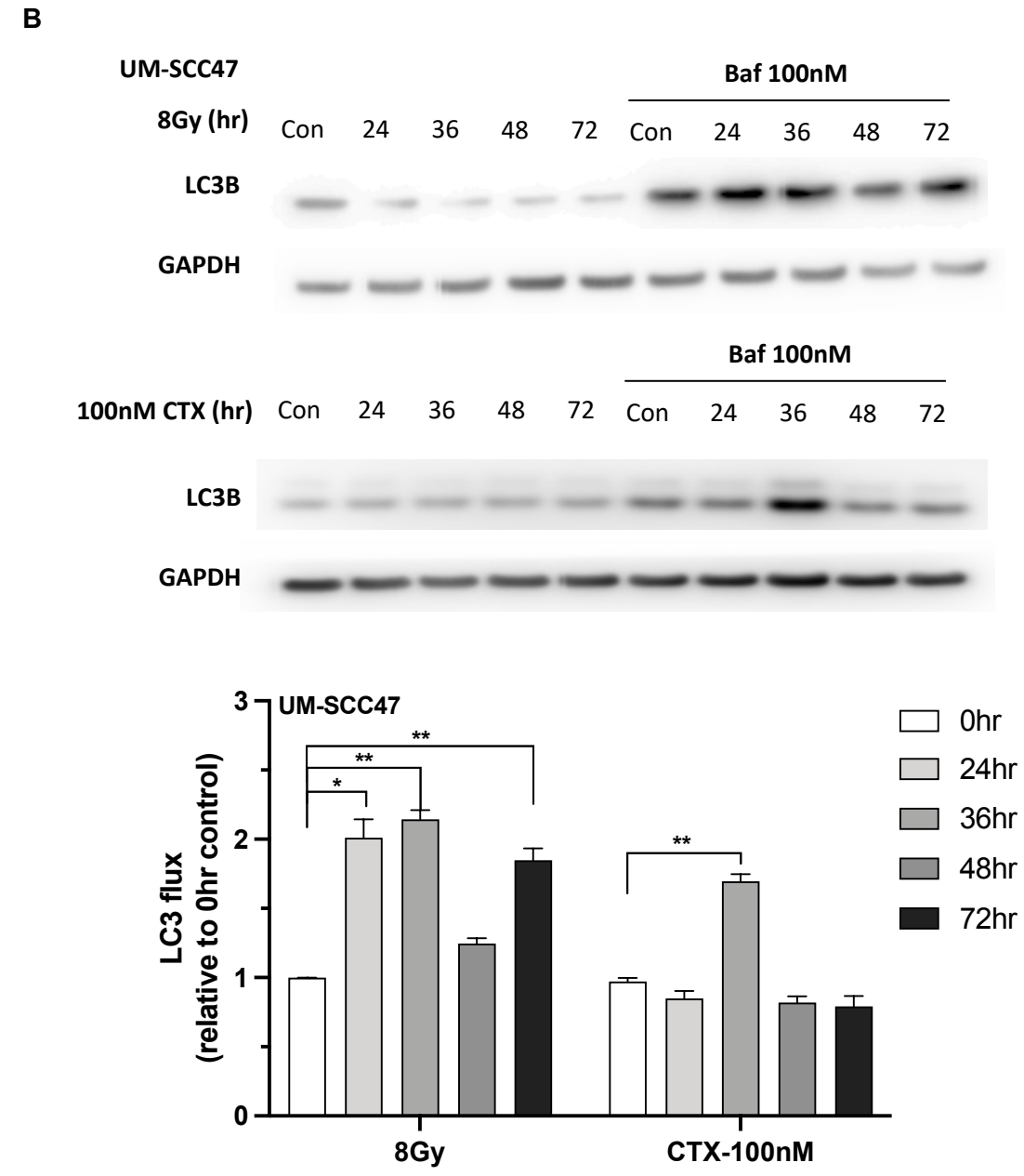
B
UM-SCC47
Baf 100nM
8Gy (hr)
Con 24 36 48 72 Con 24 36 48 72
LC3B
GAPDH
Baf 100nM
100nM CTX (hr)
Con 24 36 48 72 Con 24 36 48 72
LC3B
GAPDH
UM-SCC47
LC3 flux
(relative to 0hr control)
0hr
24hr
36hr
48hr
72hr
8Gy
CTX-100nM

Figure 2.2

C

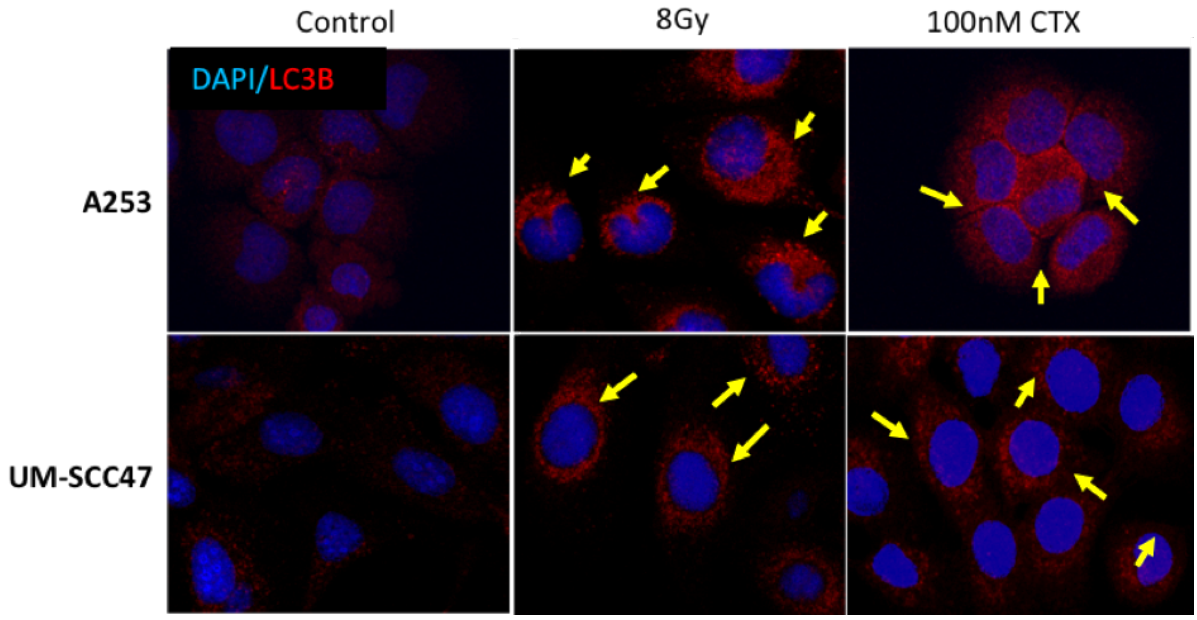

Figure 2.2 Treatment-induced autophagy is independent of HPV status in HNSCC
(A-B) Untransfected A253 cells (HPV-) and UM-SCC47 (HPV+) were treated with 100nM CTX or 8Gy irradiation both with or without 100nM Bafilomycin A1 (Baf) at indicated time points. Autophagy flux was assessed using LC3B immunoblotting for (Baf+ minus Baf-). (C) Cells were treated with 100nM CTX, 8Gy irradiation, or DMSO control for 36v hours. Baf was added to cells 4 hours prior to immunofluorescence staining for LC3 puncta counting.

Figure 2.3

A

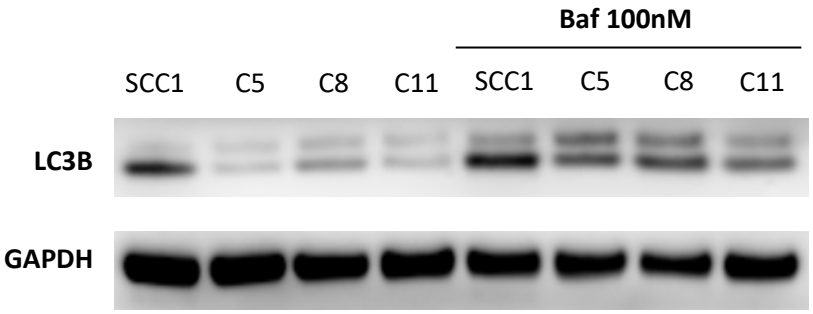
Baf 100nM
SCC1
C5
C8
C11
SCC1
C5
C8
C11
LC3B
GAPDH

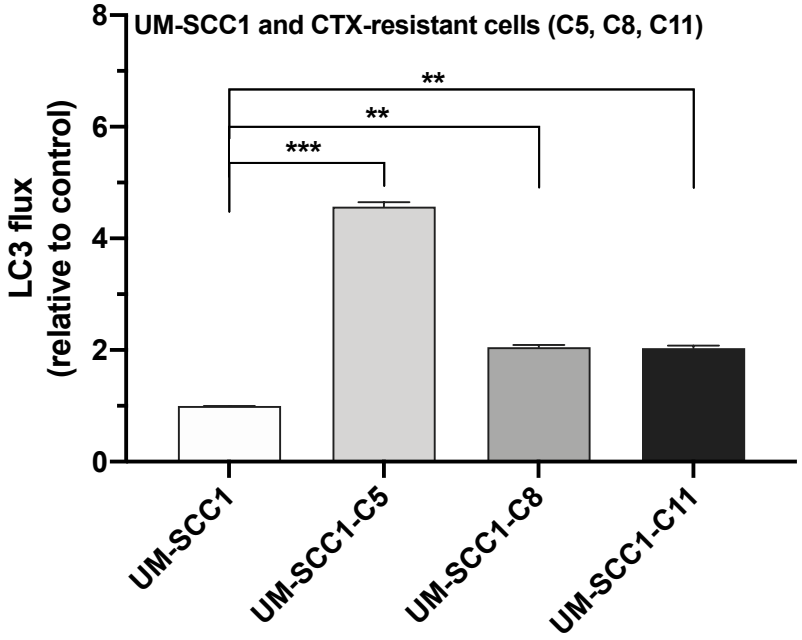
UM-SCC1 and CTX-resistant cells (C5, C8, C11)
LC3 flux
(relative to control)
8
6
4
2
0
**
**
***
UM-SCC1
UM-SCC1-C5
UM-SCC1-C8
UM-SCC1-C11

Figure 2.3

B

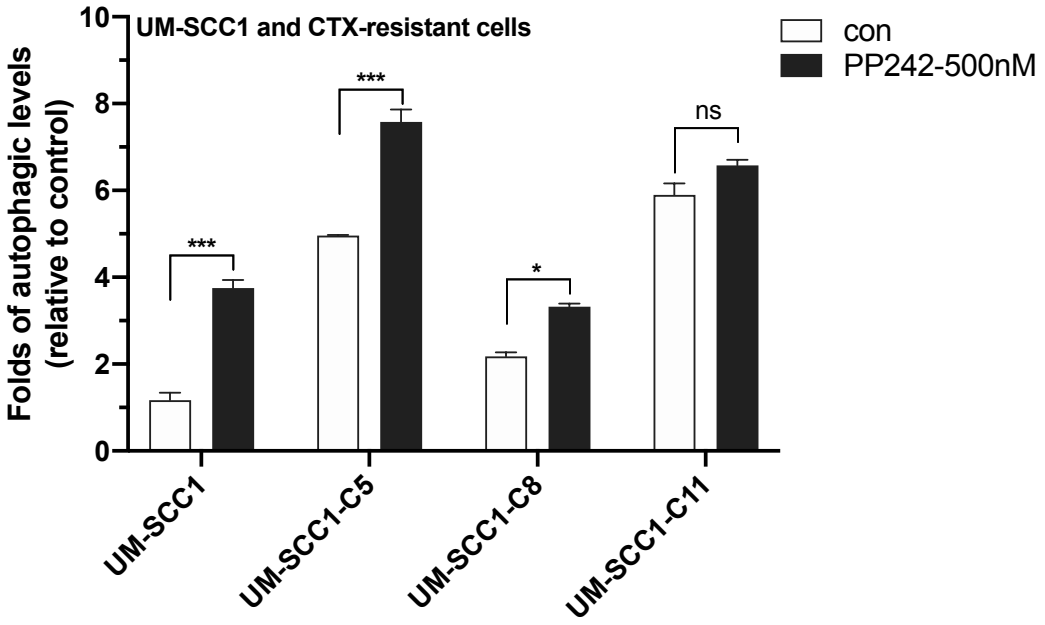
UM-SCC1 and CTX-resistant cells
con
PP242-500nM
Folds of autophagic levels (relative to control)
10
8
6
4
2
0
***
***
*
ns
UM-SCC1
UM-SCC1-C5
UM-SCC1-C8
UM-SCC1-C11

C

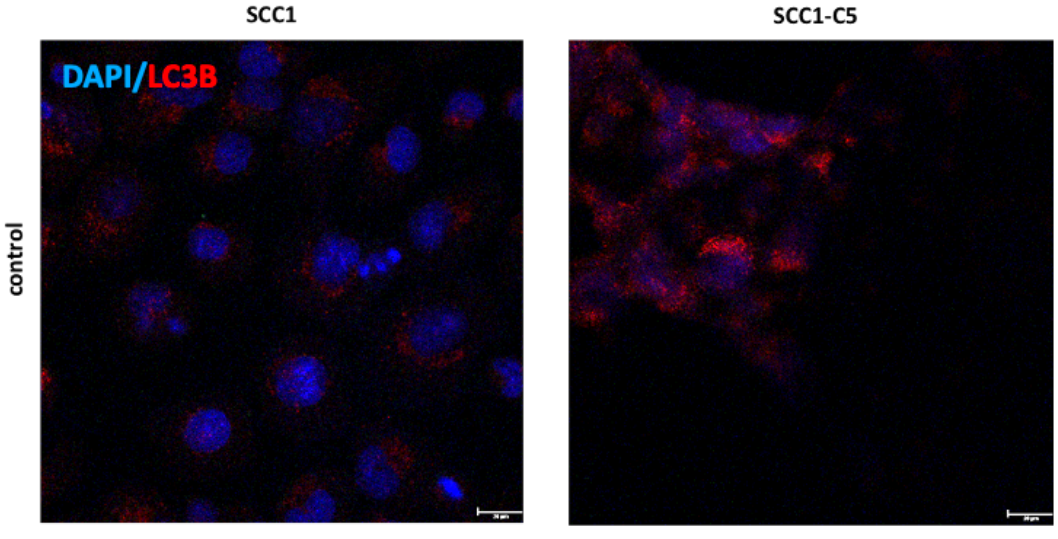
SCC1
SCC1-C5
DAPI/LC3B
control

Figure 2.3

D

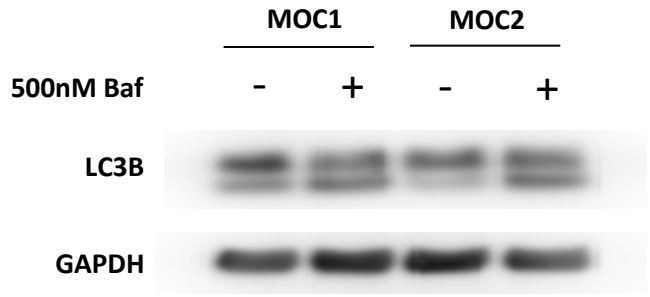
MOC1
MOC2
500nM Baf
-
+
-
+
LC3B
GAPDH

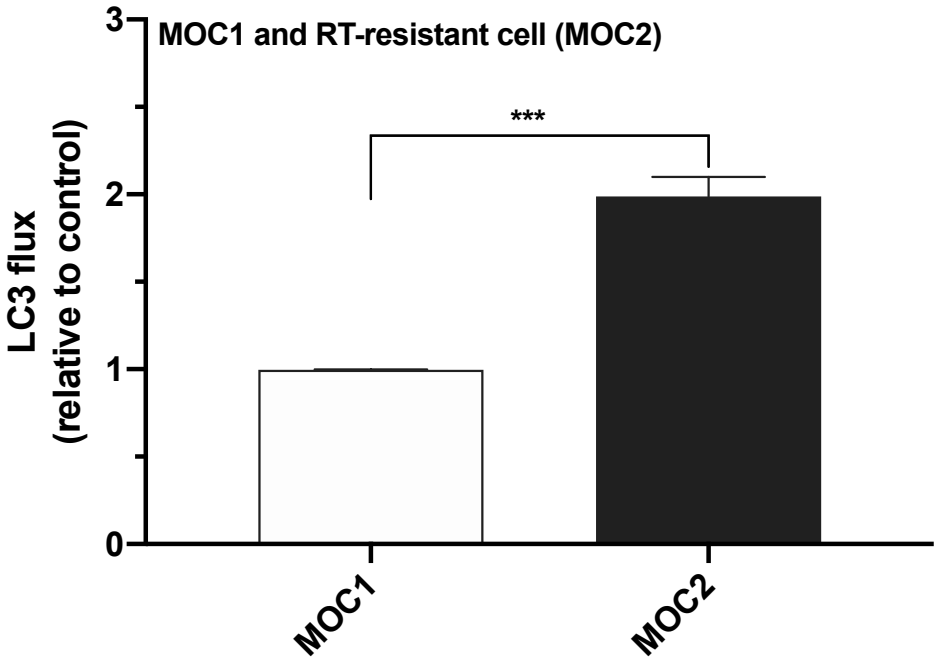
MOC1 and RT-resistant cell (MOC2)
***
LC3 flux
(relative to control)
3
2
1
0
MOC1
MOC2

Figure 2.3

E

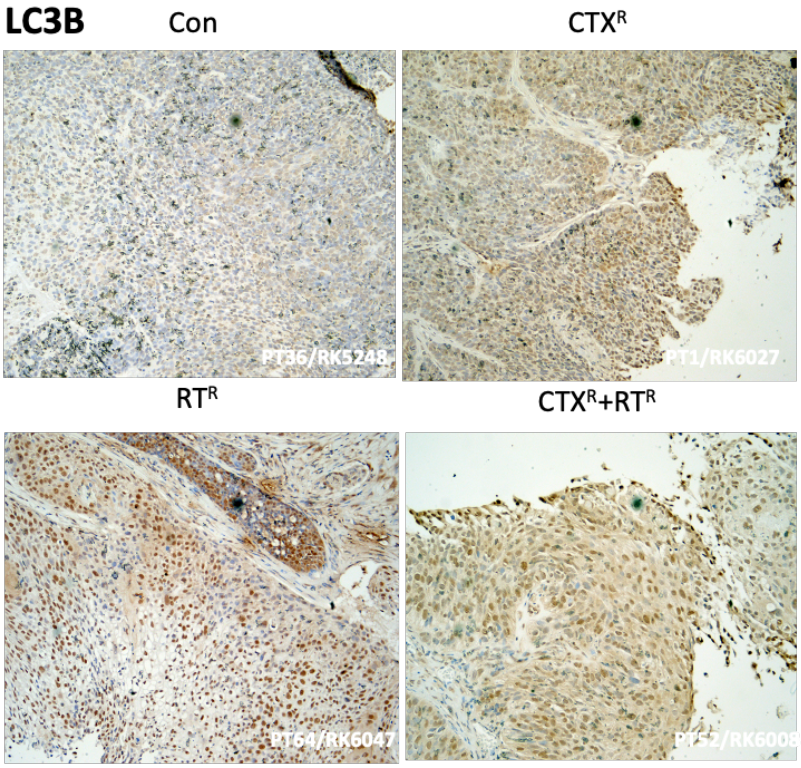

F

	Stage I/II	Stage III/IV
LC3 staining in primary tumor	8.16% (n=21)	18.79% (n=152)

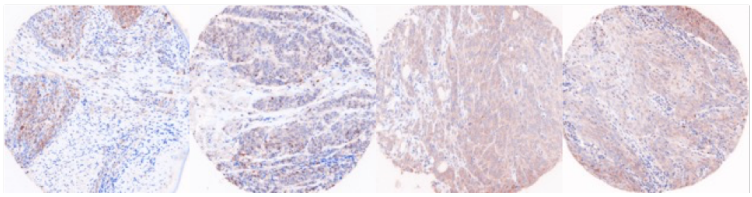

	stage I/II	stage III/IV
Avg LC3 % for primary	8.16%	18.79%
Avg LC3 % for R	14.30%	12.49%

Figure 2.3 Higher autophagy in resistant and more advanced stage HNSCC
(A-C) Cetuximab resistant cell lines (UM-SCC1-C5, C8, and C11) were assessed their basal autophagy flux or activation compared to the parental cell line (UM-SCC1). (A) 100nM Baf was added to cells to determine the autophagy flux using immunoblotting. (B) Acridine orange (AO) was used to quickly screen each cell line and determine autophagy flux in cells. PP242, mTOR inhibitor, were added (500nM, 24 hours) to cells to confirm the cells have the ability for further autophagy induction by another stimulus. (C) LC3 puncta IF staining for the assessment of basal autophagy activation but not flux in CTX-resistant or sensitive cell line. (D) Radiation resistant cell line (MOC2) were assessed its basal autophagy flux compared to the sensitive cell line (MOC1) using immunoblotting analysis. (E) Immunohistochemistry (IHC) staining for the assessment of LC3B status in PDX tissues with different drug sensitivities. (F) The analysis of TMA database across over 107 patients was used to determine the LC3 status in different malignant stage patient tissues. Samples were all stained and imagined by Vectra imaging system. The algorithm was established to calculate the LC3B area detected only in tumor tissues (LC3 and pan-cytokaretin double positive) but not in stromal tissues.

Chapter 3

Characterizing CTX- and RT-induced autophagy in HNSCC

Preface

This chapter presents work conducted over the past three years in the characterization of autophagy in HNSCC. Our group previously assessed autophagy levels across several types of samples and showed higher autophagy in resistant and more advanced stage tissues, however, the certain role of autophagy remains unclear. In this chapter we determine the role of autophagy using autophagy inhibitors including SAR405. SAR405, a Vps34 inhibitor, was administered to HNSCC cells in replacement of chloroquine (CQ) for the autophagy inhibition due to the limited effect of CQ in clinical trials.

3.1 Abstract

Autophagy induction has been associated with tumor progression [97]. However, autophagy may change its role in response to varied microenvironment conditions, leading to more complexity in characterizing autophagy. In this chapter, we determined the cellular protective role of autophagy in HNSCC using clonogenic survival and CCK8 proliferation assays. The addition of SAR405, an autophagy inhibitor, to cetuximab (CTX) or radiation (RT) improved both *in vitro* and *in vivo* tumor control over either treatment alone. Interestingly, SAR405 regulates cell cycle by arresting G1 phase rather than killing cells, although cancer cells ultimately die due to the long-term treatment. Taken together, our findings suggest that inhibition of autophagy can improve the efficacy of anticancer treatments

3.2 Introduction

Based on the dual role of autophagy, cell protector and cell killer, there are several new anticancer drugs developed to modulate autophagy in different fashions: 1) induction, and 2) inhibition. Most autophagy inducers target the mTOR/Akt signaling pathway due to the ability of this pathway to negatively regulate autophagy induction [27]. However, it caught our attention that none of the drugs were originally developed to modulate autophagy in patients. In addition, some off-target effects of autophagy inducer drugs might be attributed to the major regulation of mTOR in cell survival and cell fate. On the other side, several drugs which can block autophagy have also been developed. As of today, the only two autophagy inhibitors remained in clinical trials are chloroquine (CQ) and hydroxychloroquine (HCQ) [9]. CQ and HCQ are being used in over 50 cancer clinical trials (clinicaltrials.gov) [86, 96, 101]. However, initial results from a handful of

studies using these compounds have been underwhelming. The complex role of autophagy in both supporting cancer development and protecting against cellular stress induced by anticancer therapies emphasizes the need to determine the precise role of autophagy in HNSCC and to understand whether and how to combine autophagy modulators with these treatments.

As we described for autophagy inducers, the compounds used clinically were not developed as specific autophagy inhibitors either. Therefore, other specific autophagy modulators have been developed (i.e., SAR405). SAR405 was identified as an inhibitor to target the ATP-binding cleft of phosphatidylinositol 3-kinase, catalytic subunit type 3 (PIK3C3)/Vpas34. Recent study has shown that SAR405 disrupts late endosome and lysosome compartments and interferes LC3B-I to LC3B-II conversion which is a critical step for the initiation of autophagosome formation [129]. Our group herein screened several autophagy inhibitors and selected SAR405 for further study rather than CQ or HCQ.

3.3 Materials and methods

3.3.1 Cell lines and SAR405 preparation

Human HNSCC cell lines (UM-SCC47, A253, UM-SCC1, and UM-SCC1-C5), and syngeneic C57BL/6 (B6) mouse OSCC cell lines (MOC1 and MOC2), were cultured at low passage in standard conditions (at 37 °C in 5% CO2) as previously described. All human HNSCC cells were cultured in Dulbecco's modified Eagle's Medium (DMEM) (Corning Inc.) supplemented with 10% fetal bovine serum, 1% penicillin/streptomycin, L-glutamine, 4.5g/L glucose, and sodium pyruvate. Mouse cell lines (MOC1 and MOC2) were maintained in modified DMEM medium/F12 at a 2:1 mixture with 5% fetal bovine

serum, 1% penicillin/streptomycin, 1% amphotericin, 5ng/mL epidermal growth factor (EGF), 400 ng/mL hydrocortisone, and 5mg/mL insulin. SAR405, provided by Selleckchem (#S7682), was reconstituted in DMSO and stored at -20^{o}C until use.

3.3.2 Clonogenic survival assay

Cells were seeded into 6-well plates at specific densities, incubated overnight, and treated with indicated treatment (100nM CTX, 4Gy, or DMSO control). Once colonies averaged 50 or more cells (7-10 days) in the control wells, plates were fixed and stained with 1% (w/v) crystal violet in methanol, imaged, and colonies of 50 or more cells were counted. Survival bar graphs were generated after normalizing to the amount of cell death in control group.

3.3.3 Proliferation assay

Cells were plated in 96-well plates at densities ranging from 1,000 to 3,000 cells/well according to cell type growth rate. Twenty-four hours post-plating, cells were treated with 100nM CTX, 20μM SAR405, 4Gy irradiation, or DMSO control and incubated for 7 days. Once control wells neared full confluence, Cell Counting Kit-8 (CCK8) reagent was added (Dojindo Molecular Technologies) and absorbance measured at 450 nm on a SpectraMax i3 plate reader (Molecular Devices). The absorbance of treated wells was normalized to control wells.

3.3.4 Cell cycle

Cells were plated in 6cm dishes at densities ranging from 200,000-600,000 cells/well depending on the cell type and growth rate. Twenty-four hours post-plating, cells were treated with 100nM, 8Gy irradiation, 20μM SAR405 or DMSO control, incubated for

36 hours, and trypsinized and collected. Cells were centrifuged at 500 x g for 10 minutes, washed with PBS, pelleted again, and a single cell suspension was created in 0.5 ml PBS. 4.5 ml chilled 70% methanol was added to each tube and cells were stored in 4°C. Twenty-four hours later, cells were centrifuged at 500 x g for 10 minutes, and a single cells suspension was created in 1 ml solution of propidium iodide (Molecular probes # P3566), Triton X-100 (0.1%) (Sigma #T9284), and RNase A (Thermo Scientific #EN0531) in PBS. The samples were analyzed using the Attune NxT flow cytometer (Thermo Scientific), and the cell cycle distribution was calculated using ModFIT software (Verity Software House, Top-sham, ME).

3.3.5 LC3B and Ki67 immunohistochemistry

The expression of LC3B (CST #43566) or Ki67 (CST #9027) was detected in tumor tissue xenograft histologic sections by standard immunohistochemistry (IHC). Briefly, sections were deparaffinized, incubated in Bouins solution for 1 hour at 60ºC, washed in running tap water, and the nuclei stained with Weigert's iron hematoxylin for 15 minutes. Next, the slides were placed in Gomori's trichrome stain and incubated 20 minutes at room temperature. Finally, the tumor sections were rinsed with water, dehydrated, cleared, and cover slipped.

3.3.6 Cell line xenograft growth delay studies

Six to eight-week old female Hsd:athymic Nude-Foxn1nu (Harlan Laboratories) mice were used for growth delay studies. Mice were kept in the Association for Assessment and Accreditation of Laboratory Animal Care-approved Wisconsin Institute for Medical Research Animal Care Facility. Studies were carried out in accordance with

an animal protocol approved by the University of Wisconsin-Madison. A253 cells were grown in vitro, mixed 1:1 with Matrigel, and injected subcutaneously into bilateral flanks of nude mice at 1 x 106 cells/site. Tumor volumes were measured twice weekly with Vernier calipers and calculated according to the relationship $V=$ $\left(\frac{\pi}{6}\right) x\ (large\ diameter)\ x\ (small\ diamter)^{2}$. Once average tumor size reached ~200 mm3, mice were randomized into treatment groups. Vehicle (1% (v/v) DMSO in saline) or 100nM CTX was administered twice per week by intraperitoneal injection. SAR405 (20μM) was administered once daily by intratumoral injection. Radiation was delivered three times per wekk, 2Gy per time. The treatment arm lasted for 14 days. Eight to 10 mice (16-20 tumors) were used per treatment group.

3.3.7 Statistical analysis

A two-tailed Student's t test was used to evaluate the differences between two groups. One-way ANOVA, followed by Dunnett's or Holm-Sidak's multiple comparisons test, was used for multiple group comparisons. Data were analyzed with Prism 8 (GraphPad Software). $P < 0.05$ was considered statistically significant. All experiments were repeated at least three times and presented as means ± SEM.

3.4 Results

3.4.1 Autophagy leads to cell survival in HNSCC

Autophagy has been linked to both cell survival and cell death [33]. We examined LC3B flux using the A253-LC3 reporter cell line to test the effectiveness of several autophagy modulators (Figure 3.1). As expected, treatment with PP242 increased autophagic flux, and with SAR405, Heclin, as well as SBI-0206965 each decreased

autophagic flux. To determine the specific role of autophagy in HNSCC following CTX or RT treatment, we tested cell survival using two different methods: a clonogenic survival assay and a tetrazolium-based cell proliferation assay (CCK-8).

In the HNSCC cell line tested, the autophagy inhibitor SAR405 decreased colony formation (Figure 3.2A) but had relatively modest effects on proliferation (Figure 3.2B). The addition of SAR405 to CTX or RT treatment resulted in a further decrease in colony formation when compared to either CTX or RT alone suggesting that inhibition of autophagy with SAR405 decreases HNSCC cell survival (Figure 3.2A). Interestingly, colony formation with CTX+SAR405 was greater than that with SAR405 alone while RT+SAR405 was less than SAR405 alone suggesting possible divergent mechanisms by which CTX and RT activate autophagy.

The findings from the cell proliferation assay were consistent with our clonogenic results (Figure 3.2B). Again, RT+SAR405 appeared to be more effective than CTX+SAR405 although the difference was less stark in proliferation assays than in colony formation. To better understand the effect of SAR405 on cell proliferation, we investigated how treatment combinations affected cell cycle distribution using flow cytometry (Figure 3.3A). SAR405 arrested cells in the G1 phase. Finally, we assessed the *in vivo* impact of SAR405 on CTX and RT treated tumors. Xenografts of A253 cells were established and treated with control, CTX, or RT each with or without SAR405. Tumors were harvested 72 hours after treatment and formalin fixed, paraffin embedded tissue stained for Ki67, a cell proliferation marker, by immunohistochemistry. SAR405 decreased cell proliferation as measured by Ki67 expression (Figure 3.3B) in control, CTX, and RT treated animals. Taken together, autophagy appears to play a protective role in HNSCC cells treated with

CTX and RT because inhibition of autophagy increases treatment efficacy.

3.4.2 Combining SAR405 with CTX/RT augments the anti-cancer effect in vitro and in vivo

Finally, we investigated whether autophagy inhibition combined with RT or CTX *in vitro* and *in vivo* results in improved tumor control. Inhibition of autophagy with SAR405 significantly decreased colony formation in both CTX sensitive and CTX resistant cells (Figure 3.4A and 3.4B). The radiation sensitive MOC1 cells were sensitized to radiation by SAR405 (Figure 3.4C) whereas MOC2 cells demonstrated no response to radiation and a decrease in survival for the RT+SAR405 cells compared to RT alone suggestive of a compromise in radiation resistance using the autophagy inhibitor (Figure 3.4D).

We next established xenografts of A253 cells and randomized animals to treatment with RT, CTX, SAR405 or combination treatments. SAR405 has little effect alone (Figure 3.5). Combination treatment with RT+SAR405 (Figure 3.5A) or CTX+SAR405 (Figure 3.5B) resulted in modest tumor regression compared to the RT or CTX alone. IHC staining for LC3B demonstrated increased expression of LC3B in CTX and RT treated animals and confirmed that SAR405 inhibits autophagy *in vivo* (Figure 3.6). Taken together, these findings suggest the use of SAR405 or other autophagy inhibitors may have a role in the treatment of HNC to improve the efficacy of CTX or RT.

3.5 Discussion

This chapter we found that autophagy served as a cellular protector against anticancer therapy using several survival assays and *in vivo* mouse studies. In combination with our previous evidence shown in the chapter 2, we can determine that autophagy helps HNSCC against cellular stresses from ominous microenvironment once

malignance developed. However, it is still unclear that how much strength of autophagy and the duration of the autophagy response is involved in support of cell survival and therapeutic resistance. One of the future directions is establishing an adequate model to examine the autophagy strength in the presence of adverse microenvironmental conditions.

According to our clonogenic survival data, we noticed that SAR405 can stably enhance cetuximab and radiation efficacy in drug sensitive cell lines but not in the resistant cell lines when administered combined treatment (SAR+CTX or SAR+RT). When compared to SAR405 alone, combined treatment showed similar anticancer effect with SAR405 itself, suggesting autophagy inhibition can be effective but no synergistic effect with traditional therapy in drug resistant cells. This may result from that traditional therapy is no longer powerful enough to stimulate autophagy in drug resistant cells, highlighting the need to further study the strength of autophagy in response to varied microenvironments. Lastly, SAR405 alone showed limited effect *in vivo* until 12 days post-treatment in mice. This data is in line with the finding from Noman et al. [130] and they showed the high correlation between SAR405 and the regulation of cancer immunity, suggesting another potential role for autophagy in the cancer immune modulation.

Figure 3.1

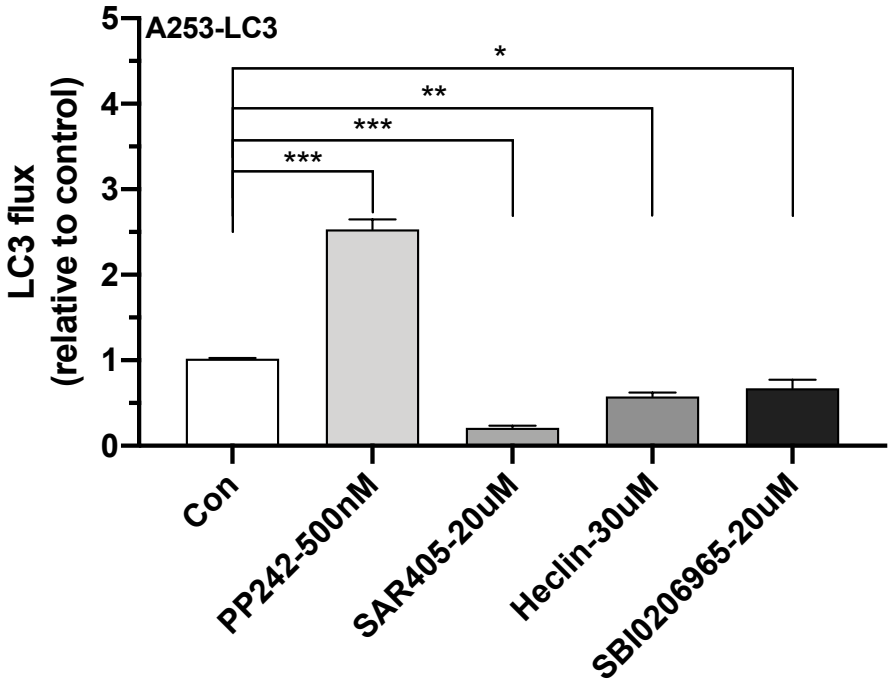
A253-LC3
LC3 flux
(relative to control)
5
4
3
2
1
0
*
**
***
***
Con
PP242-500nM
SAR405-20uM
Heclin-30uM
SBI0206965-20uM

Figure 3.1 Autophagy inhibitors are effective in HNSCC cells

Imaging cytometry-based acridine orange (AO) staining was used to screen the autophagy flux in cells with different drug treatments. All drugs were added to cells for 36 hours. PP242 was used as a positive control to autophagy inhibitors. SAR405, Heclin and SBI-0206965 are autophagy inhibitors and properly show their effectiveness in HNSCC cells.

Figure 3.2

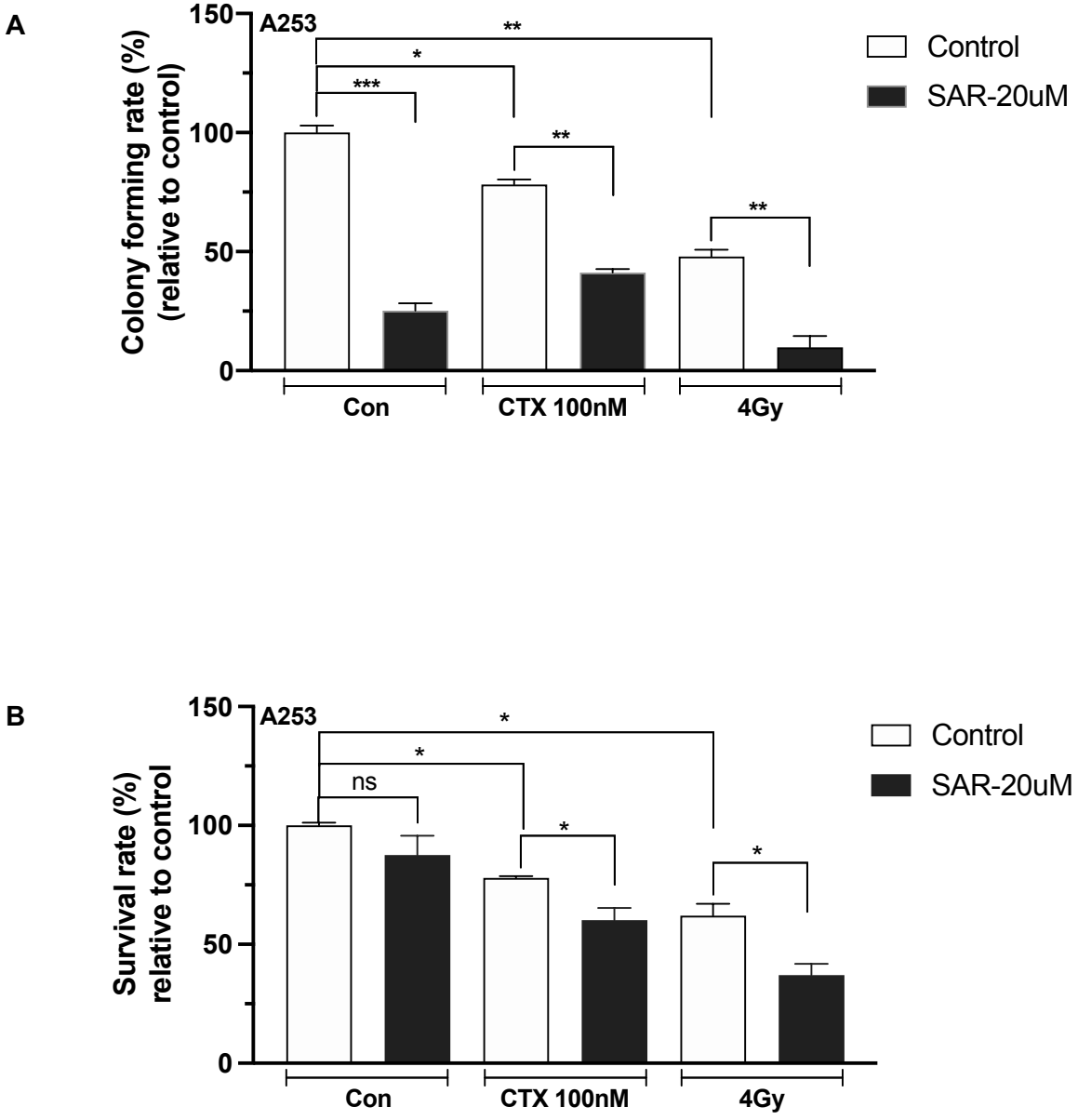
A
A253
Colony forming rate (%)
(relative to control)
150
100
50
0
**
*
***
**
**
Control
SAR-20uM
Con
CTX 100nM
4Gy
B
A253
Survival rate (%)
relative to control
150
100
50
0
*
*
ns
*
*
Control
SAR-20uM
Con
CTX 100nM
4Gy

Figure 3.2 Autophagy serves as a cell protector in HNSCC
(A) A253 cells were treated with 100nM CTX, 4Gy irradiation, or DMSO control for over 7 days, and then stained with crystal violets. Colony numbers were normalized to plate efficiency and untreated control. (B) Cells were treated with indicated drugs for 7 days and CCK-8 reagent was added to determine the cell survival rate. All numbers were normalized to the untreated control.

Figure 3.3

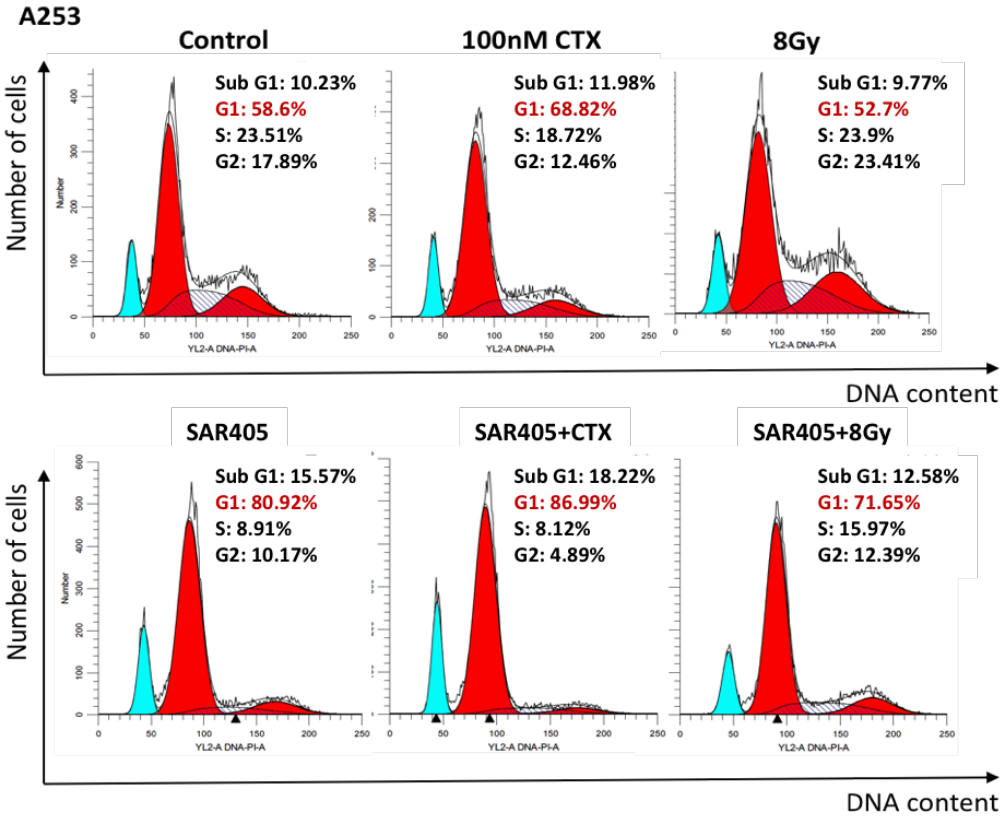
A
A253
Control
100nM CTX
8Gy
Sub G1: 10.23%
G1: 58.6%
S: 23.51%
G2: 17.89%
Sub G1: 11.98%
G1: 68.82%
S: 18.72%
G2: 12.46%
Sub G1: 9.77%
G1: 52.7%
S: 23.9%
G2: 23.41%
Number of cells
DNA content
SAR405
SAR405+CTX
SAR405+8Gy
Sub G1: 15.57%
G1: 80.92%
S: 8.91%
G2: 10.17%
Sub G1: 18.22%
G1: 86.99%
S: 8.12%
G2: 4.89%
Sub G1: 12.58%
G1: 71.65%
S: 15.97%
G2: 12.39%
Number of cells
DNA content

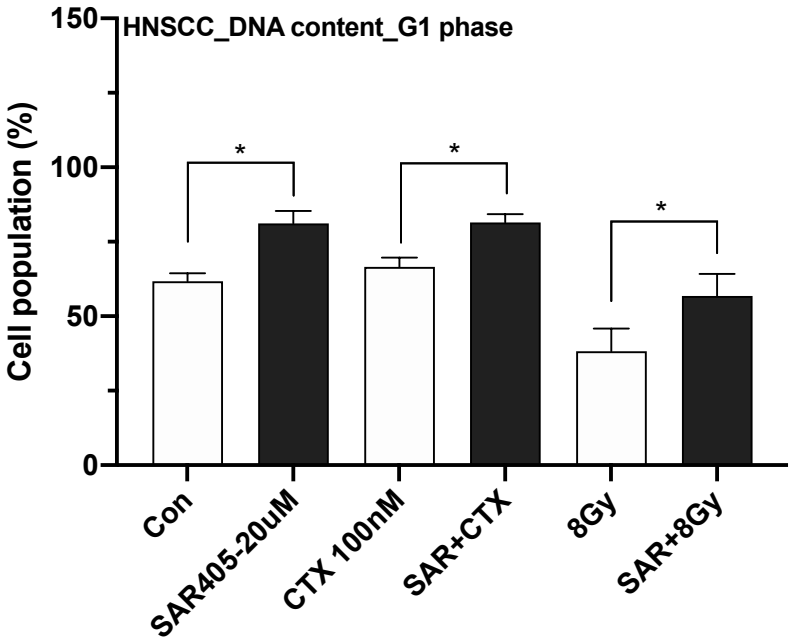
HNSCC_DNA content_G1 phase
Cell population (%)
150
100
50
0
*
*
*
Con
SAR405-20uM
CTX 100nM
SAR+CTX
8Gy
SAR+8Gy

Figure 3.3

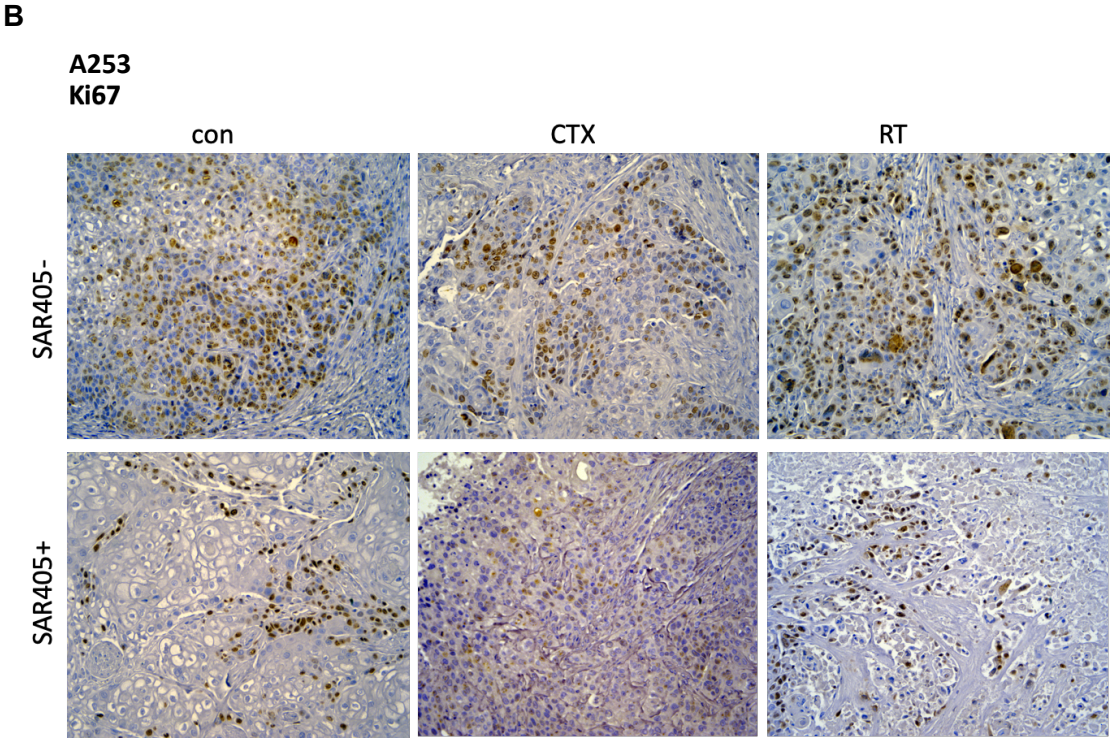

Figure 3.3 SAR405 arrests cell cycle at G1 phase in HNSCC cells
(A) Cells were treated with 100nM CTX, 20μM SAR405, 8Gy, or DMSO control for 36 hours and then collected for the cell cycle analysis using flow cytometry. The population quantified results were based on channel gating and compared to untreated control. (B) A253 cell xenograft tissues were collected 72 hours post-implantation on nude mice. IHC staining for Ki67, a proliferation marker, was used to confirm that SAR405 decreased cell proliferation through cell cycle arresting.

Figure 3.4

A

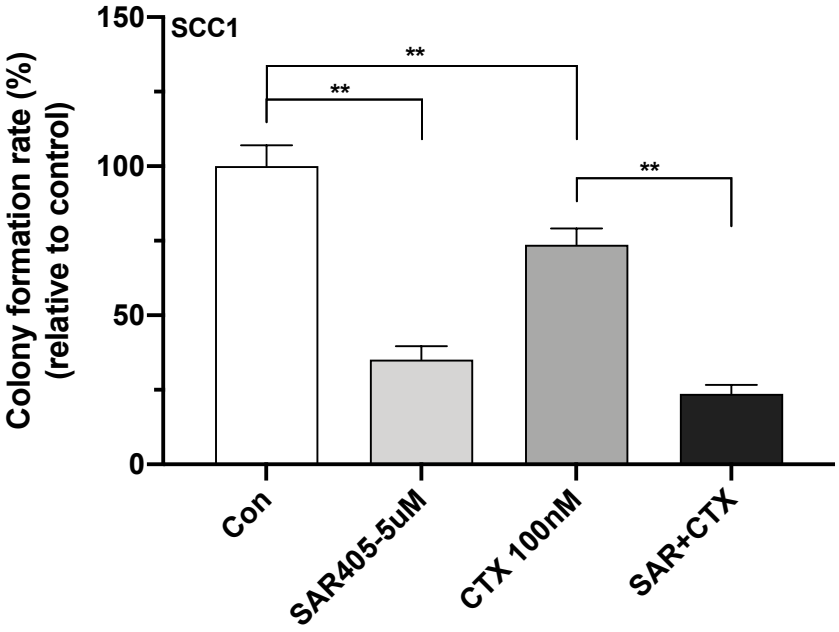
SCC1
Colony formation rate (%)
(relative to control)
150
100
50
0
**
**
**
Con
SAR405-5uM
CTX 100nM
SAR+CTX

B

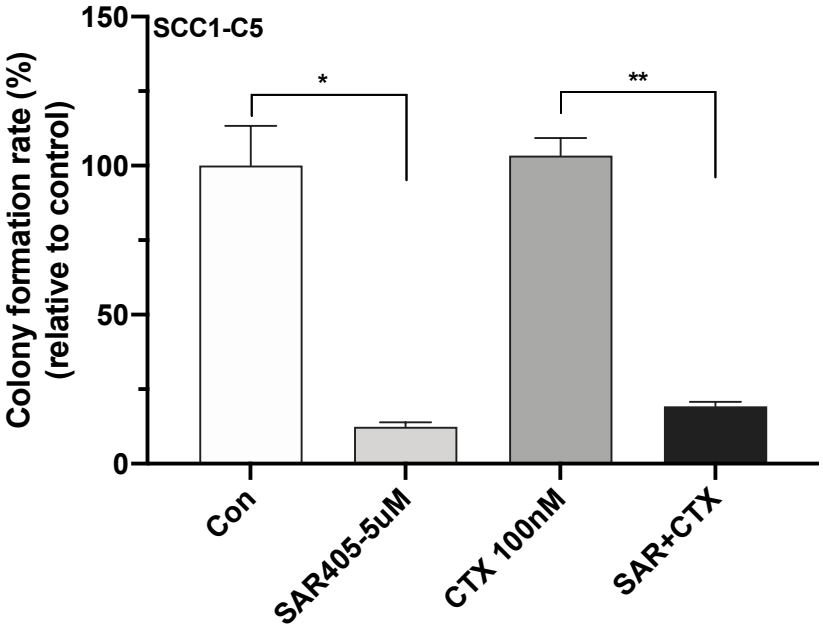
SCC1-C5
Colony formation rate (%)
(relative to control)
150
100
50
0
*
**
Con
SAR405-5uM
CTX 100nM
SAR+CTX

Figure 3.4

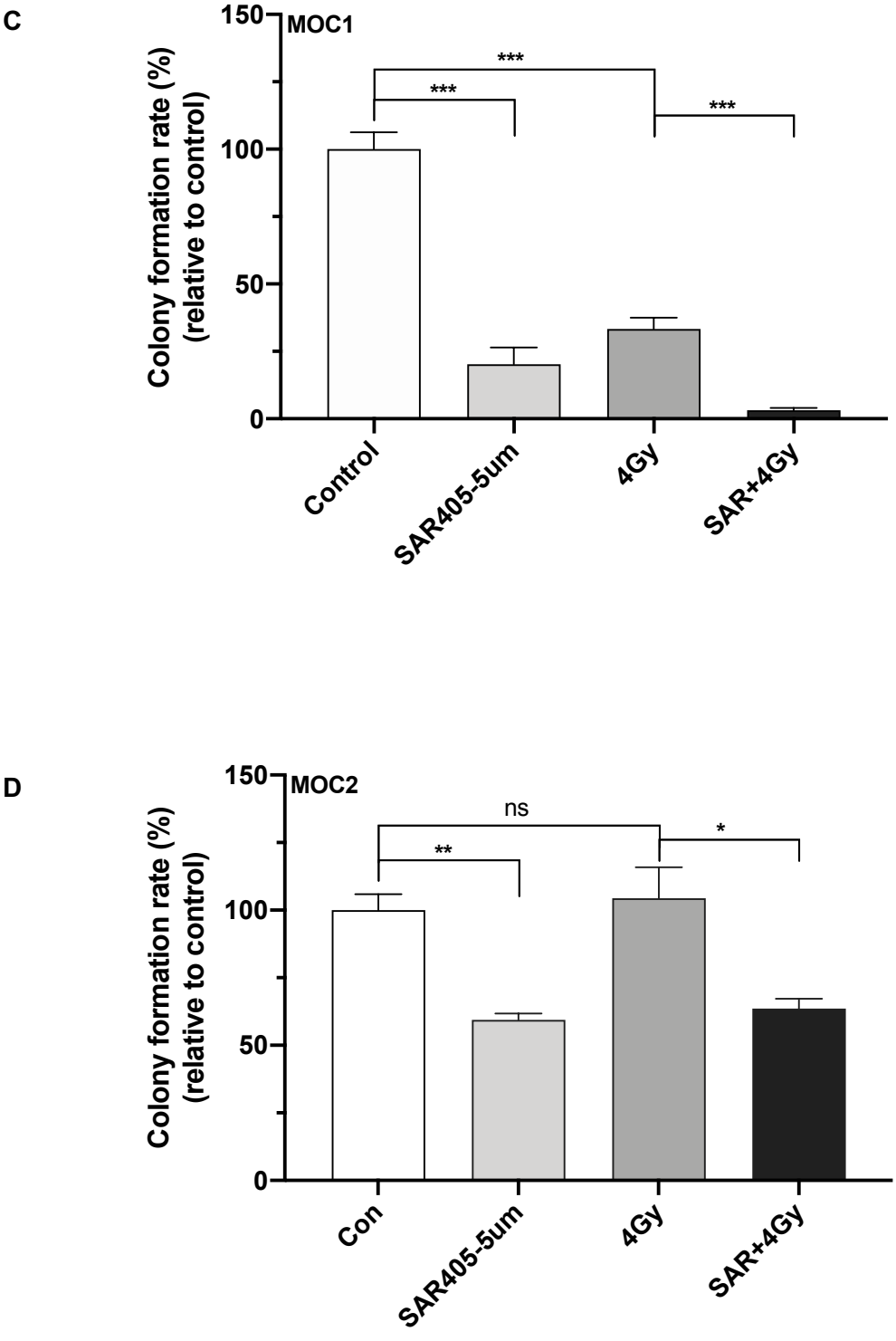
C
MOC1
Colony formation rate (%)
(relative to control)
150
100
50
0
***
***
***
Control
SAR405-5um
4Gy
SAR+4Gy
D
MOC2
Colony formation rate (%)
(relative to control)
150
100
50
0
ns
**
*
Con
SAR405-5um
4Gy
SAR+4Gy

Figure 3.4 Autophagy inhibition improves tumor controls in vitro
(A-B) Cetuximab sensitive (UM-SCC1)/ resistant (UM-SCC1-C5) cells were treated with 100nM CTX, 5μM SAR405, or DMSO control for 7days and then stained with crystal violets. (C-D) Radiation sensitive (MOC1)/ resistant (MOC2) cells were treated with 4Gy, 5μM SAR405, or DMSO control for 7days and then stained with crystal violets. Colony numbers were all normalized to plate efficiency and untreated control.

Figure 3.5

A

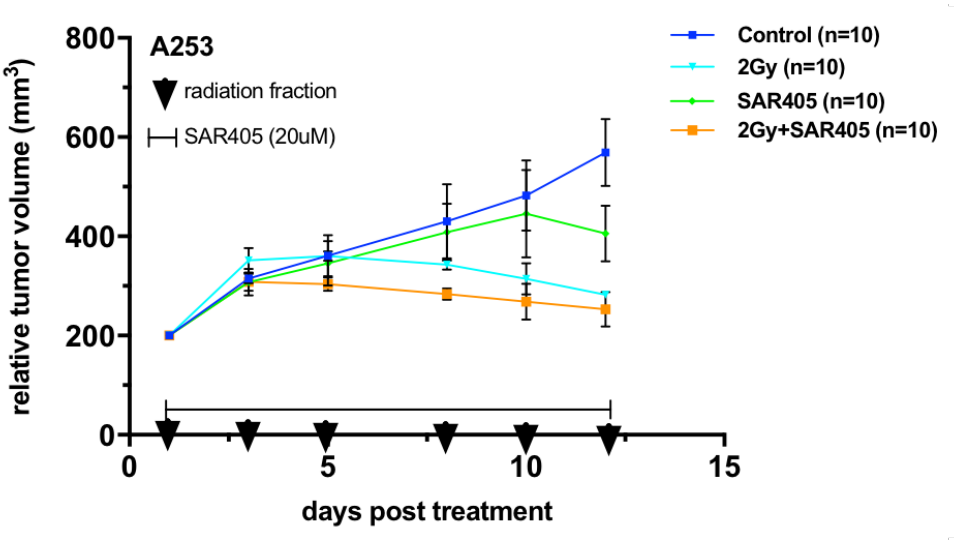
A253
radiation fraction
SAR405 (20uM)
Control (n=10)
2Gy (n=10)
SAR405 (n=10)
2Gy+SAR405 (n=10)
relative tumor volume (mm3)
800
600
400
200
0
0
5
10
15
days post treatment

B

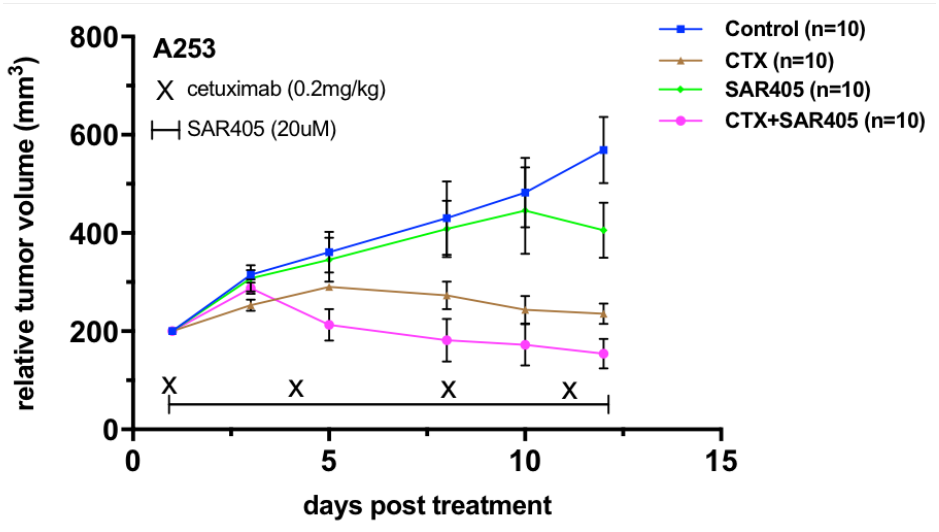
A253
X cetuximab (0.2mg/kg)
SAR405 (20uM)
Control (n=10)
CTX (n=10)
SAR405 (n=10)
CTX+SAR405 (n=10)
relative tumor volume (mm3)
800
600
400
200
0
X
X
X
X
0
5
10
15
days post treatment

Figure 3.5 Autophagy inhibition improves tumor controls in vivo
A253 cells were mixed with Matrigel (1:1) and then implanted on the nude mice flanks. Tumor sizes were started to be measured using calipers 10 days post-implantation (~200mm^3). Some xenografts were collected 3 days post-implantation for IHC analysis. All mice for radiation and cetuximab treatment were managed at the same time but we split them into two figures for better vision reason, and they thereby shared the same for group control and SAR405 alone. (A) Radiation was delivered three times a week and 2Gy per time. On the other hand, (B) cetuximab was given 2 times a week via intraperitoneal injection. SAR405 (20μM) was injected into tumor sites directly once daily. All treatments lasted for 2 weeks.

Figure 3.6

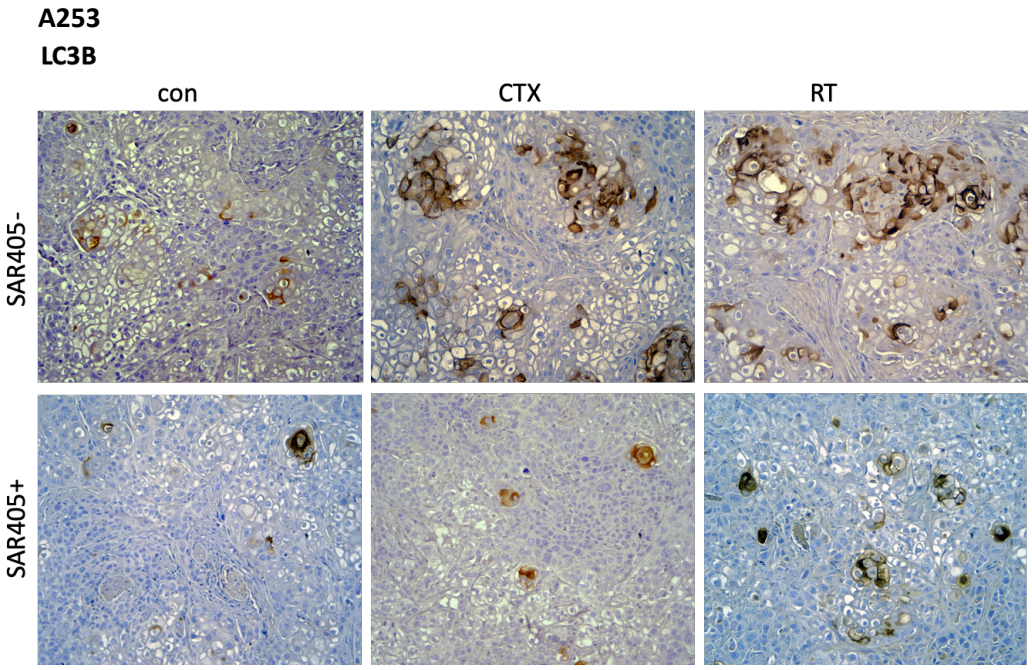

Figure 3.6 SAR405 inhibits autophagy in vivo
A253 cell xenograft tissues were collected 72 hours post-implantation on nude mice as described in Figure 3.5. IHC staining for LC3B, an autophagy marker, was used to unveil the autophagy modulation *in* v*ivo.*

Chapter 4

Mechanisms underlying CTX- and RT-induced autophagy

Preface

This chapter is conducted a series of related studies to disclose the mechanisms underlying CTX- and RT-induced autophagy over the two-year course of work. Our group identified two different subtypes of autophagy induced by CTX and RT respectively. This is a surprising finding that highlights some key therapeutical targets for each mechanism and implicates a new potential role for autophagy to be used in the future personalized cancer treatment.

4.1 Abstract

Autophagy is regulated by numbers of signaling pathways to help cells against cellular stresses. One of our collaborators, Dr. Richard Anderson, previously disclosed a mechanism involved in inactive EGFR and lysosomal-associated transmembrane protein 4B (LAPTM4B) to increase autophagy [131, 132]. We thereby hypothesized that CTX-induced autophagy is mostly governed by this EGFR/LAPTM4B machinery due to the overexpression of EGFR in HNSCC and the EGFR antibody feature of cetuximab. Knockdown of EGFR or LAPTM4B using siRNA techniques, we successfully involved this solid mechanism only in CTX- but not RT-induced autophagy.

To further understand the underlying mechanism regulating RT-induced autophagy. We have tested several possibilities and eventually the induction of reactive oxygen species (ROS)-induced mitophagy by radiation has been observed. This exciting finding highlights each cancer therapy may cause its own specific subtype of autophagy to enhance HNSCC cell survival and therapeutic resistance.

4.2 Introduction

Cells use highly conserved autophagy mechanism to maintain their homeostasis by degrading misfolded or excessive proteins, nonfunctional organelles, foreign pathogens, as well as other cellular components. Depending on the cargo, autophagy can be selective or nonselective. In nonselective autophagy, bulk portions of the cytoplasm are sequestered by the phagophore for degradation to maintain the nutrient levels in cells. This nonselective autophagy is frequently observed during starvation. Conversely, selective autophagy maintains the number and integrity of cellular organelles, as well as protects cells from pathogen invasions. Selected cargo can be

mitochondria, portions of ER, ribosomes, peroxisomes, lysosomes, lipid droplets, and others [133, 134]. Hence, the regulation of cargo transportation is important for autophagy modulation.

Studies have shown that inactive EGFR interacts with LAPTM4B at late endosome to bind Rubicon, which in turn disassociates Beclin1 from Rubicon to initiate bulk autophagy [131]. LAPTM4B is a transmembrane protein primarily located at late endosome and lysosome which is related to cellular cargo sorting and recycling [135]. Cetuximab (CTX) is an EGFR antibody frequently used in HNSCC treatment due to the overexpressed EGFR feature in HNSCC patients. Numbers of inactive EGFRs are increased by cetuximab, implicating that CTX-induced autophagy is likely involved in this EGFR/LAPTM4B machinery. In this chapter, our group is thereby firstly testing this hypothesis using RNAi technology followed by further experimental research.

For RT-induced autophagy, it might be sharing the same regulatory signaling with CTX-induced autophagy or exists another selective autophagy regulation. Radiation impacts cells through 30% direct effect and 70% indirect effect on DNA backbones. This indirect effect causes amounts of ROS through cellular water, which damages DNA or induces cell death [136]. However, mitochondria are the most important cellular organelle to manage ROS-caused oxidative stress [137]. Hence, it is our hypothesis that radiation can increase ROS leading to the induction of autophagy in mitochondria. Our group will also test this hypothesis to further understand the underlying mechanism.

4.3 Materials and methods

4.3.1 Cell lines and SAR405 preparation

Human HNSCC cell lines (UM-SCC47, A253, UM-SCC1, and UM-SCC1-C5), and

syngeneic C57BL/6 (B6) mouse OSCC cell lines (MOC1 and MOC2), were were cultured at low passage in standard conditions (at 37 °C in 5% CO2) as previously described. All human HNSCC cells were cultured in Dulbecco's modified Eagle's Medium (DMEM) (Corning Inc.) supplemented with 10% fetal bovine serum, 1% penicillin/streptomycin, L-glutamine, 4.5g/L glucose, and sodium pyruvate. Mouse cell lines (MOC1 and MOC2) were maintained in modified DMEM medium/F12 at a 2:1 mixture with 5% fetal bovine serum, 1% penicillin/streptomycin, 1% amphotericin, 5ng/mL epidermal growth factor (EGF), 400 ng/mL hydrocortisone, and 5mg/mL insulin. SAR405, provided by Selleckchem (#S7682), was reconstituted in DMSO and stored at -20^{o}C until use.

4.3.2 Immunoblot analysis

Cells were harvested and washed with PBS before freezing at -80°C. Cells were lysed with RIPA buffer supplemented 1% (v/v) with phosphatase/protease inhibitor cocktail (Cell Signaling Technologies, #5872) and sonicated. Equal amounts of protein were analyzed by SDS-PAGE, transferred to polyvinylidene diflouride membranes, and probed with specific primary antibodies overnight at 4°C. Targets were detected with NIR-conjugated anti-mouse and anti-rabbit secondary antibodies (LiCOR) and imaged on a LiCOR Odyssey FC. Specific antibodies and sources are listed in Table 1. For autophagy flux analysis, after certain drug treatments, cells were treated with or without 100nM bafilomycin A1 four hours prior to cell lysis. Protein samples were probed with LC3B primary antibody and were quantified for each sample to obtain LC3 number A (sample without Baf) and LC3 number B (sample with Baf). Subtract A from B and you have the number for autophagy flux.

4.3.3 LC3B puncta immunofluorescence (IF) and mitotracker staining

Cells were plated in 8-well chamber slides at densities ranging from 10,000 to 30,000 cells/well depending on cell type size and growth rate. Twenty-four hours post-plating cells were pre-stained with MitoTracker Red CMXRos (Thermo #M7512) and then treated with DMSO control, 100nM CTX, or irradiated with 8 Gy and incubated at 37 °C in 5% CO2 for 36 hours. 100nM bafilomycin A1 (Baf) was added to cells 4 hours prior to fixing cells with 100% methanol in PBS at indicated time points. Cells were permeabilized with 0.1% Triton-X 100 in TBST for 15 minutes, blocked with goat serum for 1 hour at 25°C, and incubated with anti-LC3B primary antibody overnight at 4°C (Table 1). Cells were then probed with Alexa Fluor 555 conjugated secondary antibody (CST #4413) for 1 hour at 25°C in the dark, and cover slipped with Fluoromount containing DAPI. The next day, they were imaged at 60x magnification using a Nikon A1RS inverted point scanning confocal microscope system.

4.3.4 Quantitative real time-polymerase chain reaction (qRT-PCR)

RNA was extracted from cultured cells using Allprep DNA/RNA Mini Kit (Qiagen, Valencia, CA) and measured by Nanodrop. RNA was used to synthesize cDNA with SuperScrip III RNase H2 Reverse Transcriptase (Invitrogen, Carlsbad, CA) with specific 3′-primers. SYBR green based gene primers (see Table 2) were used to run the qPCR. Relative mRNA levels were quantified by RT-qPCR (Bio-Rad, S1000 Thermal cycler) and normalized to housekeeping gene GAPDH. All reactions were performed in triplicate from RNA isolated from three independent biological experiments.

4.3.5 Co-immunoprecipitation (co-IP)

Cells were pelleted and lysed in NP40 buffer containing protease and phosphatase

inhibitor cocktails immediately after the end of drug treatment. Cell lysates were kept on ice through the process. Syringes with 23G needles were used to physically breakdown cell membranes. Spin cells at 14,000 rpm at 4^{o}C for 30min and collect supernatants. 250ug-500ug of proteins were used for the immune-precipitation using protein A/G plus agarose (Santa cruz #sc-2003). Indicated primary antibodies were used for immunoblotting analysis.

4.3.6 CM-H2DCFHDA ROS indicator

Cells were pre-probed with CM-H2DCFHDA for 30min followed by irradiation or drug treatment as indicated time point. Subsequent oxidation yields a fluorescent adduct which can be measured using the SpectraMax i3 Multi-Mode Microplate Reader Platform. The fluorescent wavelength (excitation/emission: 492–495/517–527nm) signal was assessed for quantification.

4.3.7 Statistical analysis

A two-tailed Student's t test was used to evaluate the differences between two groups. One-way ANOVA, followed by Dunnett's or Holm-Sidak's multiple comparisons test, was used for multiple group comparisons. Data were analyzed with Prism 8 (GraphPad Software). $P < 0.05$ was considered statistically significant. All experiments were repeated at least three times and presented as means ± SEM.

4.4 Results

4.4.1 EGFR/LAPTM4B mechanism governs CTX-induced autophagy

Inactive EGFR has been shown to form a complex with LAPTM4B to prevent Rubicon from interacting with the autophagy initiator Beclin1, thus leading to autophagy

initiation [131, 132]. Accordingly, we hypothesized that CTX-induced autophagy is dependent on the EGFR/LAPTM4B interaction due to the role of CTX as an EGFR inhibitor. Knockdown of EGFR or LAPTM4B significantly decreased autophagy as assessed by LC3B puncta (Figure 4.1A). We also assessed the mRNA levels of LAPTM4B, when treated with CTX treatment in HNSCC. RNA results showed that CTX treatment increased LAPTM4B (Figure 4.1B), suggesting that EGFR/LAPTM4B were involved in CTX-induced autophagy. Moreover, our immunofluorescence staining data is in line with the result from immunoblotting analysis (Figure 4.1C). We next investigated the protein-protein interaction between Rubicon and Beclin1 to understand whether CTX caused autophagy through EGFR/LAPTM4B machinery (Figure 4.1D). Our findings showed that lower Beclin1 proteins were detected as we immunoprecipitated Rubicon from CTX-treated cells when compared to control. This result demonstrates that EGFR/LAPTM4B complex released more Beclin1 by trapping Rubicon to increase autophagy. Taken together these results suggest that CTX activates autophagy in a LAPTM4B, Rubicon, Beclin1 dependent manner.

4.4.2 RT-induced autophagy is mitophagy controlled by PINK1/PARKIN signaling pathway

Since CTX-induced autophagy was successfully related to EGFR/LAPTM4B machinery, and RT has been shown to result in alteration of EGFR signaling, we were intrigued to understand whether RT-induced autophagy shared the same mechanism. To test this hypothesis, we again transcriptionally inhibited LAPTM4B and EGFR using si-LAPTM4B or si-EGFR. Our findings showed no effect on autophagy between control and the cells with EGFR/LAPTM4B knockdown (Figure 4.2), suggesting that RT-induced

autophagy is modulated by alternative pathways.

RT induces significant reactive oxygen species (ROS) which leads to mitochondrial stress (21) and has the potential to activate autophagy. Autophagy levels were examined using acridine orange dye combined with the ROS scavenger Trolox. Irradiated cells demonstrated an increase in ROS that can be blocked by treatment with Trolox (Figure 4.3A). Trolox treatment blocks autophagy induction by RT or ROS generated by H2O2 treatment (Figure 4.3B) strongly suggesting that RT-induced autophagy is mediated by ROS generation. We assessed mitochondrial and cytoplasmic LC3B expression in cellular fractionation extracts and showed that RT-induced autophagy was concentrated in the mitochondria (Figure 4.4A). LC3B flux in response to radiation was mostly detected in mitochondria using immunoblotting (Figure 4.4A). These results were confirmed by immunofluorescence for LC3B (green) and MitoTracker (red) (Figure 4.4B).

Recent evidence has suggested that Pink1 and Parkin signaling regulates mitophagy induction (22). We assessed alteration in Pink1 mRNA by qRT-PCR and demonstrated that RT (Figure 4.5A) but not CTX (Figure 4.5B) increases Pink1 expression. Knockdown of Pink1 blocked its RT-mediated increase (Figure 4.5A). We assessed expression of LC3B mRNA in irradiated cells treated with si-Pink1 and demonstrated that Pink1 knockdown abrogates RT-induced increase in LC3B expression (Figure 4.5C). Finally, we assessed the ability of Parkin to be immunoprecipitated with Pink1 following radiation. More Pink1 was pulled down with Parkin following radiation suggesting that radiation activates the Pink1/Parkin interaction (Figure 4.5D). This data suggests that Pink1 cooperates with Parkin to mediate RT-induced mitophagy in HNSCC.

4.5 Discussion

We determined two individual mechanisms that regulate CTX- and RT-induced autophagy respectively. However, there might be other minor signaling pathways controlling treatment-induced autophagy. For example, we also found that mTOR signaling was downregulated when cells were irradiated (data not shown), implicating that not only single type of autophagy can be induced by one type of treatment. On the other hand, mTOR inhibition is commonly considered as a switch for autophagy induction and it can be inhibited in response to several adverse microenvironment conditions, such as nutrition depletion. This highlights the complexity of autophagy regulation in cells and remains challenges to relate certain type of autophagy to each treatment. However, our findings still suggest that future drugs which target specific subtypes of autophagy may be needed to personalize treatment combinations for HNSCC patients.

Figure 4.1

A

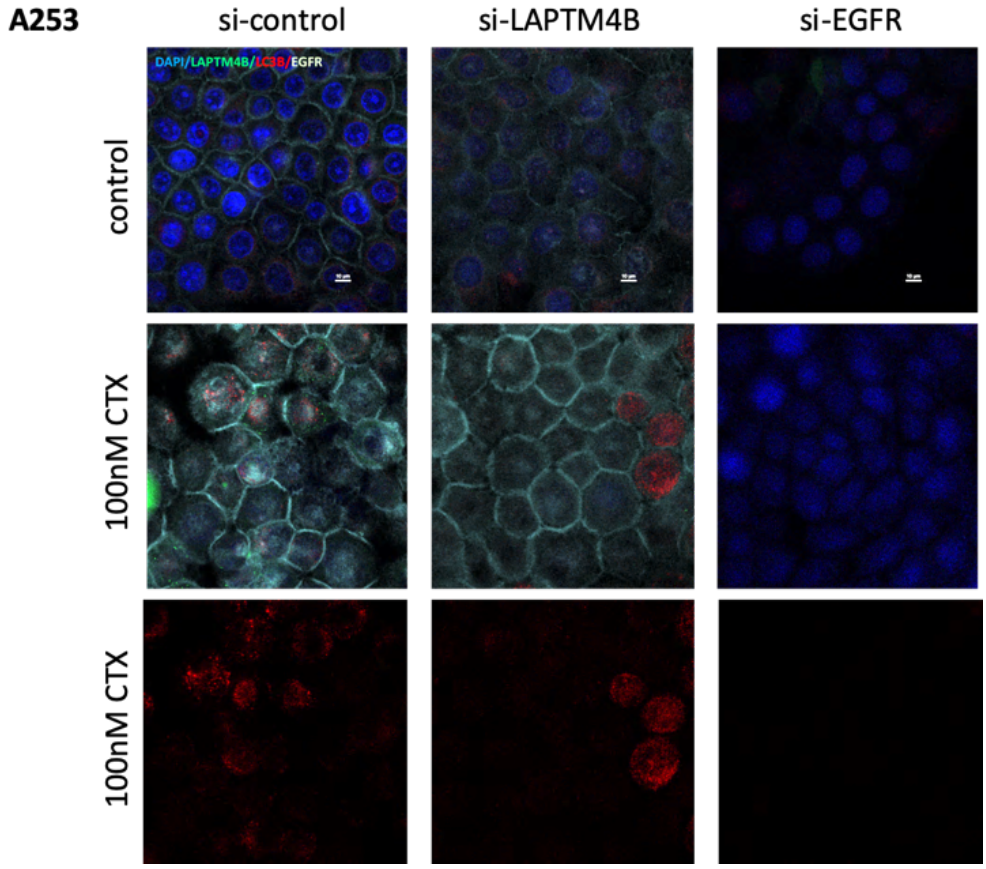
A253
si-control
si-LAPTM4B
si-EGFR
DAPI/LAPTM4B/LC3B/EGFR
control
100nM CTX
100nM CTX

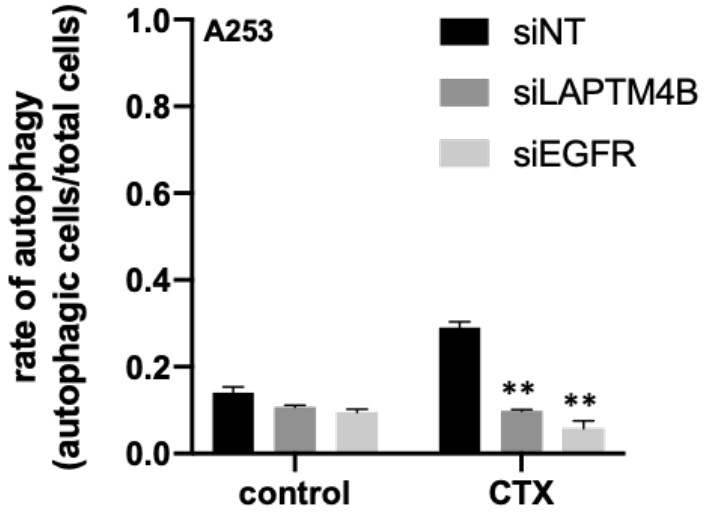
A253
siNT
siLAPTM4B
siEGFR
rate of autophagy
(autophagic cells/total cells)
1.0
0.8
0.6
0.4
0.2
0.0
**
**
control
CTX

Figure 4.1

B

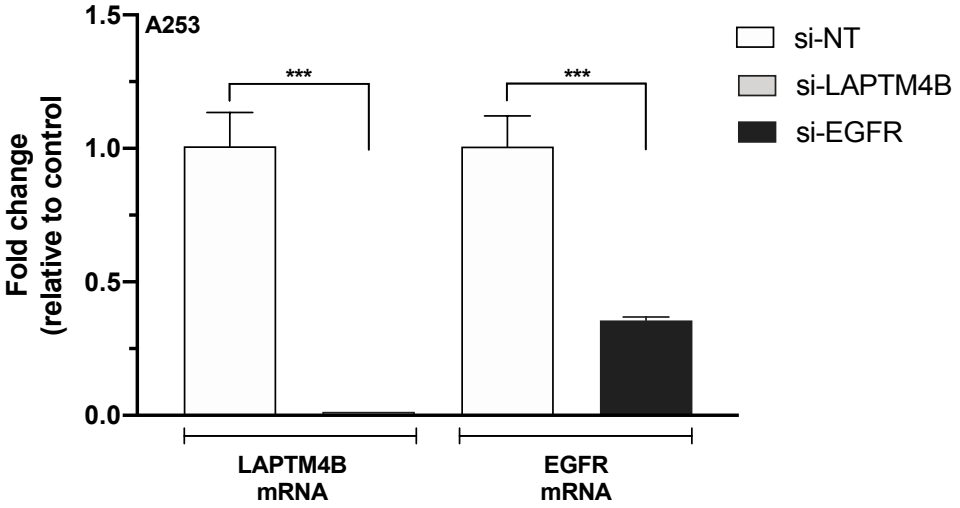
A253
1.5
1.0
0.5
0.0
Fold change
(relative to control
***
***
si-NT
si-LAPTM4B
si-EGFR
LAPTM4B
mRNA
EGFR
mRNA

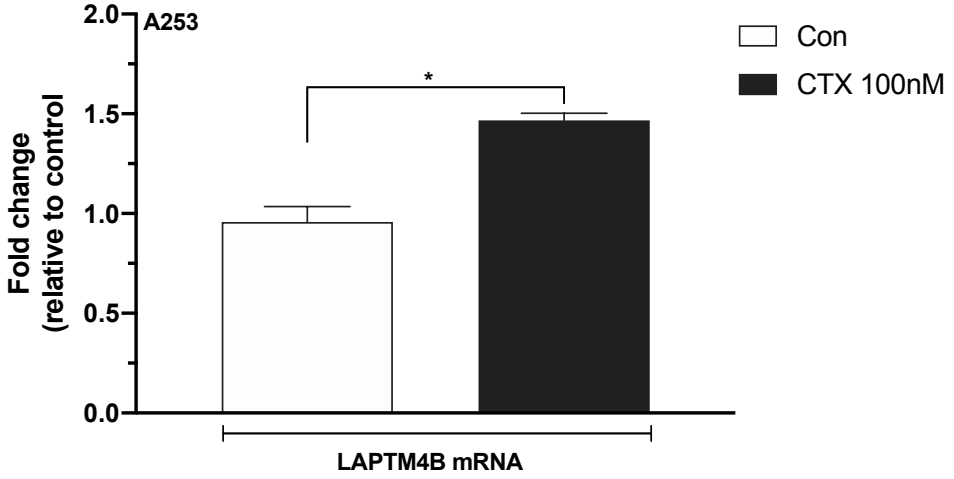
A253
2.0
1.5
1.0
0.5
0.0
Fold change
(relative to control
*
Con
CTX 100nM
LAPTM4B mRNA

Figure 4.1

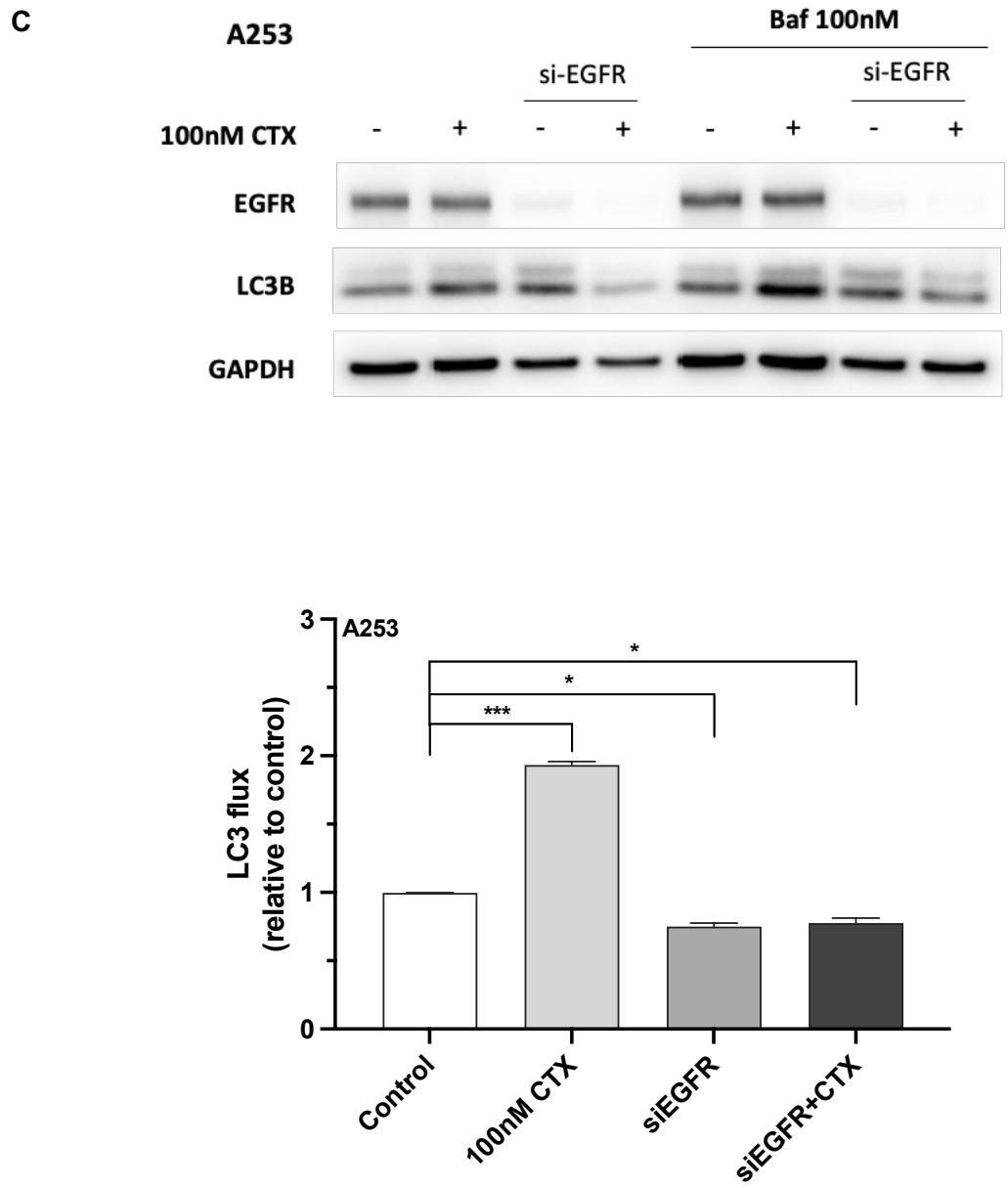
C
A253
Baf 100nM
si-EGFR
si-EGFR
100nM CTX
- + - + - + - +
EGFR
LC3B
GAPDH
A253
LC3 flux
(relative to control)
3
2
1
0
*
*
***
Control
100nM CTX
siEGFR
siEGFR+CTX

Figure 4.1

D

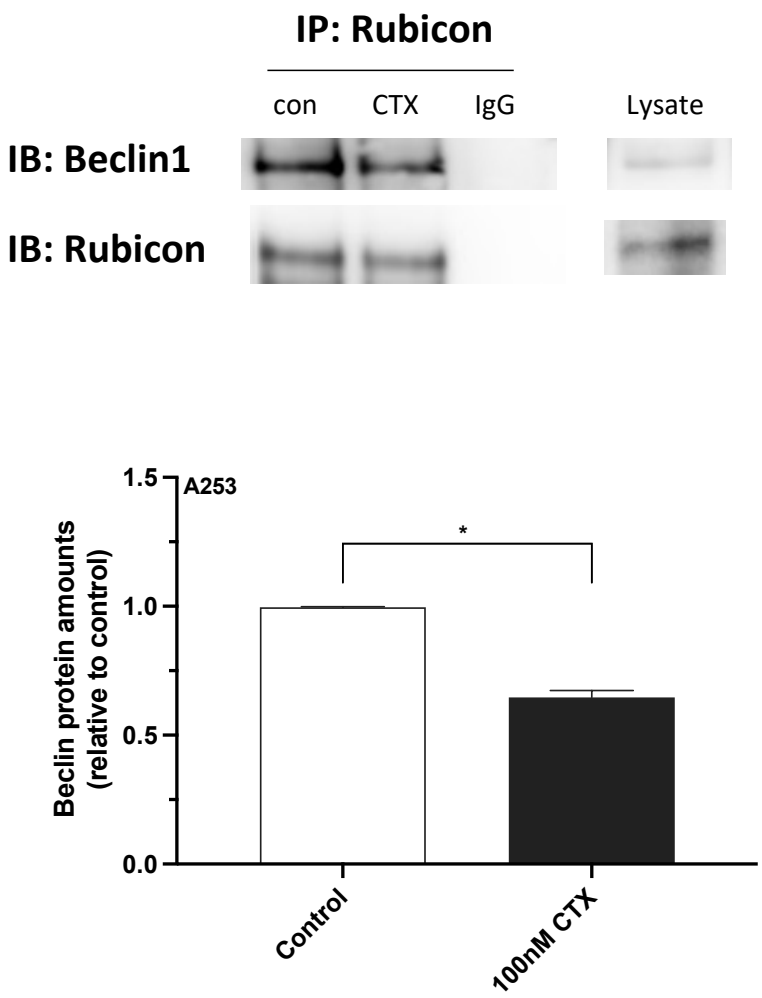
IP: Rubicon
con
CTX
IgG
Lysate
IB: Beclin1
IB: Rubicon
A253
Beclin protein amounts (relative to control)
1.5
1.0
0.5
0.0
*
Control
100nM CTX

Figure 4.1 EGFR/LAPTM4B machinery is involved in CTX-induced autophagy
(A) A253 cells were transfected with siRNAs (si-control, siEGFR, siLAPTM4B) for 72 hours using lipofectamine 2000 reagent (Invitrogen). Cells were treated with 100nM or DMSO control 36 hours post-transfection and maintained until the end of siRNA treatment. Baf was added to observe LC3 punta for counting autophagic cells. Immunofluorescence (IF) quantified data were obtained by the numbers of autophagic cells normalized to total cell numbers. (B) RNA knockdown efficiency was assessed using qPCR. Cells were transfected with each siRNA (siLAPTM4B, siEGFR) for 72 hours followed by RNA extraction for qPCR examination. Cells treated with 100nM CTX for 36 hours showed higher LAPTM4B mRNA expressions when compared to untreated control. (C) Immunoblotting analysis for LC3B was used to verify our IF data shown above (A). (D) Co-immunoprecipitation assay was performed to understand the protein-protein interaction between Rubicon and Beclin1. Cells were treated with 100nM CTX for 36 hours followed by fresh cell lysis using NP40 lysis buffer. Anti-rabbit IgG was used as the negative control and the lysate input was used for the recognition of the bands.

Figure 4.2

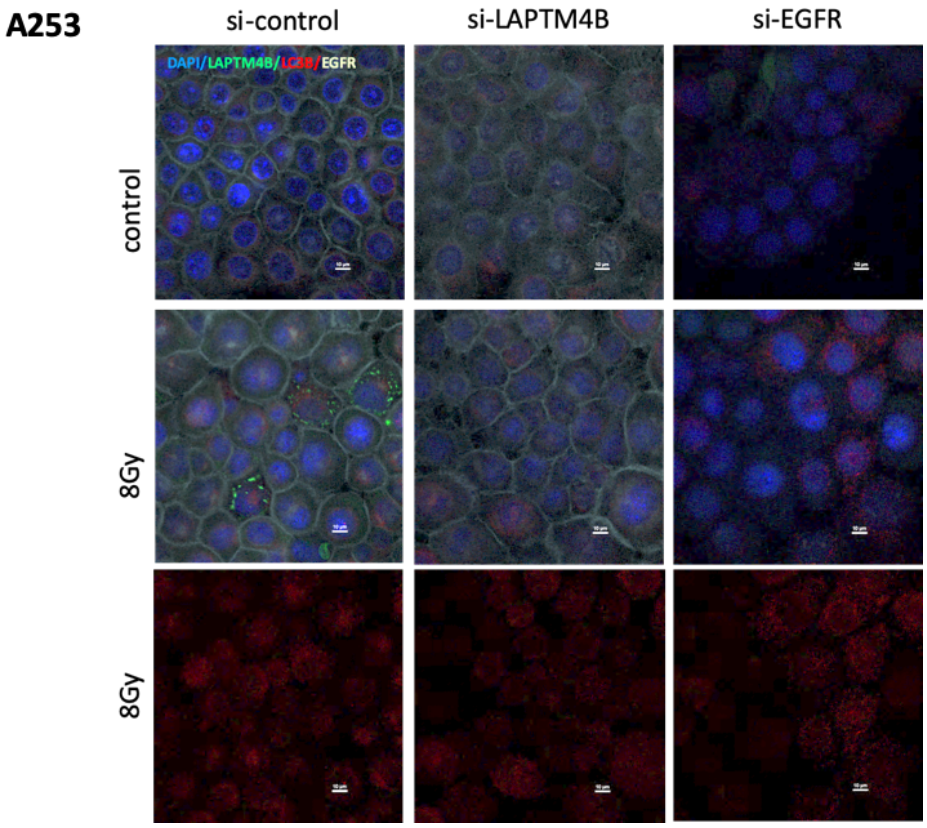
A253
si-control
si-LAPTM4B
si-EGFR
DAPI/LAPTM4B/LC3B/EGFR
control
8Gy
8Gy

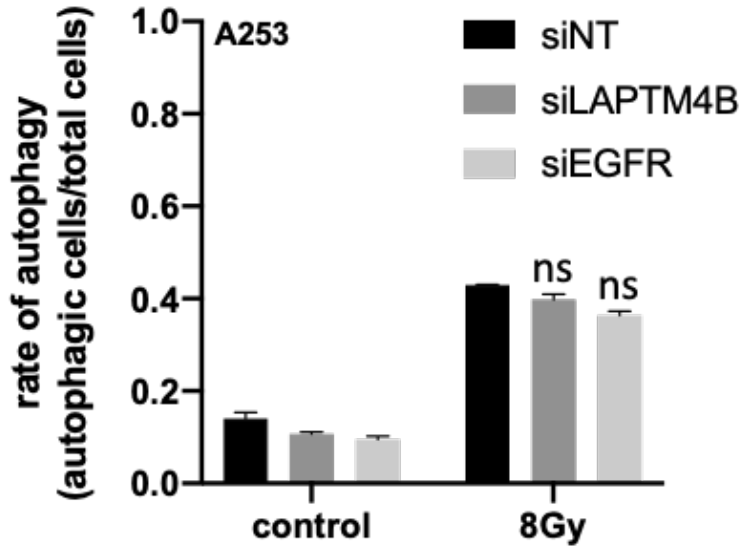
A253
siNT
siLAPTM4B
siEGFR
rate of autophagy
(autophagic cells/total cells)
1.0
0.8
0.6
0.4
0.2
0.0
ns
ns
control
8Gy

Figure 4.2 RT-induced autophagy is independent of EGFR/LAPTM4B machinery
(A) A253 cells were transfected with siRNAs (si-control, siEGFR, siLAPTM4B) for 72 hours using lipofectamine 2000 reagent (Invitrogen). Cells were irradiated with 8Gy or non-irradiated 36 hours post-transfection and maintained until the end of siRNA treatment. Autophagic cell numbers were normalized to total cells in a image for the quantification. Results showed no difference when compared to si-NT control.

Figure 4.3

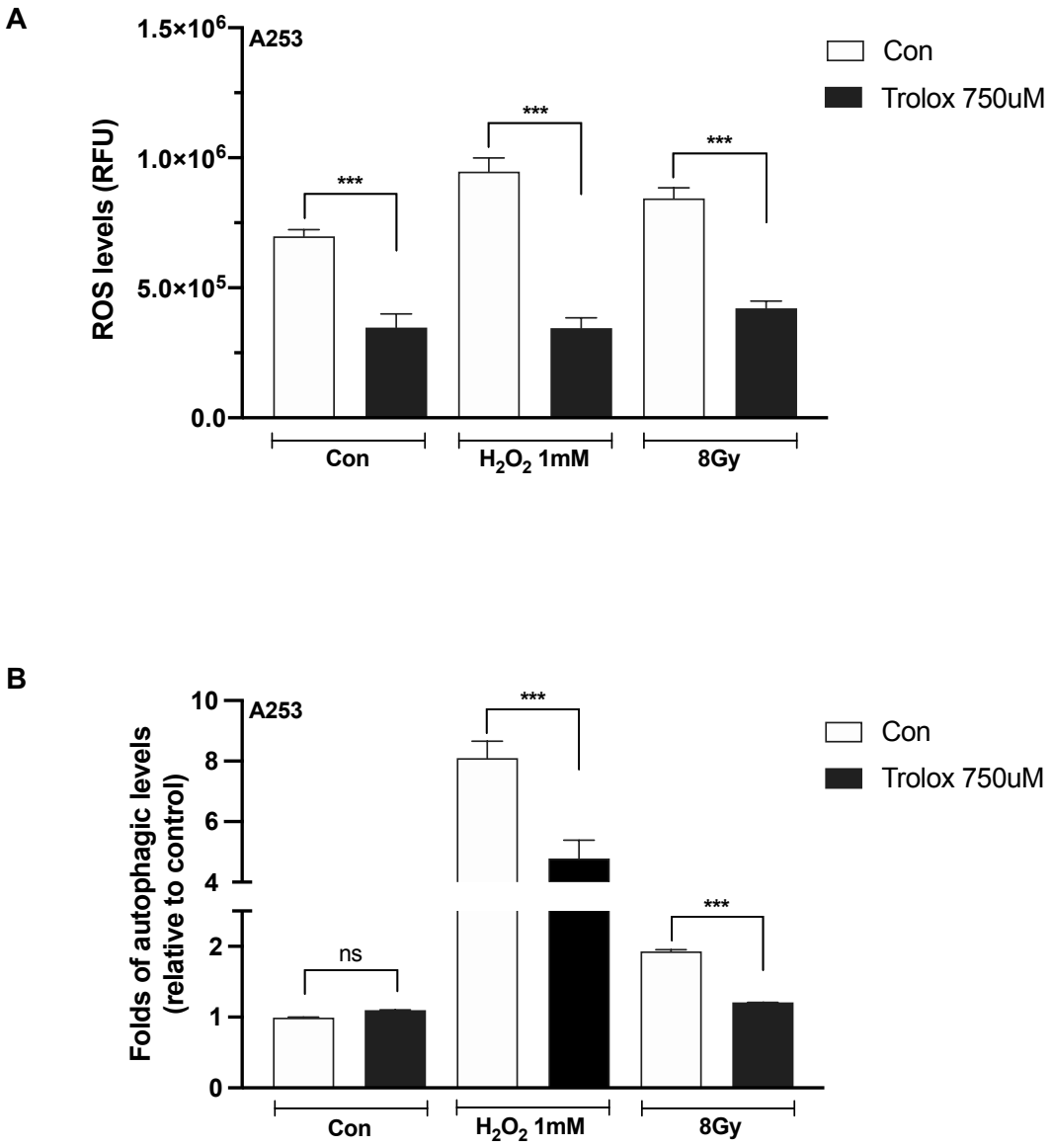
A
A253
ROS levels (RFU)
1.5×10^6
1.0×10^6
5.0×10^5
0.0
***
***
***
Con
Trolox 750uM
Con
H2O2 1mM
8Gy
B
A253
Folds of autophagic levels (relative to control)
10
8
6
4
2
1
0
ns
***
***
Con
Trolox 750uM
Con
H2O2 1mM
8Gy

Figure 4.3 RT-induced ROS increases autophagy induction
(A) A253 cells were assessed the ROS using CM-H2DCFDA. Cells were irradiated (8Gy) or treated with 1mM H_2O_2 (positive control). Trolox, a ROS scavenger, was used to determine the correlation between radiation and ROS. (B) Autophagy flux induced by ROS was assessed using acridine orange (AO) assay. Cells were treated with 1mM H_2O_2, 8Gy, or untreated control in presence or absence of 750μM Trolox for 36 hours. Autophagy levels were normalized to untreated control.

Figure 4.4

A

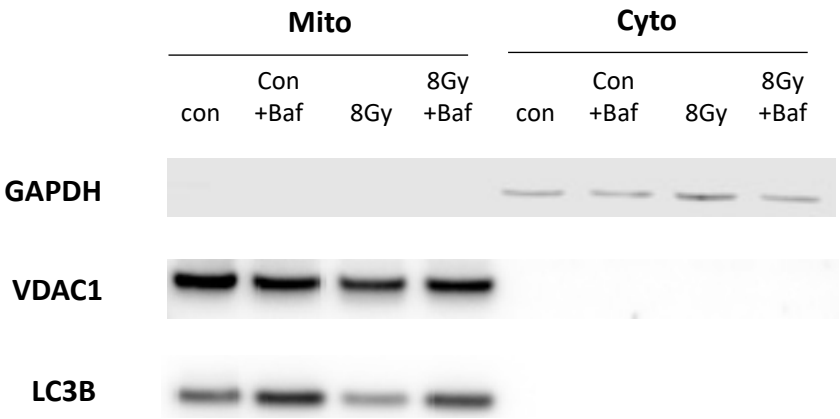
Mito
Cyto
con
Con +Baf
8Gy
8Gy +Baf
GAPDH
VDAC1
LC3B

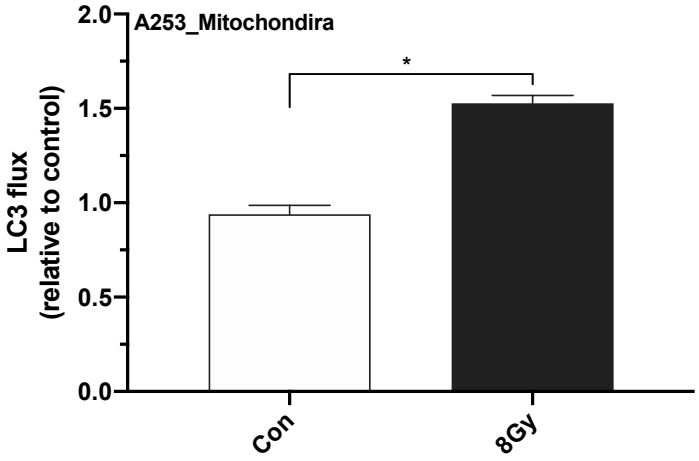
A253_Mitochondira
LC3 flux (relative to control)
2.0
1.5
1.0
0.5
0.0
*
Con
8Gy

B

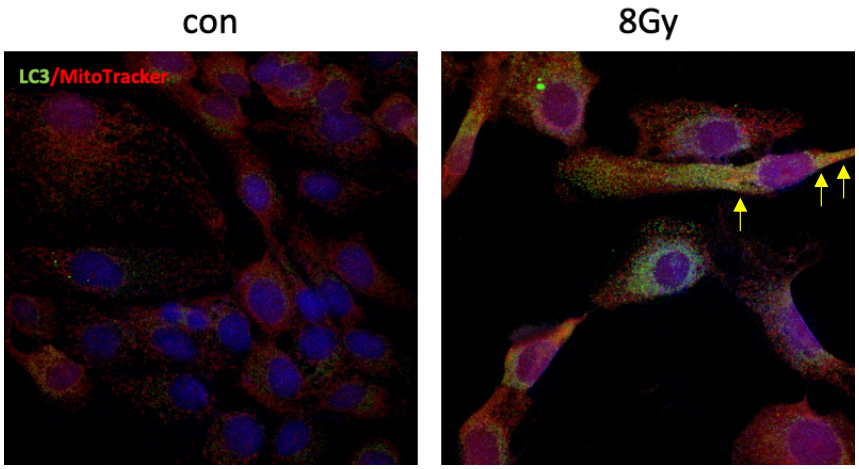
con
8Gy
LC3/MitoTracker

Figure 4.4 RT-induced autophagy mostly comes from mitochondria (mitophagy)
(A) A253 cells were irradiated (8gy) for 36 hours and cell lysates was isolated compartmentally. Mitochondrial proteins were isolated to compare protein expression located in cytoplasm. Baf was added to quantify LC3 flux for autophagy. Results were normalized to untreated control. (B) IF staining for LC3 puncta (green) combined with mitoTracker RED CMXRos (red) located LC3B. Cells were prestained with mitoTracker reagent followed by irradiation for indicated time point. Baf was added to trace LC3 puncta. Mitochondrial LC3 puncta were shown as yellow color (arrow).

Figure 4.5

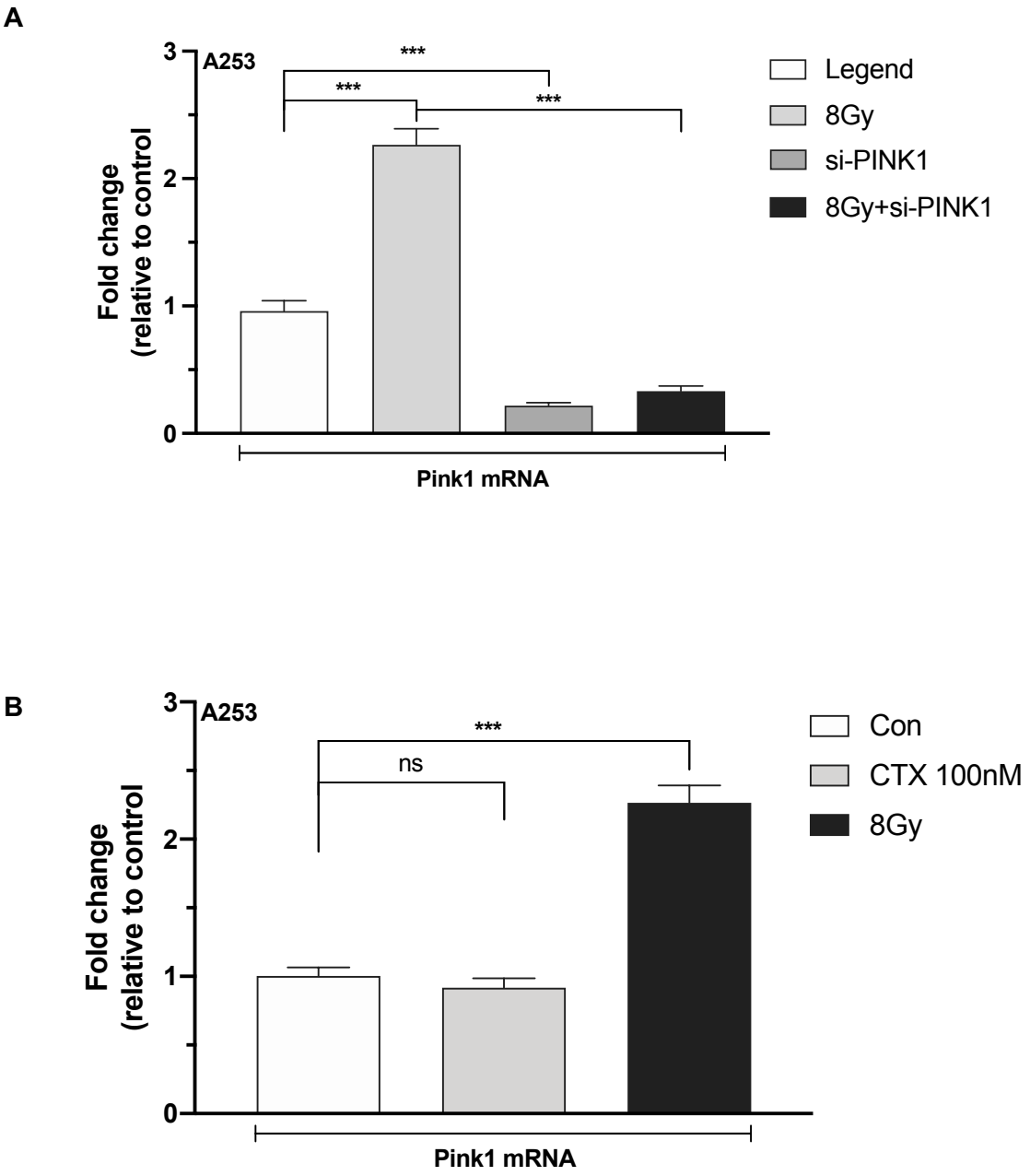
A
A253
***
***
***
Legend
8Gy
si-PINK1
8Gy+si-PINK1
Fold change
(relative to control
3
2
1
0
Pink1 mRNA
B
A253
***
ns
Con
CTX 100nM
8Gy
Fold change
(relative to control
3
2
1
0
Pink1 mRNA

Figure 4.5

C

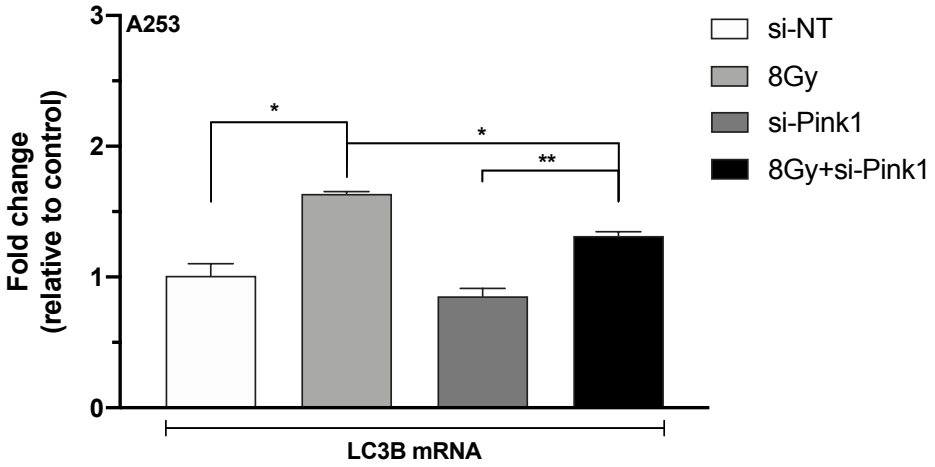
A253
Fold change (relative to control)
3
2
1
0
*
*
**
si-NT
8Gy
si-Pink1
8Gy+si-Pink1
LC3B mRNA

D


IP: Parkin
con
8Gy
IgG
IB: Pink1
IB: Parkin

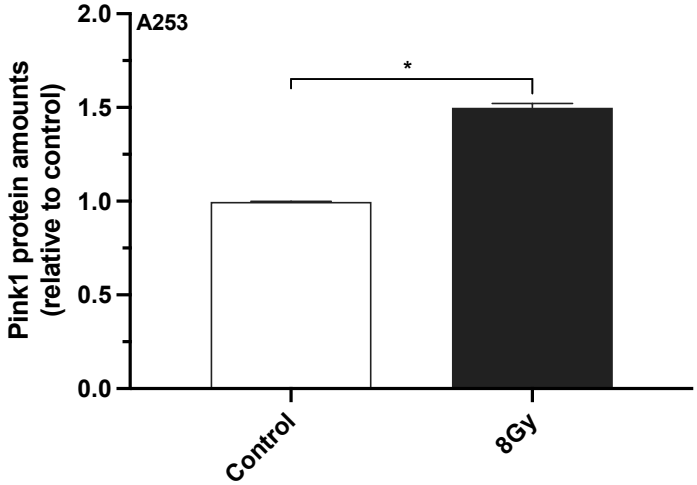
A253
Pink1 protein amounts (relative to control)
2.0
1.5
1.0
0.5
0.0
*
Control
8Gy

Figure 4.5 RT-induced mitophagy is controlled by Pink1/Parkin switch
(A and C) Pink1 and LC3B mRNA were assessed by qPCR. A253 cells were transfected with siRNA for 72 hours; Irradiated (8gy) was delivered to cells 36 hours post-transfection and cell were maintained until the end of siRNA treatment. RNAs were collected and reversed transcribed for qPCR quantification. mRNA results were normalized to untreated control. (B) Cells were treated with 100nM CTX or 8Gy for 36 hours followed by RNA isolation for further qPCR analysis. (D) Co-immunoprecipitation assay was performed to understand the protein-protein interaction between Pink1 and Parkin. Cells were irradiated (8Gy) for 36 hours followed by fresh cell lysis using NP40 lysis buffer. Anti-rabbit IgG was used as the negative control.

Chapter 5

Summary and future directions

5.1 Overview

In this last chapter I summarize the major conclusions from chapters 2-4. I will then discuss the major implications of these findings, and the important scientific questions that arise as a result. Finally, I will present some potential applications of autophagy in clinic.

5.2 Summary of thesis findings

Autophagy not only controls cellular homeostasis but also plays a critical role in cancer development leading from healthy cells to metastatic or drug resistant tumors. This complex regulation highlights the opportunities for pharmacologic intervention in the multi-step process of autophagy. However, the precise role of autophagy in cancer remains highly complex. Autophagy has been shown to play a role in both evasion of cell death and maintenance of homeostasis through cellular recycling programs, and in the promotion of cell death through large-scale degradation of cellular components [27, 40]. This dual role of autophagy poses an immense challenge to anti-cancer treatment approaches and suggests that understanding the mechanism by which individual treatments modulate autophagy is critical. Drug-induced autophagy has been employed as an attempt to kill cancer cells, particularly in those that have adopted anti-apoptotic strategies [36-38]. Meanwhile, an opposite approach has been taken wherein autophagy is inhibited as an attempt to overcome the treatment resistance conferred by autophagy [45, 46]. It should be noted that there are currently no FDA approved compounds that were developed specifically to inhibit autophagy. Rather, autophagy modulation was discovered as an off-target effect of the drugs used in these studies. Our group is thereby actively investigating whether chemotherapy and radiotherapy can be enhanced with the

addition of autophagy modulators to improve tumor control and prevent the development of therapeutic resistance, as autophagy has numerous effects on cancer treatments.

In this work, we demonstrate that autophagy is activated in HNSCC cells treated with CTX or RT. In HNSCC, autophagy plays a protective role to cell death caused by these common treatments. We observed therapy induced autophagy in both HPV-negative and HPV-positive HNSCC cells but determining the precise role for HPV oncoproteins in this process is beyond the scope of this work. In both acquired and intrinsic resistance models autophagy was higher than in related sensitive lines. This is consistent with the finding of increased autophagy in patient samples with recurrent as compared to primary tumors and in more advanced stage, compared to early-stage cancers. We readily acknowledge the limitation that LC3B immunohistochemistry in fixed tissues only provides a snapshot and does not permit one to comment on autophagic flux in these tissues. This highlights the unmet need of a clinically straightforward biomarker for autophagy measurement from patients.

CQ and HCQ are currently the only two autophagy inhibition compounds that have been tested in clinical trials. Although there were several convincing experimental data in support of their anti-cancer effects [98], the clinical trial results have shown limited efficacy [138]. These compounds act very late in autophagy by interfering with autolysosome formation which may explain their lack of efficacy [139]. In addition, it has been suggested that they do not reach sufficient intratumoral concentrations at the doses typically used in these studies (REF). Clearly, if autophagy inhibition is going to be utilized clinically more specific and effective autophagy inhibitors are needed. SAR405, the Vps34 inhibitor, can target Vps34 to block autophagy initiation, and we were thereby testing its anti-cancer

effect in this study. When used alone, SAR405 arrested the cell cycle at the G1 phase to obstruct cancer cell proliferation rather than kill cells. The addition of SAR405 to either CTX or RT showed the better tumor control compared to each individual treatment both in vitro and in vivo. SAR405 also improved control of therapy resistant cells. In order to translate these studies to clinical trials, pharmacologically active and safe autophagy inhibitors must be developed. It is also possible that autophagy inhibitors which block other autophagic processes may be better drugs. Two such compounds, SBI-0206965, an Ulk1 inhibitor, and Heclin, a NEDD4-1 inhibitor, are being developed although their ability to augment CTX and RT effects is not yet clear.

Previous studies have shown that various cellular stresses activate autophagy via the interaction between inactive EGFR and LAPTM4B [131]. Our group was intrigued to relate this mechanism to the cetuximab-induced autophagy, as cetuximab inhibits and downregulates EGFR. Whether this mechanism is seen in other cancers in which CTX is worthy of further study. Intriguingly radiation-induced autophagy was found to be independent of this EGFR/LAPTM4B machinery. Instead, mitophagy activation via a Pink1/Parkin signal transduction was related to the radiation-induced autophagy in HNSCC. These findings emphasized that there are various types of autophagy that occur in HSNCC in response to different cellular stresses and cancer treatments (Figure 5).

In conclusion, our work suggests that CTX and RT both induce autophagy in HNSCC. Furthermore, CTX and RT resistant cells demonstrate increased autophagy compared to sensitive cells suggesting a role for autophagy in the development of therapeutic resistance. We have demonstrated that CTX and RT activate autophagy through independent mechanisms but that inhibition of autophagy using a Vps34 inhibitor

can improve tumor control *in vitro* and *in vivo*.

5.3 Future directions

5.3.1 Role of autophagy in the development of personalized therapy

One of the primary challenges of modulating autophagy in cancer therapy is that, to date, none of the clinically used drugs was developed specifically as an autophagy modulator. In head and neck cancer, there are currently multiple open trials testing drugs which modulate autophagy in combination with other systemic therapies. It has been hypothesized that chemotherapy and radiation therapy can be combined with autophagy modulation (induction or inhibition) to overcome therapeutic resistance and improve tumor control. Additional preclinical research is needed to determine whether a specific subtype of autophagy should be targeted and/or whether targeting at a specific point in the autophagy pathway is preferred, implicating a novel application of autophagy in the development of personalized therapy. Further research is clearly needed to identify how and in which patients autophagy modulators are most likely to improve outcomes when combined with standard anti-cancer treatments.

5.3.2 Role of autophagy-related genes (ARGs) in the prediction of the prognosis for head and neck cancer patients

Recent studies have suggested that autophagy-related genes (ARGs) may be useful as either predictive or prognostic cancer biomarkers. This includes work in lung adenocarcinoma [140], glioblastoma [141], pancreatic adenocarcinoma [142], breast cancer [143], ovarian cancer [144], and head and neck cancer [145]. For example, in head and neck cancer, 232 ARGs in 515 patients were analyzed within the TCGA database; ARGs were highly associated with the regulation of apoptosis, the ErbB pathway, HIF-1 pathway, platinum drug resistance, PD-L1 expression, and the PD-1

checkpoint pathway [145]. These data suggest that a bioinformatical analysis can be established as a program for the autophagy score, and this score might be a potential prognostic factor for patients.

Figure 5. Graphical summary of CTX- and RT-induced autophagy

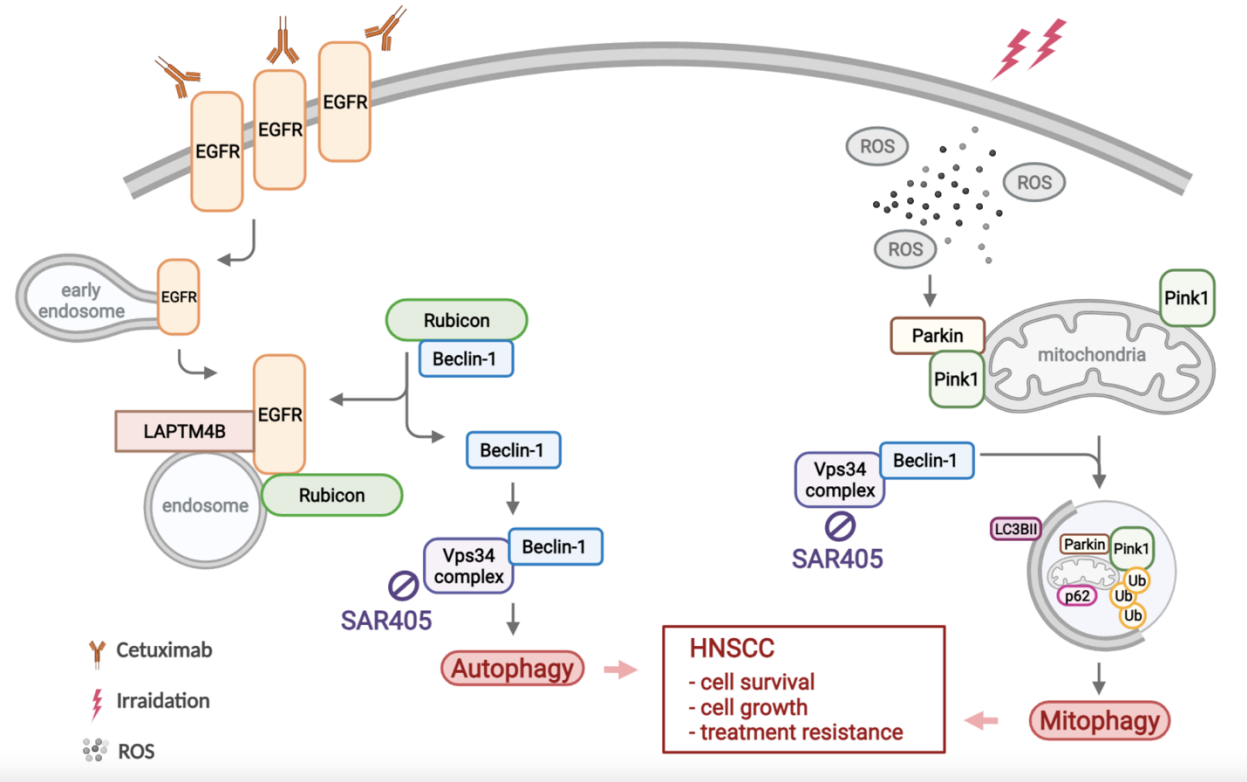

Tables

Table 1 Antibody List

Table 1 Antibody List					
Antiboies	**Concentration**	**Purpose**	**Host**	**Brand**	**Catalog number**
LC3B	1:1000	WB, IF (cell)	Rabbit	Cell Signaling	3868
LC3B	1:500	IHC	Rabbit	Cell Signaling	3868
Pink1	1:1000	WB	Rabbit	Cell Signaling	6946
Parkin	1:50	coIP	Mouse	Cell Signaling	4211
GAPDH	1:2000	WB	Rabbit	Cell Signaling	5274
LAPTM4B	1:1000	WB, IF (cell)	Rabbit	NOVUS	NBP2-61158
EGFR	1:1000	WB, IF (cell)	Rabbit	Cell Signaling	4267
Ki67	1:400	IHC	Rabbit	Cell Signaling	9027
Rubicon	1:1500	WB	Rabbit	abcam	ab92388
Rubicon	1:200	coIP	Rabbit	abcam	ab92388
Beclin-1	1:1000	WB	Mouse	Cell Signaling	4122

Table 2 Primer List

Table 2 Primer List		
h-LAPTM4B	F	5'-GTT ACC AGC AAT GAC ACT ACGG-3'
	R	5'-CTC CTT GGC AGC ACC ATT-3'
h-LC3B	F	5′-GAG AAG CAG CTT CCT GTT CTG G-3′
	R	5′-GTG TCC GTT CAC CAA CAG GAA G-3′
h-PINK1	F	5′-GTG GAA CAT CTC GGC AGG TT-3′
	R	5′-CCT CTC TTG GAT TTT CTG TAA GTG AC-3′
h-EGFR	F	5'-GTG CAG CTT CAG GAC CAC AA-3'
	R	5'-AAA TGC ATG TGT CGA ATA TCT TGA G-3'
18S	F	5'-GTA ACC CGT TGA ACC CCA TT-3'
	R	5'-CCA TCC AAT CGG TAG TAG CG-3'

References

1. Parzych, K.R. and D.J. Klionsky, *An overview of autophagy: morphology, mechanism, and regulation.* Antioxid Redox Signal, 2014. **20**(3): p. 460-73.
2. Thorburn, A., D.H. Thamm, and D.L. Gustafson, *Autophagy and cancer therapy.* Mol Pharmacol, 2014. **85**(6): p. 830-8.
3. Jin, M., X. Liu, and D.J. Klionsky, *SnapShot: Selective autophagy.* Cell, 2013. **152**(1-2): p. 368-368 e2.
4. Li, W.W., J. Li, and J.K. Bao, *Microautophagy: lesser-known self-eating.* Cell Mol Life Sci, 2012. **69**(7): p. 1125-36.
5. Khandia, R., et al., *A Comprehensive Review of Autophagy and Its Various Roles in Infectious, Non-Infectious, and Lifestyle Diseases: Current Knowledge and Prospects for Disease Prevention, Novel Drug Design, and Therapy.* Cells, 2019. **8**(7).
6. Klionsky, D.J. and P. Codogno, *The mechanism and physiological function of macroautophagy.* J Innate Immun, 2013. **5**(5): p. 427-33.
7. Ravikumar, B., et al., *Regulation of mammalian autophagy in physiology and pathophysiology.* Physiol Rev, 2010. **90**(4): p. 1383-435.
8. He, C. and D.J. Klionsky, *Regulation mechanisms and signaling pathways of autophagy.* Annu Rev Genet, 2009. **43**: p. 67-93.
9. Levy, J.M.M., C.G. Towers, and A. Thorburn, *Targeting autophagy in cancer.* Nat Rev Cancer, 2017. **17**(9): p. 528-542.
10. Seglen, P.O. and P.B. Gordon, *3-Methyladenine: specific inhibitor of autophagic/lysosomal protein degradation in isolated rat hepatocytes.* Proc Natl Acad Sci U S A, 1982. **79**(6): p. 1889-92.
11. Egan, D.F., et al., *Small Molecule Inhibition of the Autophagy Kinase ULK1 and Identification of ULK1 Substrates.* Mol Cell, 2015. **59**(2): p. 285-97.
12. Wong, P.M., et al., *The ULK1 complex: sensing nutrient signals for autophagy activation.*

Autophagy, 2013. **9**(2): p. 124-37.

13. Pattingre, S., et al., *Bcl-2 antiapoptotic proteins inhibit Beclin 1-dependent autophagy.* Cell, 2005. **122**(6): p. 927-39.
14. Vicencio, J.M., et al., *The inositol 1,4,5-trisphosphate receptor regulates autophagy through its interaction with Beclin 1.* Cell Death Differ, 2009. **16**(7): p. 1006-17.
15. Mizushima, N., et al., *A new protein conjugation system in human. The counterpart of the yeast Apg12p conjugation system essential for autophagy.* J Biol Chem, 1998. **273**(51): p. 33889-92.
16. Mizushima, N., et al., *Mouse Apg16L, a novel WD-repeat protein, targets to the autophagic isolation membrane with the Apg12-Apg5 conjugate.* J Cell Sci, 2003. **116**(Pt 9): p. 1679-88.
17. Hemelaar, J., et al., *A single protease, Apg4B, is specific for the autophagy-related ubiquitin-like proteins GATE-16, MAP1-LC3, GABARAP, and Apg8L.* J Biol Chem, 2003. **278**(51): p. 51841-50.
18. Klionsky, D.J., et al., *Guidelines for the use and interpretation of assays for monitoring autophagy in higher eukaryotes.* Autophagy, 2014. **4**(2): p. 151-175.
19. Hanada, T., et al., *The Atg12-Atg5 conjugate has a novel E3-like activity for protein lipidation in autophagy.* J Biol Chem, 2007. **282**(52): p. 37298-302.
20. Fujita, N., et al., *An Atg4B mutant hampers the lipidation of LC3 paralogues and causes defects in autophagosome closure.* Mol Biol Cell, 2008. **19**(11): p. 4651-9.
21. Birgisdottir, A.B., T. Lamark, and T. Johansen, *The LIR motif - crucial for selective autophagy.* J Cell Sci, 2013. **126**(Pt 15): p. 3237-47.
22. Rusten, T.E., et al., *ESCRTs and Fab1 regulate distinct steps of autophagy.* Curr Biol, 2007. **17**(20): p. 1817-25.
23. Gutierrez, M.G., et al., *Rab7 is required for the normal progression of the autophagic pathway in mammalian cells.* J Cell Sci, 2004. **117**(Pt 13): p. 2687-97.

24. Weber, T., et al., *SNAREpins: minimal machinery for membrane fusion.* Cell, 1998. **92**(6): p. 759-72.

25. Filimonenko, M., et al., *Functional multivesicular bodies are required for autophagic clearance of protein aggregates associated with neurodegenerative disease.* J Cell Biol, 2007. **179**(3): p. 485-500.

26. Marino, G., et al., *Self-consumption: the interplay of autophagy and apoptosis.* Nat Rev Mol Cell Biol, 2014. **15**(2): p. 81-94.

27. Bhat, P., et al., *Modulating autophagy in cancer therapy: Advancements and challenges for cancer cell death sensitization.* Biochem Pharmacol, 2018. **147**: p. 170-182.

28. Tasdemir, E., et al., *A dual role of p53 in the control of autophagy.* Autophagy, 2014. **4**(6): p. 810-814.

29. Gao, W., et al., *Upregulation of human autophagy-initiation kinase ULK1 by tumor suppressor p53 contributes to DNA-damage-induced cell death.* Cell Death Differ, 2011. **18**(10): p. 1598-607.

30. Luo, S., et al., *Bim inhibits autophagy by recruiting Beclin 1 to microtubules.* Mol Cell, 2012. **47**(3): p. 359-70.

31. Hou, W., et al., *Autophagic degradation of active caspase-8: a crosstalk mechanism between autophagy and apoptosis.* Autophagy, 2010. **6**(7): p. 891-900.

32. Luo, S. and D.C. Rubinsztein, *Apoptosis blocks Beclin 1-dependent autophagosome synthesis: an effect rescued by Bcl-xL.* Cell Death Differ, 2010. **17**(2): p. 268-77.

33. Bhutia, S.K., et al., *Autophagy: cancer's friend or foe?* Adv Cancer Res, 2013. **118**: p. 61-95.

34. Kenific, C.M., A. Thorburn, and J. Debnath, *Autophagy and metastasis: another double-edged sword.* Curr Opin Cell Biol, 2010. **22**(2): p. 241-5.

35. Takahashi, Y., et al., *Bif-1 interacts with Beclin 1 through UVRAG and regulates autophagy and tumorigenesis.* Nat Cell Biol, 2007. **9**(10): p. 1142-51.

36. Li, Z., et al., *Genetic and epigenetic silencing of the beclin 1 gene in sporadic breast tumors.* BMC Cancer, 2010. **10**: p. 98.

37. Gao, X., et al., *Loss of heterozygosity of the BRCA1 and other loci on chromosome 17q in human prostate cancer.* Cancer Res, 1995. **55**(5): p. 1002-5.

38. Aita, V.M., et al., *Cloning and genomic organization of beclin 1, a candidate tumor suppressor gene on chromosome 17q21.* Genomics, 1999. **59**(1): p. 59-65.

39. Chavez-Dominguez, R., et al., *The Double-Edge Sword of Autophagy in Cancer: From Tumor Suppression to Pro-tumor Activity.* Front Oncol, 2020. **10**: p. 578418.

40. Yun, C.W. and S.H. Lee, *The Roles of Autophagy in Cancer.* Int J Mol Sci, 2018. **19**(11).

41. Wang, Y., et al., *Beclin-1 suppresses gastric cancer progression by promoting apoptosis and reducing cell migration.* Oncol Lett, 2017. **14**(6): p. 6857-6862.

42. Kang, M.R., et al., *Frameshift mutations of autophagy-related genes ATG2B, ATG5, ATG9B and ATG12 in gastric and colorectal cancers with microsatellite instability.* J Pathol, 2009. **217**(5): p. 702-6.

43. Mrakovcic, M. and L.F. Frohlich, *p53-Mediated Molecular Control of Autophagy in Tumor Cells.* Biomolecules, 2018. **8**(2).

44. Liu, E.Y. and K.M. Ryan, *Autophagy and cancer--issues we need to digest.* J Cell Sci, 2012. **125**(Pt 10): p. 2349-58.

45. Guo, J.Y., et al., *Activated Ras requires autophagy to maintain oxidative metabolism and tumorigenesis.* Genes Dev, 2011. **25**(5): p. 460-70.

46. Liu, H., et al., *Down-regulation of autophagy-related protein 5 (ATG5) contributes to the pathogenesis of early-stage cutaneous melanoma.* Sci Transl Med, 2013. **5**(202): p. 202ra123.

47. Bishop, E. and T.D. Bradshaw, *Autophagy modulation: a prudent approach in cancer treatment?* Cancer Chemother Pharmacol, 2018. **82**(6): p. 913-922.

48. Kim, B.M., et al., *Therapeutic Implications for Overcoming Radiation Resistance in*

Cancer Therapy. Int J Mol Sci, 2015. **16**(11): p. 26880-913.

49. Sui, X., et al., *Autophagy and chemotherapy resistance: a promising therapeutic target for cancer treatment.* Cell Death Dis, 2013. **4**: p. e838.

50. Santini, J., et al., *Characterization, quantification, and potential clinical value of the epidermal growth factor receptor in head and neck squamous cell carcinomas.* Head Neck, 1991. **13**(2): p. 132-9.

51. Kalyankrishna, S. and J.R. Grandis, *Epidermal growth factor receptor biology in head and neck cancer.* J Clin Oncol, 2006. **24**(17): p. 2666-72.

52. Marquard, F.E. and M. Jucker, *PI3K/AKT/mTOR signaling as a molecular target in head and neck cancer.* Biochem Pharmacol, 2020. **172**: p. 113729.

53. Yu, J.S. and W. Cui, *Proliferation, survival and metabolism: the role of PI3K/AKT/mTOR signalling in pluripotency and cell fate determination.* Development, 2016. **143**(17): p. 3050-60.

54. Rikiishi, H., *Autophagic action of new targeting agents in head and neck oncology.* Cancer Biol Ther, 2012. **13**(11): p. 978-91.

55. Wakeling, A.E., et al., *ZD1839 (Iressa): an orally active inhibitor of epidermal growth factor signaling with potential for cancer therapy.* Cancer Res, 2002. **62**(20): p. 5749-54.

56. Pernas, F.G., et al., *Proteomic signatures of epidermal growth factor receptor and survival signal pathways correspond to gefitinib sensitivity in head and neck cancer.* Clin Cancer Res, 2009. **15**(7): p. 2361-72.

57. Cheng, Y., et al., *MK-2206, a novel allosteric inhibitor of Akt, synergizes with gefitinib against malignant glioma via modulating both autophagy and apoptosis.* Mol Cancer Ther, 2012. **11**(1): p. 154-64.

58. Han, W., et al., *EGFR tyrosine kinase inhibitors activate autophagy as a cytoprotective response in human lung cancer cells.* PLoS One, 2011. **6**(6): p. e18691.

59. Abdelgalil, A.A., H.M. Al-Kahtani, and F.I. Al-Jenoobi, *Erlotinib.* Profiles Drug Subst

Excip Relat Methodol, 2020. **45**: p. 93-117.

60. Vergez, S., et al., *Preclinical and clinical evidence that Deoxy-2-[18F]fluoro-D-glucose positron emission tomography with computed tomography is a reliable tool for the detection of early molecular responses to erlotinib in head and neck cancer.* Clin Cancer Res, 2010. **16**(17): p. 4434-45.
61. Orcutt, K.P., et al., *Erlotinib-mediated inhibition of EGFR signaling induces metabolic oxidative stress through NOX4.* Cancer Res, 2011. **71**(11): p. 3932-40.
62. Eimer, S., et al., *Autophagy inhibition cooperates with erlotinib to induce glioblastoma cell death.* Cancer Biol Ther, 2011. **11**(12): p. 1017-27.
63. Summy, J.M. and G.E. Gallick, *Treatment for advanced tumors: SRC reclaims center stage.* Clin Cancer Res, 2006. **12**(5): p. 1398-401.
64. Talamonti, M.S., et al., *Increase in activity and level of pp60c-src in progressive stages of human colorectal cancer.* J Clin Invest, 1993. **91**(1): p. 53-60.
65. Aligayer, H., et al., *Activation of Src kinase in primary colorectal carcinoma: an indicator of poor clinical prognosis.* Cancer, 2002. **94**(2): p. 344-51.
66. Lang, L., et al., *Combating head and neck cancer metastases by targeting Src using multifunctional nanoparticle-based saracatinib.* J Hematol Oncol, 2018. **11**(1): p. 85.
67. Fury, M.G., et al., *Phase II study of saracatinib (AZD0530) for patients with recurrent or metastatic head and neck squamous cell carcinoma (HNSCC).* Anticancer Res, 2011. **31**(1): p. 249-53.
68. Rothschild, S.I., et al., *MicroRNA-106a targets autophagy and enhances sensitivity of lung cancer cells to Src inhibitors.* Lung Cancer, 2017. **107**: p. 73-83.
69. Wu, Z., et al., *Autophagy Blockade Sensitizes Prostate Cancer Cells towards Src Family Kinase Inhibitors.* Genes Cancer, 2010. **1**(1): p. 40-9.
70. Sunada, H., et al., *Monoclonal antibody against epidermal growth factor receptor is internalized without stimulating receptor phosphorylation.* Proc Natl Acad Sci U S A,

1986. **83**(11): p. 3825-9.

71. Tejani, M.A., R.B. Cohen, and R. Mehra, *The contribution of cetuximab in the treatment of recurrent and/or metastatic head and neck cancer.* Biologics, 2010. **4**: p. 173-85.

72. Vermorken, J.B., et al., *Platinum-based chemotherapy plus cetuximab in head and neck cancer.* N Engl J Med, 2008. **359**(11): p. 1116-27.

73. Wheeler, D.L., et al., *Epidermal growth factor receptor cooperates with Src family kinases in acquired resistance to cetuximab.* Cancer Biol Ther, 2009. **8**(8): p. 696-703.

74. Li, C., et al., *Dasatinib blocks cetuximab- and radiation-induced nuclear translocation of the epidermal growth factor receptor in head and neck squamous cell carcinoma.* Radiother Oncol, 2010. **97**(2): p. 330-7.

75. de Mello, R.A., et al., *Cetuximab plus platinum-based chemotherapy in head and neck squamous cell carcinoma: a retrospective study in a single comprehensive European cancer institution.* PLoS One, 2014. **9**(2): p. e86697.

76. Li, X., et al., *Roles of autophagy in cetuximab-mediated cancer therapy against EGFR.* Autophagy, 2010. **6**(8): p. 1066-77.

77. Foon, K.A., et al., *Preclinical and clinical evaluations of ABX-EGF, a fully human anti-epidermal growth factor receptor antibody.* Int J Radiat Oncol Biol Phys, 2004. **58**(3): p. 984-90.

78. Kawaguchi, Y., et al., *Cetuximab induce antibody-dependent cellular cytotoxicity against EGFR-expressing esophageal squamous cell carcinoma.* Int J Cancer, 2007. **120**(4): p. 781-7.

79. Kruser, T.J., et al., *Augmentation of radiation response by panitumumab in models of upper aerodigestive tract cancer.* Int J Radiat Oncol Biol Phys, 2008. **72**(2): p. 534-42.

80. Vermorken, J.B., et al., *Cisplatin and fluorouracil with or without panitumumab in patients with recurrent or metastatic squamous-cell carcinoma of the head and neck (SPECTRUM): an open-label phase 3 randomised trial.* Lancet Oncol, 2013. **14**(8): p.

697-710.

81. Giannopoulou, E., et al., *Autophagy: novel action of panitumumab in colon cancer.* Anticancer Res, 2009. **29**(12): p. 5077-82.

82. Tam, S.Y., V.W. Wu, and H.K. Law, *Influence of autophagy on the efficacy of radiotherapy.* Radiat Oncol, 2017. **12**(1): p. 57.

83. Paglin, S., et al., *Rapamycin-sensitive pathway regulates mitochondrial membrane potential, autophagy, and survival in irradiated MCF-7 cells.* Cancer Res, 2005. **65**(23): p. 11061-70.

84. Kim, K.W., et al., *Autophagy for cancer therapy through inhibition of pro-apoptotic proteins and mammalian target of rapamycin signaling.* J Biol Chem, 2006. **281**(48): p. 36883-90.

85. Wu, S.Y., et al., *Ionizing radiation induces autophagy in human oral squamous cell carcinoma.* J buon, 2014. **19**(1): p. 137-44.

86. Chaachouay, H., et al., *Autophagy contributes to resistance of tumor cells to ionizing radiation.* Radiother Oncol, 2011. **99**(3): p. 287-92.

87. Grácio, D., et al., *An overview on the role of autophagy in cancer therapy.* Hematology & Medical Oncology, 2017. **2**(1).

88. Apel, A., et al., *Blocked autophagy sensitizes resistant carcinoma cells to radiation therapy.* Cancer Res, 2008. **68**(5): p. 1485-94.

89. Hausch, F., et al., *FKBPs and the Akt/mTOR pathway.* Cell Cycle, 2013. **12**(15): p. 2366-70.

90. Aissat, N., et al., *Antiproliferative effects of rapamycin as a single agent and in combination with carboplatin and paclitaxel in head and neck cancer cell lines.* Cancer Chemother Pharmacol, 2008. **62**(2): p. 305-13.

91. Iwamaru, A., et al., *Silencing mammalian target of rapamycin signaling by small interfering RNA enhances rapamycin-induced autophagy in malignant glioma cells.*

Oncogene, 2007. **26**(13): p. 1840-51.

92. Lin, C.I., et al., *Autophagy induction with RAD001 enhances chemosensitivity and radiosensitivity through Met inhibition in papillary thyroid cancer.* Mol Cancer Res, 2010. **8**(9): p. 1217-26.

93. Rini, B.I., *Temsirolimus, an inhibitor of mammalian target of rapamycin.* Clin Cancer Res, 2008. **14**(5): p. 1286-90.

94. Bozec, A., et al., *The mTOR-targeting drug temsirolimus enhances the growth-inhibiting effects of the cetuximab-bevacizumab-irradiation combination on head and neck cancer xenografts.* Oral Oncol, 2011. **47**(5): p. 340-4.

95. Yazbeck, V.Y., et al., *Temsirolimus downregulates p21 without altering cyclin D1 expression and induces autophagy and synergizes with vorinostat in mantle cell lymphoma.* Exp Hematol, 2008. **36**(4): p. 443-50.

96. Mauthe, M., et al., *Chloroquine inhibits autophagic flux by decreasing autophagosome-lysosome fusion.* Autophagy, 2018. **14**(8): p. 1435-1455.

97. New, J., et al., *Secretory Autophagy in Cancer-Associated Fibroblasts Promotes Head and Neck Cancer Progression and Offers a Novel Therapeutic Target.* Cancer Res, 2017. **77**(23): p. 6679-6691.

98. Briceno, E., S. Reyes, and J. Sotelo, *Therapy of glioblastoma multiforme improved by the antimutagenic chloroquine.* Neurosurg Focus, 2003. **14**(2): p. e3.

99. Sotelo, J., E. Briceno, and M.A. Lopez-Gonzalez, *Adding chloroquine to conventional treatment for glioblastoma multiforme: a randomized, double-blind, placebo-controlled trial.* Ann Intern Med, 2006. **144**(5): p. 337-43.

100. Maes, H., et al., *Tumor vessel normalization by chloroquine independent of autophagy.* Cancer Cell, 2014. **26**(2): p. 190-206.

101. Gao, L., et al., *Autophagy blockade sensitizes human head and neck squamous cell carcinoma towards CYT997 through enhancing excessively high reactive oxygen*

species-induced apoptosis. J Mol Med (Berl), 2018. **96**(9): p. 929-938.

102. Barnard, R.A., et al., *Phase I clinical trial and pharmacodynamic evaluation of combination hydroxychloroquine and doxorubicin treatment in pet dogs treated for spontaneously occurring lymphoma.* Autophagy, 2014. **10**(8): p. 1415-25.

103. Boone, B.A., et al., *Safety and Biologic Response of Pre-operative Autophagy Inhibition in Combination with Gemcitabine in Patients with Pancreatic Adenocarcinoma.* Ann Surg Oncol, 2015. **22**(13): p. 4402-10.

104. Patil, S., R.S. Rao, and A.T. Raj, *Dual Role of Autophagy in Oral Cancer.* J Int Oral Health, 2015. **7**(6): p. i-ii.

105. Rubinsztein, D.C., P. Codogno, and B. Levine, *Autophagy modulation as a potential therapeutic target for diverse diseases.* Nat Rev Drug Discov, 2012. **11**(9): p. 709-30.

106. Buchser, W.J., et al., *Cell-mediated autophagy promotes cancer cell survival.* Cancer Res, 2012. **72**(12): p. 2970-9.

107. Kumar, P., et al., *Autophagy and transporter-based multi-drug resistance.* Cells, 2012. **1**(3): p. 558-75.

108. Holohan, C., et al., *Cancer drug resistance: an evolving paradigm.* Nat Rev Cancer, 2013. **13**(10): p. 714-26.

109. Iida, M., et al., *Targeting the HER Family with Pan-HER Effectively Overcomes Resistance to Cetuximab.* Mol Cancer Ther, 2016. **15**(9): p. 2175-86.

110. Klionsky, D.J., et al., *Guidelines for the use and interpretation of assays for monitoring autophagy.* Autophagy, 2012. **8**(4): p. 445-544.

111. Jiang, P. and N. Mizushima, *LC3- and p62-based biochemical methods for the analysis of autophagy progression in mammalian cells.* Methods, 2015. **75**: p. 13-8.

112. Mizushima, N., T. Yoshimori, and B. Levine, *Methods in mammalian autophagy research.* Cell, 2010. **140**(3): p. 313-26.

113. Tanida, I., et al., *Lysosomal turnover, but not a cellular level, of endogenous LC3 is a*

marker for autophagy. Autophagy, 2005. **1**(2): p. 84-91.

114. Yoshii, S.R. and N. Mizushima, *Monitoring and Measuring Autophagy.* Int J Mol Sci, 2017. **18**(9).

115. Thome, M.P., et al., *Ratiometric analysis of Acridine Orange staining in the study of acidic organelles and autophagy.* J Cell Sci, 2016. **129**(24): p. 4622-4632.

116. Fowler, T.L., et al., *High-throughput detection of DNA double-strand breaks using image cytometry.* Biotechniques, 2015. **58**(1): p. 37-9.

117. Park, N.H., et al., *Immortalization of normal human oral keratinocytes with type 16 human papillomavirus.* Carcinogenesis, 1991. **12**(9): p. 1627-31.

118. Elrefaey, S., et al., *HPV in oropharyngeal cancer: the basics to know in clinical practice.* Acta Otorhinolaryngol Ital, 2014. **34**(5): p. 299-309.

119. Ang, K.K., et al., *Human papillomavirus and survival of patients with oropharyngeal cancer.* N Engl J Med, 2010. **363**(1): p. 24-35.

120. Marur, S., et al., *HPV-associated head and neck cancer: a virus-related cancer epidemic.* Lancet Oncol, 2010. **11**(8): p. 781-9.

121. Lassen, P., et al., *The influence of HPV-associated p16-expression on accelerated fractionated radiotherapy in head and neck cancer: evaluation of the randomised DAHANCA 6&7 trial.* Radiother Oncol, 2011. **100**(1): p. 49-55.

122. Posner, M.R., et al., *Survival and human papillomavirus in oropharynx cancer in TAX 324: a subset analysis from an international phase III trial.* Ann Oncol, 2011. **22**(5): p. 1071-1077.

123. Judd, N.P., et al., *Comparative analysis of tumor-infiltrating lymphocytes in a syngeneic mouse model of oral cancer.* Otolaryngol Head Neck Surg, 2012. **147**(3): p. 493-500.

124. Onken, M.D., et al., *A surprising cross-species conservation in the genomic landscape of mouse and human oral cancer identifies a transcriptional signature predicting metastatic disease.* Clin Cancer Res, 2014. **20**(11): p. 2873-84.

125. Moore, E., et al., *Established T Cell-Inflamed Tumors Rejected after Adaptive Resistance Was Reversed by Combination STING Activation and PD-1 Pathway Blockade.* Cancer Immunol Res, 2016. **4**(12): p. 1061-1071.

126. Huang, J., et al., *Survival, recurrence and toxicity of HNSCC in comparison of a radiotherapy combination with cisplatin versus cetuximab: a meta-analysis.* BMC Cancer, 2016. **16**: p. 689.

127. Reyes-Gibby, C.C., et al., *Survival patterns in squamous cell carcinoma of the head and neck: pain as an independent prognostic factor for survival.* J Pain, 2014. **15**(10): p. 1015-22.

128. Forastiere, A.A., et al., *Concurrent chemotherapy and radiotherapy for organ preservation in advanced laryngeal cancer.* N Engl J Med, 2003. **349**(22): p. 2091-8.

129. Pasquier, B., *SAR405, a PIK3C3/Vps34 inhibitor that prevents autophagy and synergizes with MTOR inhibition in tumor cells.* Autophagy, 2015. **11**(4): p. 725-6.

130. Noman, M.Z., et al., *Inhibition of Vps34 reprograms cold into hot inflamed tumors and improves anti-PD-1/PD-L1 immunotherapy.* Sci Adv, 2020. **6**(18): p. eaax7881.

131. Tan, X., et al., *A kinase-independent role for EGF receptor in autophagy initiation.* Cell, 2015. **160**(1-2): p. 145-60.

132. Tan, X., et al., *LAPTM4B is a PtdIns(4,5)P2 effector that regulates EGFR signaling, lysosomal sorting, and degradation.* EMBO J, 2015. **34**(4): p. 475-90.

133. Kirkin, V. and V.V. Rogov, *A Diversity of Selective Autophagy Receptors Determines the Specificity of the Autophagy Pathway.* Mol Cell, 2019. **76**(2): p. 268-285.

134. Johansen, T. and T. Lamark, *Selective Autophagy: ATG8 Family Proteins, LIR Motifs and Cargo Receptors.* J Mol Biol, 2020. **432**(1): p. 80-103.

135. Liu, X.R., et al., *Structure analysis and expressions of a novel tetratransmembrane protein, lysosoma-associated protein transmembrane 4 beta associated with hepatocellular carcinoma.* World J Gastroenterol, 2004. **10**(11): p. 1555-9.

136. Kim, W., et al., *Cellular Stress Responses in Radiotherapy.* Cells, 2019. **8**(9).

137. Van Houten, B., V. Woshner, and J.H. Santos, *Role of mitochondrial DNA in toxic responses to oxidative stress.* DNA Repair (Amst), 2006. **5**(2): p. 145-52.

138. Bernard, M., et al., *Dual Inhibition of Autophagy and PI3K/AKT/MTOR Pathway as a Therapeutic Strategy in Head and Neck Squamous Cell Carcinoma.* Cancers (Basel), 2020. **12**(9).

139. Yang, Y.P., et al., *Application and interpretation of current autophagy inhibitors and activators.* Acta Pharmacol Sin, 2013. **34**(5): p. 625-35.

140. Wang, X., et al., *Development and validation of a survival model for lung adenocarcinoma based on autophagy-associated genes.* J Transl Med, 2020. **18**(1): p. 149.

141. Wang, Y., et al., *A risk signature with four autophagy-related genes for predicting survival of glioblastoma multiforme.* J Cell Mol Med, 2020. **24**(7): p. 3807-3821.

142. Yue, P., et al., *Development of an autophagy-related signature in pancreatic adenocarcinoma.* Biomed Pharmacother, 2020. **126**: p. 110080.

143. Lin, Q.G., et al., *Development of prognostic index based on autophagy-related genes analysis in breast cancer.* Aging (Albany NY), 2020. **12**(2): p. 1366-1376.

144. An, Y., et al., *Development of a Novel Autophagy-related Prognostic Signature for Serous Ovarian Cancer.* J Cancer, 2018. **9**(21): p. 4058-4071.

145. Jin, Y. and X. Qin, *Development of a Prognostic Signature Based on Autophagy-related Genes for Head and Neck Squamous Cell Carcinoma.* Arch Med Res, 2020. **51**(8): p. 860-867.